Evaluation of Blasting Efficiency in Surface Mines

Abinash Parida

Department of Mining Engineering
National Institute of Technology Rourkela

Evaluation of Blasting Efficiency in Surface Mines

Dissertation submitted to the

National Institute of Technology Rourkela

in partial fulfilment of the requirements

of the degree of

Master of Technology (Research)

in

Mining Engineering

by

Abinash Parida
(Roll Number: 613 MN 3003)

under the supervision of

Prof. Manoj Kumar Mishra

Department of Mining Engineering
National Institute of Technology Rourkela

December, 2016

Department of Mining Engineering
National Institute of Technology Rourkela

December 14, 2016

Certificate of Examination

Roll Number: 613MN3003

Name: Abinash Parida

Title of Dissertation: Evaluation of Blasting Efficiency in Surface Mines

We the below signed, after checking the dissertation mentioned above and the official record book (s) of the student, hereby state our approval of the dissertation submitted in partial fulfilment of the requirements of the degree of Master of technology (Research) Engineering at National Institute of Technology Rourkela. We are satisfied with the volume, quality, correctness, and originality of the work.

---	---
	Prof. Manoj Ku. Mishra
(Co-Supervisor)	(Principal Supervisor)
---	---
Prof. A. K. Satpathy	*Prof. S. K. Das*
Member (MSC)	Member (MSC)
---	---
Prof. H. B. Sahu	*Name of Examiner*
Member (MSC)	Examiner

Prof. B.K. Pal

Chairman (MSC)

Department of Mining Engineering
National Institute of Technology Rourkela

December 14, 2016

Prof. Manoj Kumar Mishra

Associate Professor and H.O.D
Department of Mining Engineering

Supervisor's Certificate

This is to certify that the work presented in this dissertation entitled " Evaluation of Blasting efficiency in surface Mines" by "*Abinash Parida''*, Roll Number 613MN3003, is a record of original research carried out by him/her under my supervision and guidance in partial fulfilment of the requirements of the degree of *Master of technology (Research)* in *Mining Engineering*. Neither this dissertation nor any part of it has been submitted for any degree or diploma to any institute or university in India or abroad.

Prof. Manoj K Mishra

Declaration of Originality

I, Abinash Parida, Roll Number 613MN3003 hereby declare that this dissertation entitled "*Evaluation of Blasting Efficiency in Surface Mines*" represent my original work carried out as a postgraduate student of NIT Rourkela and, to the best of my knowledge, it contains no material previously published or written by another person, nor any material presented for the award of any other degree or diploma of NIT Rourkela or any other institution. Any contribution made to this research by others, with whom I have worked at NIT Rourkela or elsewhere, is explicitly acknowledged in the dissertation. Works of other authors cited in this dissertation have been duly acknowledged under the section "Bibliography". I have also submitted my original research records to the scrutiny committee for evaluation of my dissertation.

I am fully aware that in case of any non-compliance detected in future, the Senate of NIT Rourkela may withdraw the degree awarded to me on the basis of the present dissertation.

December 14, 2016

NIT Rourkela

Abinash Parida

Acknowledgment

This dissertation would not have been completed without the help of my empathetic and supportive supervisor Prof. M. K. Mishra. I heartfelt thank him for his unconditional help, constant effort for improving my work, providing time to time feedback and never giving upon me.

I am indebted to my Master Scrutiny Committee (MSC) members Prof. A. K. Satpathy, Department of Mechanical Engineering, Prof. S. K. Das, Department of Civil Engineering, Prof. H. B. Sahu, and Prof. B K Pal, Chairman Department of Mining Engineering of our institute for their kind co-operation and insightful comments throughout, which has been instrumental in the success of thesis..

I also express my thankfulness to all the faculties and staff members of the department, specifically Mr. P. N. Mallick and Mr. Bhaskar Jena for their continuous help and assistance. Special thanks to Mr. Harinandan Kumar for his kind cooperation and support during the research work. I also thankful to mines manager Mr. A.K. Dey of Daitari region and Mr. B. Kalo from Koira region for their assistance and help. Lastly, my sincere thanks to my parents and all my friends who encourage me to complete my research work.

December 14, 2016

Abinash Parida

NIT Rourkela

Abstract

Drilling and blasting are the major unit operations in opencast mining. In spite of the best efforts to introduce mechanization in the opencast mines, blasting continue to dominate the production. Beside the production in open cast mining blasting and vibration also cause environmental problem. In bench blast design, not only the technical and economic aspects, such as block size, uniformity and cost, but also the elimination of environmental problems resulting from ground vibration, air blast and fly rock should be taken into consideration. The evaluation of ground vibration components plays an important role in the minimization of the environmental complaints. Odisha is rich in iron ore deposit and the mines invariably need blasting for loosen the rock mass. These are frequent complaints from the people surrounding the zone about adverse effect of blasting. This study is an attempt to evaluate same of those aspects. Two active iron ore mine have been considered for the analysis of ground vibration, air over pressure, flyrock as well as fragmentation parameters. There exist a few established approaches as USBM, Langefors-Kilstrom, Ambraseys-Hendron, Indian standard and CMRI to predict those. In this investigation the utility of those approaches are evaluated. It was observed that the two region Koira and Daitarido not confirm strongly to the five approaches. Artificial neural network is a technique that is gain wide acceptance even in heterogeneous condition. This study also finds that the prediction by ground vibration, air over pressure and fly rock by ANN would be better alternative. Model equation has also been developed with ANN approach. Mutual relations between stemming length, depth, fragmentation size, powder factor, explosive charge have also been determined.

Keywords**:** *Blasting*; *Ground Vibration*; *Frequency; Air Noise*; *Flyrock*; *Fragmentation*

Contents

List of Figures

List of Tables

List of Algorithms

Chapter 1
Introduction

Mineral resources are backbone of industry and industry needs metal and non-metals as row material. Mineral resources are extracted by both underground mining method and open cast mining method. In both the case extraction of mineral is done by loosening the rock or coal. Surface mining is the most popular method of ore excavation worldwide. Drilling and blasting operation is the first element of the ore extraction process. Blasting is the most energy efficient stage in the comminution system and has an energetic efficiency of 20 to 35% as compared to efficiency of 15% and 2% by crushing and grinding respectively [1]. There exists a strong relation between blast properties and efficiency of crushing and grinding [2]. The primary purpose of blasting is rock fragmentation and displacement of the broken rock. Blasting operations may impose excessive noise and vibration on communities. Excessive levels of structural vibration caused by ground vibration from blasting can result in damage to, or failure of, structures. The intensity of ground vibration depends on various parameters which can be categorized into two classes-Controllable parameters and Uncontrollable parameters.

Controllable parameters are mainly related to explosive characteristics (initiation system, initiation sequence, no of free faces, buffers, explosives energy, charge geometry, loading method) and blast hole design parameter (hole diameter, hole depth, sub drill depth, hole inclination, collar height, stemming, blast pattern, burden to spacing ratio, blast size and configuration and blasting direction, initiating system, initiating sequence, no of free faces, explosive types, explosive energy, charge geometry, loading method while others are uncontrollable parameters which is natural and is related to geological conditions, rock characteristic etc. Ground vibrations are generally quantified by means of particle velocities at particular ground locations. Currently the most widely accepted single measurement of ground vibration considered potentially damaging is Peak Particle Velocity (PPV). PPV is defined as the speed by which earth particles move or pass a particular site. Ground vibration is an integral part of the process of rock blasting.

Dynamic stresses in surrounding rock mass around blast hole is set due to sudden acceleration of rock mass by detonating gas pressures on the hole walls. This sets up a wave motion in the ground. The wave motion spreads concentrically from the blast site in all direction and gets attenuated due to spreading of fixed energy over a greater mass of material and away from its origin. In rock blasting, it is generally understood that both the stress wave and gas pressurization make significant contribution to rock fragmentation. When an explosive detonates in a hole, the pressure can exceed 10 GPa (100,000 atm.) sufficient to scatter the rock near the hole and also generate a stress wave that travel

outwards at a velocity 3000-5000m/s [3]. Leading front of stress wave is compressive but it closely followed by tensile stress that are mainly responsible for rock fragmentation. Compressive wave converts into tensile stress when it reaches a nearby exposed surface. Rock breaks much easily in tension than in compression and fracture progress backward from the free surface. The desired degree of fragmentation depends on the type and size of equipment, which is used for the subsequent handling of the fragments. The properties of fragmentation such as size and shape are very important for optimization of production. Three factors that control the fragment size distribution are rock structure, quantity of explosive, and its distribution within the rock mass.

1.1 Objectives

The goal of the investigation is to develop a correlation between parameters as PPV, distance and explosive quantity fragmentation size. The aim is achieved by addressing the following specific objectives particularly with reference to iron ore mines.

- Prediction of PPV with a few established approaches as USBM, Langefors-Kilstrom, Ambraseys-Hendron, Indian standard and CMRI.
- Development of mutual relation between Peak Particle Velocity, explosive used and distance of structure from field studies.
- Evaluation of field measured values against predicted values.
- Prediction of PPV for ANN approach and comparison with measured.
- Evaluation of relation between PPV, mean fragmentation size, depth, powder factor, Air over pressure and dominant frequency and fly rock.

1.2 Methodology

The aim and objectives are proposed to be achieved through well determined steps. The methodology involves the following:

- Critical review of literature to understand blasting and its effect.
- Visit to mines to observe the actual phenomena and collect the data.
- Field experimentation by measuring ground vibration and air over pressure.
- Fragmentation analysis.
- Model development by ANN.

The following flow chart shows the broad step by step approach adopted for the investigation

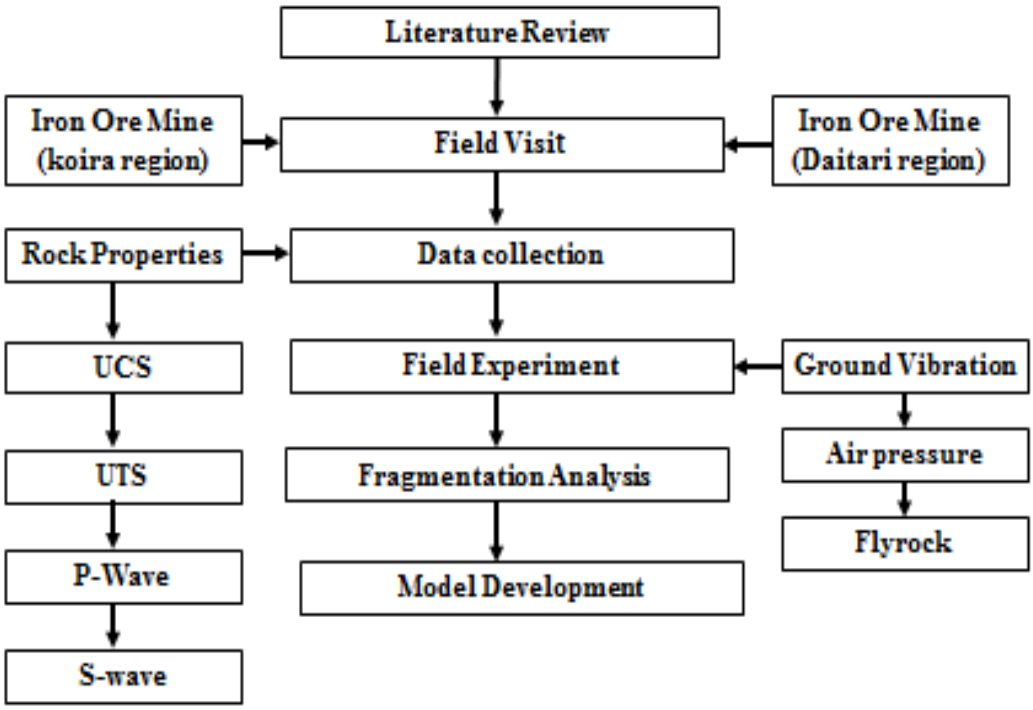

Chapter 2

Literature review

Mining is the second most endeavours of human kind after agriculture. It is one of the primary industries of civilization. Over the ages, mining activity has undergone phenomenal changes: from manual cutting tools to remote operated motorized machine. Typically mining is a five stage activity: prospecting, exploration, development, exploitation and reclamation. Among the development stage involves the opening of a mineral deposit and exploitation is with the actual recovery of minerals in quantity. The mining method selected for the exploitation depends on factor as characteristics of mineral deposit and the limits imposed by safely, technology, and environment and economics. Broadly two methods surface and underground are adopted. Surface mining include mechanical excavation in large scale and is the predominant procedure worldwide. The process involves breaking or loosening the rock, ore and waste in to minimum size and to extract largest possible size at minimum cost. Drilling and blasting are necessary to penetrate and fragment the rock mass and is given a generic term rock breakage. In surface mines, the site is started by removal of over burden and weathered material on the rock formation. After the removal of over burden, ore winning takes place.

2.1 Breakage

The freeing or loosening of large masses of harder rock from the earth is called rock breakage. It involves two steps: (A) Rock penetration i.e. drills a hole in the rock mass and (B) Rock fragmentation i.e. breaks the rock in to manageable size. The rock fragmentation is usually carried out by chemical energy using explosive although these exists many other approaches. But rock fragmentation by explosive is the dominant method.

2.2 Rock blasting

Rock blasting is the process which consists of several operations such as drilling blast holes, charging explosives into the holes, connecting the holes by suitable blasting pattern with surface delay and igniting by safety fuse or exploder. Rock is affected when explosives are detonated. Total charge is converted into hot gas and intense shock pressure. The rock is crushed and fractured by intense shock pressure and separated from each fracture by gas pressure. The shock energy creates fracture in the rock mass. Gas pressure expands the fracture and also helps in move the rock from original position. There are three zones explain [4]such as

- Strong shock zone
- Non-linear zone
- Elastic zone

In the first zone radial compressive stress exceed the dynamic compressive strength of surrounding rock mass. As a result crushing of rock occurs due to compression. In the second zone, fracturing of rock mass is possible due to tangential stress. Tangential stress is produced due to reflection of compressive wave at free face. After wave passage, the high temperature and pressure gas flow through the fracture crack. As a result crack expansion and rock movement occurs. Third zone extends to a distance of twenty to fifty radii of blast hole where fracturing of rock occurs from plastic deformation to brittle elastic fracturing [5]. According to [6], absence of free face shock waves travel through the ground and generate ground vibration. This zone is known as seismic zone.

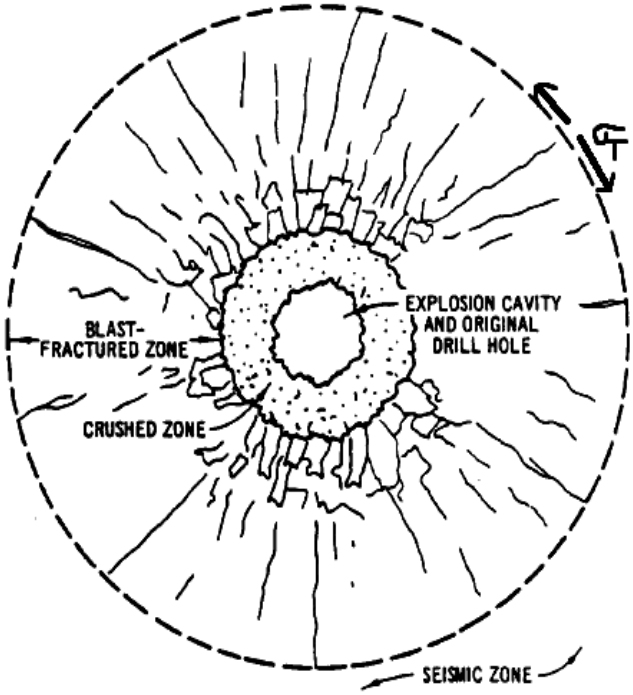

Figure 2.1: location of different zone of rock fragmentation

2.3 Parameter affecting blasting

There are two parameters that affect blasting such as controllable and uncontrollable parameter.

2.3.1 Controllable parameters

2.3.1.1 Explosive

Explosive is a solid or liquid substance or a mixture of substance produce high pressure heat and large volume of gases in a short period when exploded by external means. Explosives are classified in to two types.

- Low explosive
- High explosive

Low explosive when explode, deflagration occurs and reaction moves slower than the sound. Gun powder, propellants in ammonium nitrates and rocket propellants are example of low explosive.

High explosive produces large volume of gases with high pressure heat when explode at velocity 1500-8000 m/s. High explosives are two types such as primary explosive and secondary explosives. Primary explosives are initiated by detonator and used as base charge. On application of weak mechanical shock, spark or flame to base charge, it initiates column charge without deflagration. Secondary explosives are detonated by shock wave and shock waves are generated by detonation of primary explosive. Secondary explosives are nitro-glycerine, emulsion, slurries, watergels, ANFO and other powder explosive.

Explosive possess certain characteristics and properties such as effective energy, detonation velocity, detonation pressure, density, sensitivity, water resistance, physical characteristics, fume characteristics, storage life.

2.3.1.2 Effective energy

Effective energy is defined as the total energy released by the explosive to break the rock.

2.3.1.3 Strength

The strength of explosive is defined as the maximum potential energy stored in the explosive composition. It is expressed as either unit volume (cm^3) or unit mass known as relative weight strength (RWS).

$$RWS = \frac{Calculated\,Strength\left(\frac{MJ}{kg}\right)}{Calculated\,Strength\,of\;ANFO\left(\frac{MJ}{kg}\right)} \quad (1)$$

$$RBS = RWS \times \frac{Density\;of\;Explosive}{Density\;of\;ANFO} \quad (2)$$

$$ANFO = 0.84\left(\frac{g}{cm^3}\right) \quad (3)$$

Table 2.1: RWS and RBS of some common explosives

Product	Density (g/cc)	Energy (MJ/kg)	Explosion Pressure (GPa)	RWS	RBS
Bulk ANFO	0.84	3.75	22	100	100
Bulk Emulsion	1.25	2.92	31	77	115
TNT Slurry(22% TNT)	1.48	3.37	59	89	158
Heavy ANFO(30% Emulsion)	1.23	3.45	41	92	135
Doped Emulsion(30% AN)	3.45	3.29	37	87	130

2.3.1.4 Detonation velocity

The detonation velocity is defined as the speed at which the detonation wave travels through a column of explosive. Factors affecting the detonation velocity are explosive type, diameter, temperature and priming.

2.3.1.5 Type of explosive

The VOD of common explosive falls in the range between 3000m/s to 5000m/s. Higher VOD of explosive has the high ability of shattering of rock. So at the time of blasting of rock, explosive is selected according to VOD of explosive and strength of rock.

2.3.1.6 Diameter

The VOD of explosive depends upon the diameter of explosive. The VOD of explosive increases with increase of diameter of explosive until the steady state velocity of explosive is reached. Explosive has a critical diameter i.e. the minimum diameter at which detonation process sustains itself once initiated. If explosive's diameter is smaller than critical diameter, the detonation of explosive will not be supported due to un-confinement. In case of longer diameter than critical, detonation will be supported due to confinement. For ANFO explosive, diameter of 225 mm or more gives VOD of 4000 m/s to 5000 m/s while diameter below 50 mm, the VOD is less than 2500 m/s[15].

2.3.1.7 Density

Density of explosive is defined as mass of explosive to unit volume. It is expressed as g/cm^3. Some densities of explosives are 0.80 g/cm^3 (ANFO) and 0.80 to1.80 g/cm^3 (watergels, emulsion, etc.). The strength of explosive increase with increase in density. So in case of hard ground larger explosive quantity are required. Critical density of an explosive is the density of explosive beyond which explosive loses its sensitivity and unable to detonate if adequate primer is available. The density of a few commonly used explosives is as follows

- Loosely poured ANFO = 0.80 g/cc
- Pneumatically charge ANFO = 0.95 to1.10 g/cc
- Slurries and emulsions = 0.80 to 1.5 g/cc
- Cast Boosters = 1.60 g/cc

2.3.1.8 Sensitivity

The sensitivity is the explosive's propagating ability. Two types of explosives are generally found. One is cap-sensitivity and another is non-cap sensitivity. First one is detonated by detonator and another is initiated by cap sensitivity explosive.

2.3.1.9 Detonating pressure

The pressure produced when detonating wave pass through a column of explosive. It is depends upon VOD and density of explosive.

2.3.1.10 Initiation sequence

Initiation sequence is important for proper fragmentation. Two parameters that affect vibration sequence are

1) Delay interval
2) Delay pattern or connection

Delay interval is the time gap between two conjugative holes. The explosive is detonated by shock or detonation which provided by detonator. There are two types of detonator available namely electrical and non-electrical. Both electric or non-electric delay is used as surface delay and in hole delay. In hole delay system provide time gap between each downline initiation and detonation of corresponding explosive charge. Performance of any multi-hole blast depends on interaction between adjacent blast hole. Time delay between blast hole influence the overall blast result. Shorter delay is provided for small diameter blast hole with small burden and spacing. Longer delay provides adequate relief for large diameter blast hole with large burden.

Hole sequence or delay pattern is most important parameter in blasting. The connection of blast hole in surface mines may be series/parallel/diagonal or 'V' pattern.

2.3.1.11 Blast design

Blast design is most important parameter that not only influence blasting cost but also influences fragmentation, vibration and air blast etc. The blast design parameters are bench height, hole diameter, burden, spacing, stemming height etc.

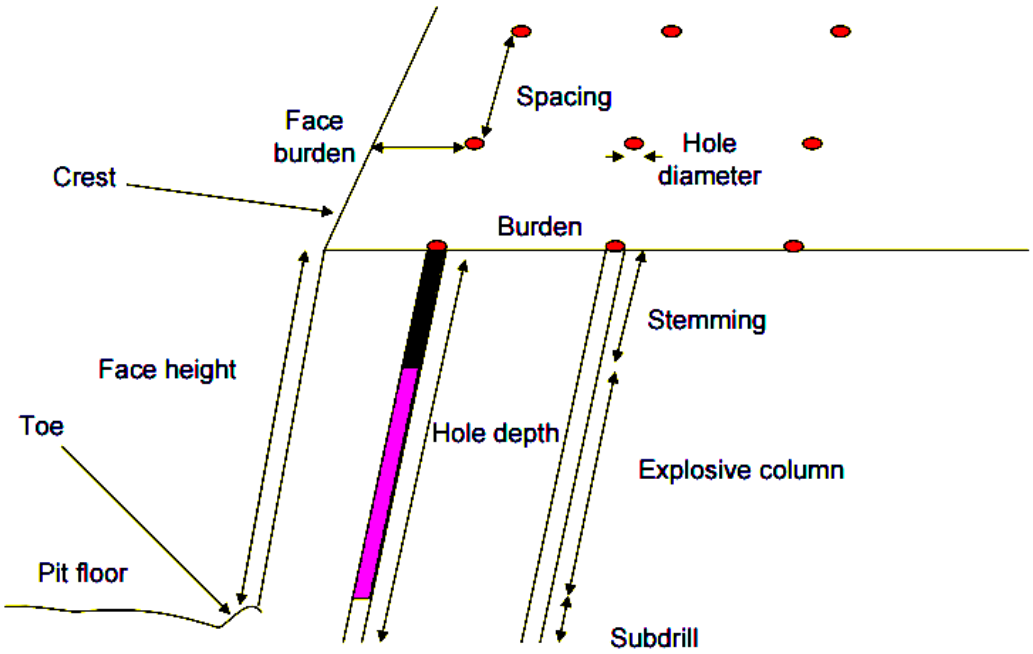

Figure 2.2: Blast design layout

2.3.1.12 Bench height

Bench height is defined as vertical distance between the upper and lower surface of each bench called bench height. According to [7] suggested that bench height should not be more than 62 times the hole diameter. Because the use of large diameter blast holes in shallow faces prevents the efficient charge distribution while small diameter blast holes in high faces can be in effective due to effect of blast hole deviation.

2.3.1.13 Blast hole diameter

The factor that are considered to be considered at the time of selecting blast hole diameter.

- Rock mass properties
- Rock pile characteristics
- Bench height
- Explosive distribution
- Relative economics of different type of drilling equipment

According to [7] Diameter (D) should not be exceed $0.016 \times$ H (bench height).

2.3.1.14 Burden

The perpendicular distance from blast hole to the nearest free face is known as burden. It has the following relation:

B = 25D to 40D

B = 25D to 30D for hard rock

B = 30D to 35D for medium rock

B = 35D to 40D for soft rock

B and D are burden and diameter respectively.

In other term inter row distance is known as burden. For desired fragmentation and control blasting, burden is depend upon hole diameter, rock type and explosive strength etc.

Table: 2.2: some formulas for estimation of burden [8]

Konya,[9]	$B = 3.15 D_e (SGe / SGr)^{0.33}$
Langefors and kihlstrom, [10]	$B_m = 0.958 D_e (r_e / cof (S_D / B_D))^{1/2}$
Ash formulae, [11]	$B_m = 38 D_e (r_e / r_r)^{0.5}$
Vutukuri and Bhandari, [12]	$B = 0.024 \times D_e + 0.85$
Rajmeny *et al*., [13]	$B = 0.028 \times D_e - 0.074$

(Where, B = burden and B_m = maximum burden; D_e = diameter of hole; SG_e and SG_r are specific gravity of explosive and specific gravity of rock respectively; r_e and r_r are density of explosive and density of rock respectively.)

2.3.1.15 Spacing

The distance between two adjacent hole measured perpendicularly to burden and parallel to free face is known as spacing. The spacing depends upon burden. If Spacing is equal to burden, then they form grid pattern which is applicable for massive rock breaking. Large spacing and small burden causes more twisting and tearing of rock and also lesser splitting and back break is observed. In case of smaller spacing than burden causes splitting between blast holes and back break. In open cast blast design, spacing and burden ratio should be 1.25 for better result.

Table 2.3: Some Empirical formula for rock blasting

Vutkuri and Bhandari [14]	$S = 0.9 \times B + 0.91$
Rajmeny et al. [15]	$S = 0.024 \times D + 0.9$

Where, S = spacing; B = burden; D = diameter

2.3.1.16 Stemming

Stemming is the covering of material (mud, clay and drill cutting) in the remaining part of blast hole after putting the explosive charge. Stemming not only enhances fragmentation but also reducing high pressure gas venting to atmosphere.

2.3.1.17 Powder factor

Powder factor is defined as volume of rock broken (m^3) per unit charge amount (kg) consumption and depends on parameters as volume of rock, charge amount, explosive strength, drilling diameter, rock type, geological weaknesses, etc. Specific charge is just reciprocal of powder factor. Powder factor depends upon rock type, explosive strength, degree of mechanization, drill hole diameter, pattern of drilling, explosive density etc.

Table 2.4: **S**ome Examples of Consumption of High Explosives with rock type

Rock type	**Explosive consumption (kg/m^3)**
Soft clay, slate, heavy loam	0.3-0.5
Marl, coal, gypsum, soft limestone,	0.35-0.55
Sand stone, shale, marly limestone	0.45-0.6
Granite, limestone and sand stone	0.6-0.7
Coarse grained granite, basalt, weathered genesis	0.7-0.75
Hard genesis, granite genesis, basalt	0.85
Gabbro and basalt	0.9

2.3.2 Uncontrollable Parameter

2.3.2.1 Rock parameter affecting Blasting

2.3.2.1.1 Density

Density is defined as mass per unit volume of rock mass. The density is expressed as dry density, bulk density and saturated density. Dry density of a rock means rock is

completely dry (void contains only air). Bulk density means rock mass contains some liquid and air in its pores. Saturated density means rock mass is fully saturated.

2.3.2.1.2 Moisture content

Moisture content in rock is the ratio of weight of water in the voids to the weight of dry sample in the voids. Moisture content is determined by drying at a temperature from 105 to110 degree centigrade. Natural moisture content in sample means the sample taken from ground by excavation and boring. Excess natural moisture content indicates the rock is more porous. If confining pressure of rock mass increase, it means there is decrease in moisture content and rock is stronger.

2.3.2.1.3 Thermal properties

Change in the thermal temperature induce crack in the rock mass due to thermal strains produce in the rock mass by thermal stress. So shock energy and gas energy passes through the crack of rock and causing ground vibration, air noise and fly rock etc.

2.3.2.1.4 Anisotropy

Rock mass is always anisotropic due to existence in bedding plane. The bedding planes are the plane of weakness which separates the sedimentary and stratified rocks in different layers. Anisotropic material shows some weakness in a particular direction.

2.3.2.1.5 Joints

Joint is defined as the fracture or crack in the rock mass due to reduce in volume of rock mass by tensile and compressive stress.

2.3.2.1.6 Uniaxial Compressive strength

UCS test is intended for strength classification and characterisation of intact rock. Specimen for this test should be circular cylinder having height to diameter ratio 2.5-3.0 and diameter of NX core size. P wave and powder factor depend upon compressive strength. According to [16] P wave increases linearly with compressive strength. UCS of rock also affects powder factor (Table 2.5).

Table 2.5:Classification of the UCS of rocks with powder factor [17]

Rock Type	UCS (MPa)	PF (kg/m^3)
Very low strength	1-5	0.15-0.25
Medium strength	5-25	0.25-0.35
High strength	25-30	0.4-0.5
Very high strength	50-100	0.7-0.8
Very high Strength	100-250	-
Extremely High strength	250	-

The compressive strength (σ_c) is calculated by

$$\sigma_c = \frac{F}{A} \tag{4}$$

(Where, σ_c = Compressive strength, F = Compressive load, A= initial cross-section of the sample)

2.3.2.1.7 Tensile strength

Tensile strength of rock sample is mainly intended for classification and characterisation of intact rock sample having diameter 54 mm about NX size and thickness should be equal to sample radius. The most common method for determination of tensile test is Brazilian test method. In this test the rocks fail in biaxial stress field (one principal stress is tensile while other is compressive). During blasting rock is fractured by combination of two waves such as compressive and tensile. The tensile fracture occurs when reflected tensile wave exceeds the tensile strength of rock and slabbing occur [18]. The tensile strength of the specimen is calculated by

$$\sigma_t = \frac{F}{\Pi D t} \tag{5}$$

(Where, F = load at failure (N), D = distance (m), t = thickness of test specimen)

2.3.2.1.8 Ultrasonic velocity

Ultrasonic testing is a non-destructive testing techniques based on the propagation of ultrasonic waves in the rock sample to measure P wave and S wave velocity. The test was done by two sensors to opposite surface of specimen. Honey was used for better contact and transmission of waves between platen and sample. Samples were prepared NX size of height to diameter varies 2 to 2.5m.The equation of P wave and S wave is expressed as

$$V_p = \sqrt{\frac{K + \frac{4}{3}\mu}{\rho}} \tag{6}$$

$$V_s = \sqrt{\frac{\mu}{\rho}} \tag{7}$$

(Where, V_p and V_s are P wave and S wave, μ and ρ are density and bulk modulus.)

2.4 Principle of fragmentation by explosive

The primary purpose of rock blasting is fragmentation of rock and assessment of blast induced impacts such as ground vibration and Air blast. According to [19], nearly 20% of the energy is transferred as shock wave to surrounding. The remaining part of explosive is released as gases of very high temperature and pressure. The pressure on the bore hole wall increases instantaneously. When the explosive detonate with the movement of walls elastically, these occurs a pressure drop. The difference between total work done by the gas and the amount of energy stored elastically around the bore hole is the energy

responsible for creation of shock wave that contributes to the ground breaking process. Shock wave results in wave propagation and particle velocity. The resultant effect is in creation of several environmental impacts as air over pressure ground vibration, fly rock and back break around the blasting zone[20-21].

Table 2.6: Different factor that influence ground vibration [22]

Variable within the control of mine operators	Influence on ground motion significant	Moderately significant	Insignificant
1.Charge weight per delay	X		
2. Delay interval	X		
3. Burden and spacing		X	X
4. Stemming (amount)			X
5. stemming (type)			X
6. Charge length and diameter			X
7. Angle of bore hole			
8. Direction of initiation		X	
9. Charge weight per blast			X
10. Charge depth			X
11. Bare vs. Covered prima cord			X
12. Charge confinement	X		
Variables not in the control of mine operator			
1. General surface terrain			X
2. Type and depth of overburden	X		
3. Wind and weather condition			X

Hence the prediction of ground vibration is important. It is difficult to predict the magnitude, frequency and duration of ground vibration due to amplitude influences. Typically it depends on maximum in explosive charge per particularly delay interval and the distance between the blast hole and the measuring point through all the variables as rock type, topographically, blasting pattern, explosive type characteristics of ground motion, etc. It is difficult to establish common generic approach to take into account all these factor into the elasto-plastic equation of motion and predict the particle velocity. So empirical approaches have been developed extensively for ground vibration prediction.

2.5 Characteristics of ground vibration

2.5.1 Ground vibration

With the explosive charging in the blast hole, intense strain waves transmit to the surrounding rock, typically it involves a shoving (compressive) wave being transmitted from bore hole wall at the speed of sound. The particle velocity associated with them also move outward. When it reaches a free face, the wave tends to reflect and travel back from the free face “jerking” the rock material on its way. As rock is weak in tension it fails, typically occurring at a free face, termed “spalling”. Simultaneously with compressive wave, stretching (tension) action in the tangential (circumferential) direction is also

transmitted. These two (compressive radial and tensile tangential) move outward at a speed of sound in the rock medium. The energy carried by these waves are called strain energy and is responsible for fragmentation attributed to different breakage mechanism as crushing, radial cracking and reflection breakage. This is the crushed zone i.e. the vicinity of the bore hole and radial fracture zone in compassed a volume of permanently deformed rock. Strain wave intensity reduces with radial distance and at a location where no permanent damage occurs in the rock mass. It is typically beyond the fragmentation zone. These strain waves propagate through the medium in the form of elastic waves, oscillating the particle through which it travels. These waves in the elastic zone are common as ground vibration that closely confirm to visco-elastic behaviour [23]. The ground vibration is detuned as the wave motion that travels away from the blast site to nearby areas Singh [24-25].

2.5.2 Types of Vibration Waves

Several types of waves form due to interaction between vibrations and the propagating media. There are mainly two types of vibration waves observed such as body waves and surface waves.

2.5.3 Body waves

Body waves travel through the medium such as soil and rock. Body waves are generally two types P wave and S wave.

2.5.4 P wave

The p wave is faster compression wave move in the direction of propagation wave. They move in solid, liquid and gaseous medium.

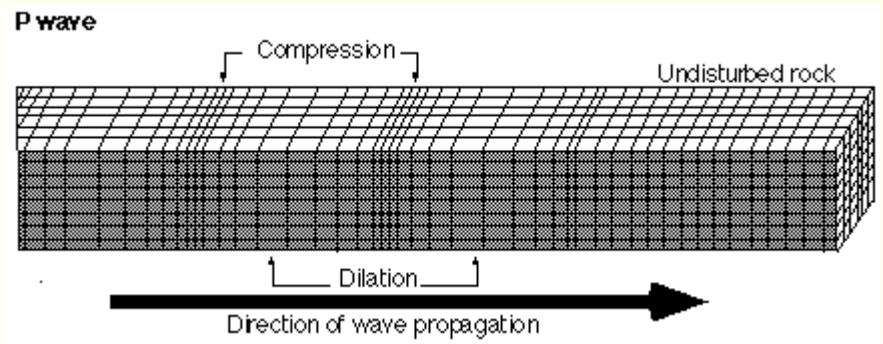

Figure 2.3: shows particle motion in P wave [26]

2.5.5 S wave

The S wave is shear wave move slower than P wave but travel through the medium at right angles to the wave propagation direction. It moves only solid medium.

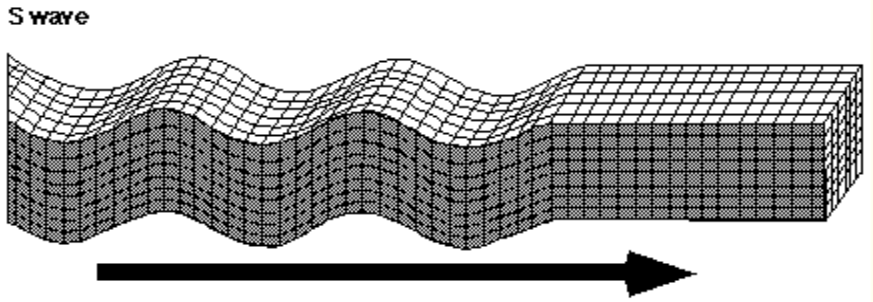

Figure 2.4: shows particle motion in S wave [26]

2.5.6 Surface wave

Surface wave are transmitted along a surface (upper part of surface). There are two types of surface wave such as R-wave and L wave.

2.5.7 R-wave

The R-waves travel slowly than the P wave and S wave. But the motion of particle is elliptical in the vertical plane and in the same direction as the propagation. So the particle motion is two dimensional instead of one dimensional like Body wave. The motion of R waves is similar to the forward motion of water wave but only difference is water wave make half circular motion whereas R wave make elliptical motion in solid medium.

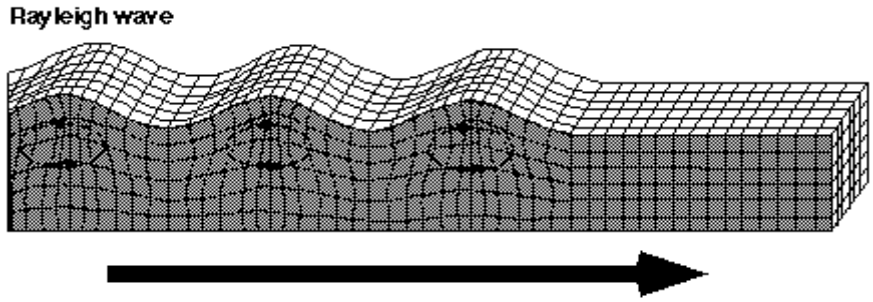

Figure2.5: shows particle motion in R wave[26]

2.5.8 L wave

Love waves are faster than the Rayleigh waves and particle motion is transverse direction to that of propagation. The love waves cannot be recorded by vertical geophone due to horizontal particle motion.

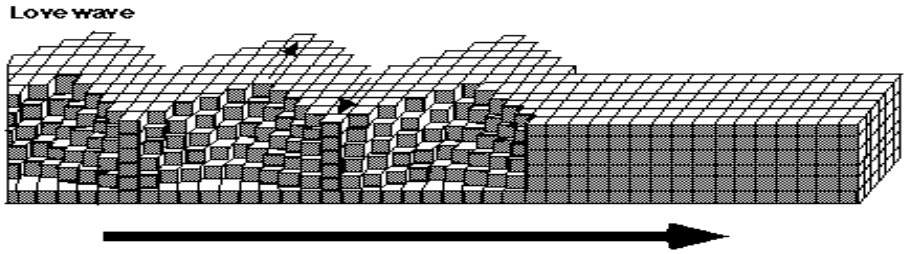

Figure 2.6: shows particle motion in L waves [26]

2.5.9 Ground vibration direction

There are three ground vibrational directions such as

- Transverse
- Vertical
- Longitudinal

Transverse is the horizontal motion of wave at right angle to the blast. Vertical is the up and down movement of the wave. Longitudinal is the horizontal movement along a line between the monitoring point and the blast site.

2.5.10 Peak particle velocity

Peak particle velocity is the maximum particle velocity over total recorded time where the peak vector sum is the resultant particle component. The resultant particle velocity is the square root of sum of individual component of particle velocity. Usually a few blasts are monitored at different distances for ground vibration. The data collected are fitted to model with empirical constants. There exist many propagation equations. The more common equation is given by

$$V = K \times W^a \times R^b \quad (8)$$

Where, V=Ground Vibration (mm/s), W =Maximum charge (kg), R=Distance (m), K, a, b= site constants.

The parameter V is either particle displacement, particle velocity or particle acceleration. Typically the peak particle velocity is the most commonly used parameter and is closely related to damage [27-28]. The actual formula used for peak particle velocity prediction varies considerably and few of those represented below.

The ground wave front form a column charge (L/D>6) is considered as expanding cylinder whose volume varies the square of its radium. It gives the peak ground motion is inversely proportional to the square of distance from the blast point [29]. The equation is

$$V = K(SD)^{-B} \quad (9)$$

Where, V = Peak Particle velocity, mm/s, K = Ground transmission coefficient, B = Specific geotechnical constant, SD = Scaled distance (m/kg)

The site constant for a mine is calculated by regression analysis of the data sets.

Table 2.7: Site constants for a few hard Rock Mines [30]

Type of Mines	Number of blasts	Number of data	K	B	R	Frequency
Iron ore	4	16	66.44	1.17	0.79	3-14
	6	15	100	1.40	0.96	2-15
	3	10	48.60	0.80	0.72	2-16
	13	38	69.30	1.16	0.87	2-20
	26	79	70.30	1.16	0.85	2-20
	260	260	65.75	1.15	0.66	2-30
Copper ore	21	24	303.75	1.54	0.75	5-20
Zinc ore	10	31	211.82	1.42	0.86	11-75

(Where, R = correlation coefficient, k and b are site constant.)

2.5.11 USBM Predictor Equation

The USBM predictor equation [31] shows scaled distance as the function of radial distance and square root of maximum charge per delay. It is denoted as

$$v = K\left(\frac{R}{\sqrt{Q_{MAX}}}\right)^{-B} \tag{10}$$

Where, v =PPV, R=radial Distance and Q= maximum charge per delay.

The site constant value K and B are determined by plotting the PPV and scaled distance in log-log scale.

2.5.12 Langefors-Kilstrom Equation

According to Langefors-Kilstrom [10], scaled distance is the square root of charge per delay divided by two third of radial distance. It is denoted by

$$\upsilon = K\left(\sqrt{\frac{Q_{MAX}}{R^{\frac{2}{3}}}}\right)^{B} \tag{11}$$

The site constant K and B is determined by plotting PPV with scaled distance in Graph.

2.5.13 Ambraseys-Hendron Equation

According to Ambraseys-Hendron [32], scaled distance is the ratio of radial distance to the cube root of maximum charge. The peak particle velocity equation is denoted by

$$\upsilon = K\left(\frac{R}{Q^{\frac{1}{3}}_{MAX}}\right)^{-B} \tag{12}$$

The site constant equation is determined by plotting PPV and scaled distance in log-log scale.

2.5.14 Indian Standard Equation

According to Indian standard [33], scaled distance is the ratio of two third of maximum charge per delay to the radial distance. The PPV equation is denoted by

$$\upsilon = K\left(\frac{Q_{MAX}{}^{\frac{2}{3}}}{R}\right)^{B} \tag{13}$$

The site constant k and B are determined by plotting PPV and scaled distance in graph.

2.5.15 CMRI Equation

Many studies have been carried out to establish an efficient blast vibration predictor based on wave propagation law [35]. The decrease in amplitude of ground vibration was considered as only due to geometrical spreading and was given by [34]

$$V = n + k\left(\frac{D}{\sqrt{Q}}\right)^{-1} \quad (14)$$

Where, Empirical constant 'n' is related to rock properties and geological discontinuities. The other parameter k is related to change weight, distance from blast source, charge diameter, delay interval, burden, spacing etc.[36]. The following table 2.7 shows values of same of site constants as determined in situ [36].

Table 2.8: Values of site constants for Iron ore Mines

Equation	B	K	N	R^2
USBM [29]	1.80138	303.736	-	0.761
LFKH [10]	2.50391	30.0096	-	0.748
AMHEN [30]	1.72116	2471.13	-	0.769
IS [31]	1.87793	30.0096	-	0.748
CMRS [32]	-	91.9117	0.28874	0.845

2.5.16 Zero crossing frequency and Fast Fourier transform frequency

The frequency is the no of times object makes up and down motion in one second. The zero-crossing frequency is the inverse of the time period between two consecutive zero-crossing at the peak. So it is the approximate frequency of the Peak Particle Velocity. Fourier frequency function or FFT (Fast Fourier Transform) to transform the ground motion time domain in to frequency domain.

2.5.17 Wave Propagating velocity and Attenuation

If the bore hole with compressive wave called Ground vibration is a wave motion created from explosive source and the wave propagate at a speed from blasting point is known as propagating velocity. The vibration wave velocity is reduced when wave travel far from originating point called seismic attenuation. Particle motion in ground vibration is similar to floating object in water. The distance between two crest points of a complete wave is known as wavelength. The speed at which the wave moves outward from the originating point or source of disturbance point called propagation velocity and the up down motion of object in water is known as particle motion.

2.5.18 Ground vibration effects on nearby structure

Blasting can cause damage to structure. It does not depend on distance of blast from the structure. It depends upon resonant frequency of structure and vibration frequency.

Damage occurs in residential structure when vibration frequency and resonant frequency matches.

2.5.19 Types of Blast effects

- **Major:** The permanent distortion or damage to structure.
- **Minor:** Only small crack appears in the structure.
- **Threshold:** expansion of previous crack in the structure.

2.5.20 Resonation and Amplification Factor

In blast induced ground vibration, frequency of ground vibration exceed the natural frequency 4 to 10 Hz of structure. As a result structure is resonated. Amplification factor is defined as ratio of amplitude of structure to ground amplitude [37]. The increase in amplitude of the structure with respect to ground amplitude due to transfer of seismic wave from ground to structure is known as Amplification.

2.5.21 Damage effect in terms of Peak particle velocity and frequency

DGMS criterion [38]

Depending upon type of structure and dominant frequency, the peak particle velocity (PPV) should not exceed respective frequency (Table 2.8)

Table 2.9: DGMS guidelines for different structure

Type of Structure	Dominant excitation frequency, Hz		
	<8 HZ	8-25 HZ	>25 HZ
(A) Buildings/Structures not belonging to the owner			
1. Domestic houses/structures(Kuchha, brick and cement)	5	10	15
2. Industrial building	10	20	25
3. Objects of historical importance andsensitive structures	2	5	10
(B) Building belonging to owner with limited span of life			
1. Domestic houses/structures(Kuchcha, brick & cement)	10	15	25
2. Industrial building(RCC and framed structures)	15	25	30

Langefors and Kihilstrom's criterion[10]

Damage effects are described by peak particle velocity, and frequency by Langefors and khilstrom

Table 2.10: Langefors and Kihilstrom's damage criterion for different rock described by peak particle velocity

Damage Effects	**Peak Particle velocity**					
	Sand, gravel, clay below water level; c=1,000-1,500 m/sec		Moraine, slate, or soft limestone; c=2,000-3000 m/sec		Granite, hard limestone, diabase; c =4,500-6,000 m/sec	
	mm/sec	in/sec	mm/sec	in/sec	mm/sec	in/sec
No noticeable crack formation	18	0.71	35	1.4	70	2.8
Fine crack and falling plaster	30	1.2	55	2.2	100	3.9
Crack formation	40	1.6	80	3.2	150	5.9
Severe crack	60	2.4	115	4.5	225	8.9

(Where, c is Propagation velocity in media)

USBM Criterion [31]

The figure 2.6 shows the safe blasting vibration criteria with peak particle velocity from

0.5 to 2 inch/sec having two frequency ranges for residential structure involving frequency, velocity, displacement as proposed by USBM. The lower frequency (>40Hz) has ability to more damage than higher frequency (<40 Hz). The lower frequency ground vibration with 0.75 in/sec and 0.5 in/sec for gypsum board houses and plaster on lath interiors. High frequency with maximum particle velocity 2 in/sec is recommended for all houses.

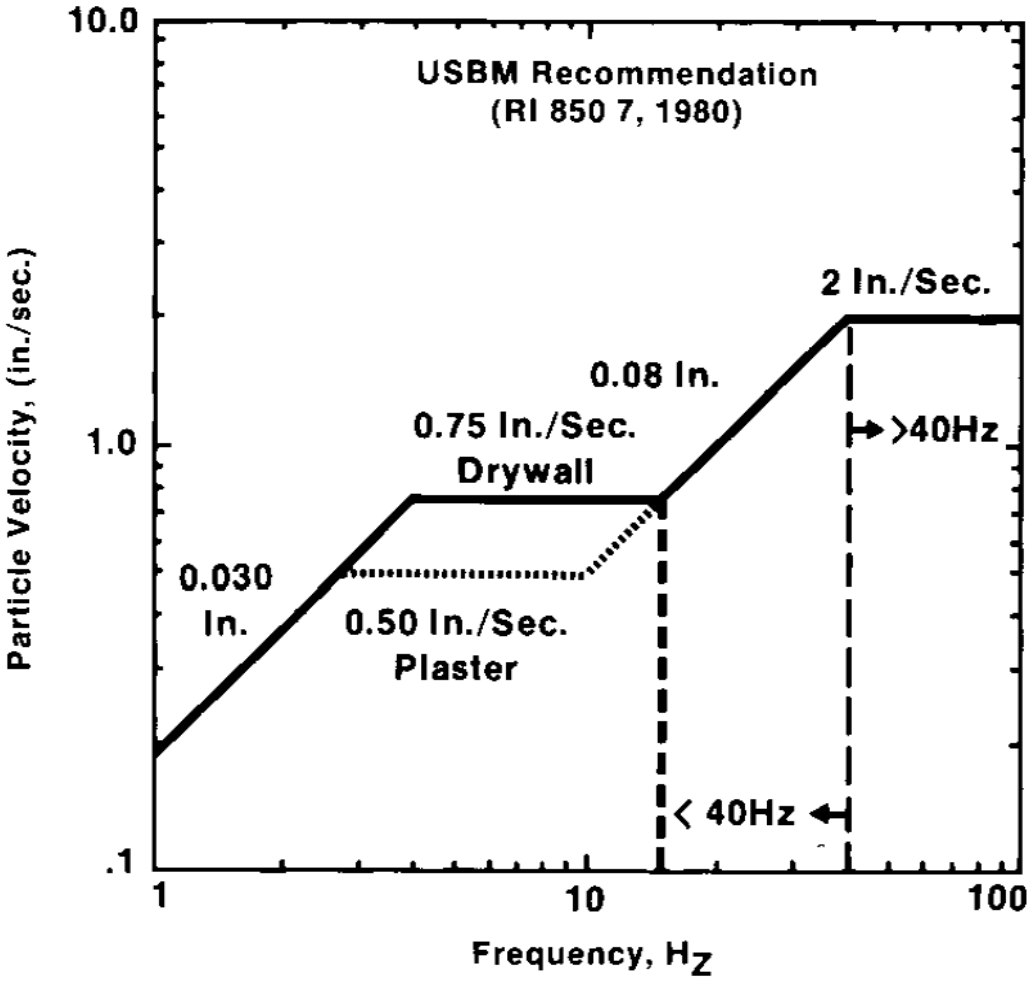

Figure 2.7: Safe levels of blasting vibration of structure[31]

German DIN standard, 4150 [39]

German Institute of standard developed criteria for vibration effects on structures based on peak particle velocity, frequency and type of structures. This criterion is illustrated in table 2.2 [40].

Table 2.11: guideline value of vibration velocity, DIN 4150 [40]

Line	Type of structure	Vibration Velocity (mm/sec)		
		Foundation frequency		
		Less than 10 Hz	10 to 50 Hz	50 to 100 Hz
1	Building used for commercial purposes, industrial buildings and building of similar design	20	20-40	40-50
2	Dwelling and building of similar design and/or used	5	5-15	15-20
3	Structures that, because of their sensitivity to vibration, do not correspond to those listed in lines 1 and 2 and are of great intrinsic value (e.g. building that are under a preservation order)	3	8-10	8-10
• For frequencies above 100 Hz, at least the values specified in this column shall be applied				

2.6 Air overpressure

One of the principal disturbances created by surface blasting is air blast. In the surface blast, a part of the total blast energy escapes in to the atmosphere which is usually above speed of the sound, typically at 300m/sec in normal air [22]. This over pressure wave is atmospheric. It is transmitted away from blast sites in the form of wave that travel at the called Air Blast or Air Over Pressure (AOP) [41]. Noise is the audible and infrasonic part of this wave spectrum from 20 Hz to 20 KHz [42]. Audible air blast is called noise and those inaudible to the human ear are called concussions [43].With detonation of explosives, transient air blast pressure waves get generated that lost for a about second. Cause of air blast was proposed as under [44].

- Rock pressure pulse due to detonation of explosives.
- Escape of gases from the blast hole when the stemming is ejected.
- Escape of gases through the fractures created in the rock masses face.
- Detonation of initiating cord in the open air.
- Displacement of bench at the bench face.
- Collision between projected fragments of rock.

Air blast adversely impacts the house through the roofs, walls and windows of the structures through rarely causing heaving damage [45]. In addition it causes annoyance to the people living around mining areas. The main four reasons are discussed below.

2.6.1 Air Pressure Pulse

Each blast hole acts as (APP) source. From front row blast hole, air pressure pulses are generated and moves forcefully by the help of next rows pulses. But far behind the face, due to dispersion and refraction in pulses loses its APP spikes.

2.6.2 Rock pressure pulse

Rock pressure pulse is generated by vertical component of ground vibration. The relation between Rock pressure pulse (lb/in^2) and vertical component (in/s) is

$$RPP = 0.0015 \times V \quad (15)$$

Where, RPP is Rock pressure pulse and V is the vertical component of ground vibration.

2.6.3 Gas release pulse and stemming release pulse

These pulses depend upon stemming, spacing, burden and detonation velocity. GRP and SRP appear as series of spikes which are superimposed on the APP.

2.6.4 Types of Air noise

Air over pressure is of three types as

- Audible noise (Direct noise)
- Inaudible noise(Combination with ground motion which produce structural motion and produce noise)
- High audible noise (produce crack in windows)

Table 2.12: Noise level and consequence [90]

Sl. No.	Air noise level in (dB)	Description
1	115	Threshold of complaints
2	134	Bureau of mines recommended safe level of blasting
3	140	Historical Proven safe level
4	151	Occasional windows break
5	171	General windows break
6	180	Possible structure damage

The lower frequency portion of the air blast is not audible but excites structures causing secondary and audible rattle within a structure [29]. There are reports also that the response noise within a structure is the source of many complaints [46].

Parameters that influence air over pressure are maximum charge per delay, burden and spacing, detonator accuracy, stemming, charge depth and factors that arise from secondary blasting like weak strata, direction of initiation etc. [21]. However many authors have suggested that the most influential parameters are maximum charge per delay and distance from the blast face [47]. Though there exists several empirical approaches to predict air over pressure the use of cube root scaled distance factor is the most common.

It is given as

$$SD = DW^{-0.33} \quad (16)$$

(Where D = Distance (m), W = explosive charge per weight (Kg), SD = Scaled distance (Kg/m^3))

The predictor equation takes the form of

$$AOP = H(SD)^{-B} \tag{17}$$

Where, AOP is air over pressure (dB), H and B are site factors. The site factors, H and B as defined for same blasting condition are given below (Table 2.12)

Table 2.13: Site Factors as developed elsewhere[21]

References	Description	H	B
Siskind *et al.*[48]	Quarry blasts, behind face	622.000	0.515
	Quarry blasts, direction of initiation	19,010.000	1.120
	Quarry blasts, front of face	22,182.000	0.966
Hopler [49]	Confined blasts for AOP suppression	1906.000	1.100
	Blasts with average burial of the charge	19,062.000	1.100
Hustrulid [22]	Detonations in air	185,000.000	1.200
Kuzu *et al.* [45]	Quarry blasts in competent rocks	261.54.000	0.706
	Quarry blasts in weak rocks	1833.800	0.981
	Overburden removal	21,014.000	1.404
Hajihassani *et al.*[50]	Quarry blasts, front of face(distance of 300 m)	10,909.000	1.090
	Quarry blasts, front of face (distance of 600m)	959.480	0.450

Kahriman [51] investigated about 73 blast events in a limestone mine and developed a relation as below with correlation coefficient of 0.72.

$$PPV = \left(340 \times \frac{R}{\sqrt{W}}\right)^{-1.79} \tag{18}$$

Where, PPV = peak particle velocity, R = Distance, W = maximum charge per delay.

Khandelwal *et al*. [52] predicted the peak particle velocity (PPV) by using few important and widely used predictors and computed results are compared with actual field data. The same input–output data sets have been also used for the prediction by artificial neural network (ANN).

Uysal [53] found that ground vibration decreased when burden increased. He also observed that correlation coefficient increased when particle velocity decreased with respect to increased burden.

Nateghi [54] predicted ground vibration induced by blasting near underground and surface excavation. He considered different rock formation, detonator and explosive for prediction of peak particle velocity prediction. Also he analyzed scaled distance and peak particle velocity statistically from 498 events that recorded from 216 blast shots. Then he

analyzed particle velocity and frequency according to measure level to the neighbouring concrete structure based on equation

Where v = peak particle velocity, SD = scaled distance, R = Distance, Q = maximum charge per delay. He found dynamic site factor K and B changes from 170-660 and 0.87-1.71 for Aghajhari formation where 350-420 and 0.95-1.63 for Bhaktiary conglomerate site.

Sasastojadinovic *et al.*[55] Established relation between peak particle velocity of ground vibration and residual deformation of structure. They measured total 10 PPV data from six locations, during four blasts. They develop an equation for peak particle velocity at 50% confidence interval was

$$PPV = 33613\left(\frac{R}{\sqrt{Q}}\right)^{-1.2997} \tag{21}$$

Also they established a relation between PPV and residual deformation was

$$\frac{\Delta S}{S} = f(V_{50}) \tag{22}$$

Dehghani and pour [56] studied blast vibration at copper mines in Iran. The Sarcheshmeh copper ore mine is situated 160 km southwest of Kerman and 50 km south of Rafsanjan city, Kerman province, in $55^0$52’ 13” longitudes and $29^0$15’ 70” latitude. The mine is at 2500 m above sea level. They used back propagation algorithm for prediction of PPV and used a mathematical model in which vibration is a function of most important parameters such as powder factor, charge per delay and burden.

Caylak [57] investigated rock mass properties and directional vibration by using different geophysical methods such as electrical resistivity, seismic reflection and multi-channel analysis of surface wave. They considered seismic S wave, P wave velocity, electrical resistivity and sending information for alluvium, clay limestone and found that these geophysical properties were vary from place to place. They evaluate the structure hazard parameter such as frequency; acceleration and particle velocity with respect to geophysical properties vary from place to place. They evaluated the structural hazard parameter such as frequency, acceleration and particle velocity with respect to geophysical properties. They found that ground vibration show different spreading properties in different location and different hazard risk depending on the geological structure of the region.

Hosseini and Baghikhani [58] measured ground vibration components for 78 blast events in order to predict PPV for the site over a period of 12 months. A seismograph and analysis software (Siesmowin software) was used in this study. Seismograph analyse blast vibration with an integrated tri-axial geophone. Each transducer measured velocities on

three mutually perpendicular axes (V_x, V_y, V_z). PPV is the resultant of V_x, V_y, V_z. They used predictor equation such as USBM, Ambraseys–Hendron and Indian Standrad Equation to predict PPV value. Among all, USBM equation shows more correlation coefficient of 0.8858 with empirical factors such as

$$PPV = 129.6\left(\frac{R}{\sqrt{Q}}\right)^{-1.7792} \quad (23)$$

Mandal [59] carried out experiment on wide blast geometry (burden and spacing) with respect to depth blast holes and location of measurements i.e. measurement made at higher altitude (grater vertical distance) with respect to horizontal distance from vibrating source and found higher vertical component than longitudinal and orthogonal component. He concluded that vertical component generate more stress on structure.

Sailu *et al.* [60] found relation between blast efficiency of explosive and uniaxial compressive strength of calcite, dolomite and granite. They found compressive strength for granite (133.55 MPa), calcite (78.91 MPa) and dolomite (71.17 MPa) respectively.

They observed that with decrease in blasting efficiency, uniaxial compressive strength increase.

Choudhary and Sanu[61] predict uniaxial compressive strength of rocks on powder factor using Schmidt rebound number of rock mass. They observed that powder factor increases as rebound value or uniaxial compressive strength increases.

Mohan and Dey [62] experimented with a wide range of charge per delay i.e. from 0.025 kg to 500 kg over a distance varying from 0.5 m to 1km. They predicted PPV equation as

$$PPV = 7972\left(\frac{D}{W^{\frac{1}{2}}}\right) \quad (24)$$

Karkar and Rathore [63] carried out investigation in two iron ore blocks and studied sixteen and fourteen blast holes respectively. They determined the relation between PPV, distance and explosive for sixteen blast holes as.

$$PPV = 161.1 \times (SD)^{-0.928} \quad (25)$$

For fourteen blast holes, the equation obtained was

$$PPV = 112 \times (SD)^{0.785} \quad (26)$$

2.7 Rock Fragmentation

Rock fragmentation is the process where large volume of rock mass converts to small pieces during blasting with explosive. At the time of initiation of explosive, a large amount of energy is released through chemical reaction which causes breakage in rock by

high pressure gases .The amount of gases produce exceed 10 GPa [10]. The shock wave produces from instantaneous pressure that travels at a speed of 3000-5000m/s. The high Pressure not only expands the wall of the hole but also shatters the adjacent area of drill hole due to vast amount of tangential strain and stresses [64]. Due to high travelling speed of shock wave, initial crack forms in the rock within millisecond. The shock wave positive value falls to negative value resulting compression wave to tangential wave when compression wave reflects from free face. During first stage, radial cracks occur. In second stage, scrabbling occurs which means the radial cracks occur by compression stress expands due to tensile stress. In third stage, last breakage occurs due to high pressurized gases produced by blast in which expanded cracks separated from each other.

2.7.1 Mechanical properties of rock mass affect fragmentation

Rock fragmentation mainly depends upon compressive strength and tensile strength. Crushing and grinding of rock is done by static loading of rock. But in case of blasting, rock fragmentation occurs due to both static and dynamic loading through explosive reaction.

2.7.1.1 Prediction Equation of fragmentation

The relation between the mean fragmentation size and powder factor has been expressed by Kuznestov [65] as a function of rock type such as

$$\overline{X} = A(\frac{V_o}{Q_T})^{0.8} Q_T^{1/6} \tag{27}$$

But Cunningham [66]modified above Kuznestov equation as

$$\overline{X} = A(\frac{V_o}{Q_T})^{\frac{4}{5}} Q_T^{\frac{1}{6}} (\frac{S_{ANFO}}{115})^{\frac{-19}{30}} \tag{28}$$

Where, $\overline{X}$ = Mean fragmentation size(cm), A = rock factor = 7 for medium rock,10 for hard, V_0 = Rock volume(m^3), Q_T = mass of explosive (Kg) and S_{ANFO} = relative weight strength of explosive to ANFO(ANFO=100).

Gheibie *et al.* [67] analysed the data from sungun mines and proposed equation to predict ROM size distribution. The Rosin-Rammler function is used as the size distribution with X_m as central parameter and n', as the uniformity index:

$$X_m = 0.073BI\left(\frac{V_0}{Q_e}\right)^{\frac{4}{5}} Q_e^{\frac{1}{6}}\left(\frac{S_{anfo}}{115}\right)^{\frac{-19}{30}} \tag{29}$$

$$n' = 1.88 * n * BI^{-0.12} \tag{30}$$

Where, X_m = the mean fragment size (cm), V_0 = the rock volume broken per blast hole (m^3), Q_e = the mass of explosive being used (kg), S_{anfo} = the relative weight strength of the explosive to ANFO (ANFO = 100), n' = modified uniformity index, n = uniformity index (Cunningham) and BI = Blastability index.

Bahramiet *et al.*[68] adopted Cosine amplitude method (CAM) to identify the most sensitive factors affecting rock fragmentation. In this method, all of the data pairs are expressed in common X-space. The data pairs used to construct a data array X defined as:

$$X = \{x_1, x_2, x_3, \ldots\ldots x_m\} \tag{31}$$

$$X_i = \{x_{i1}, x_{i2}, x_{i3}, \ldots\ldots x_{im}\} \tag{32}$$

Each of the elements, Xi, in the data array X is a vector of lengths of m, that is:
Thus, each of the pairs is a point in m-dimensional space, where each point requires m coordinates for a full description. Each element of a relation, r_{ij}, results in a pair wise comparison of two data pairs. The strength of the relation between the data pairs, x_i and x_j is expressed by the following membership function:

$$\frac{\sum_{k=1}^{m} x_{ik} x_{jk}}{\sum_{k=1}^{m} x^2_{ik} \sum_{k=1}^{m} x^2_{jk}} \tag{33}$$

The most effective parameters on the fragmentation are blastability index (G), charge per delay (J), burden (C), SMR (F) and powder factor (E).

2.8 Flyrock

Flyrock is important issue for blaster. Injuries due to flyrock was 68% of all blasting related injuries in surface coal, metal and nonmetal mines between the period from 1978 to 2001 [69]. Flyrock is defined as the rock propelled by the force of explosion generated from explosive in confined form in blast hole beyond the blast hole [70]. According to [71]three tons of flyrock travels a distance of 980 ft. during blasting. When explosive is detonated in blast hole, high pressure energy with gas energy is generated. The pressure is the cause of fragmentation while high pressure is responsible for bursting of rock masses from the bench. Fly rock is generated due to mismatch of the distribution of explosive energy, type of confinement of explosive charge and mechanical strength of explosive energy.

2.8.1 Factor causing the mismatch

- Change in the rock resistance due to presence of joints, cracks, layers of mud, slit and soft material in the host rock.
- High explosive concentration causes migration of explosive charge in to fissures, voids and mud seams.
- Deviation of blast holes causing radiation in burden and spacing.
- Improper stemming.
- Poor blast design

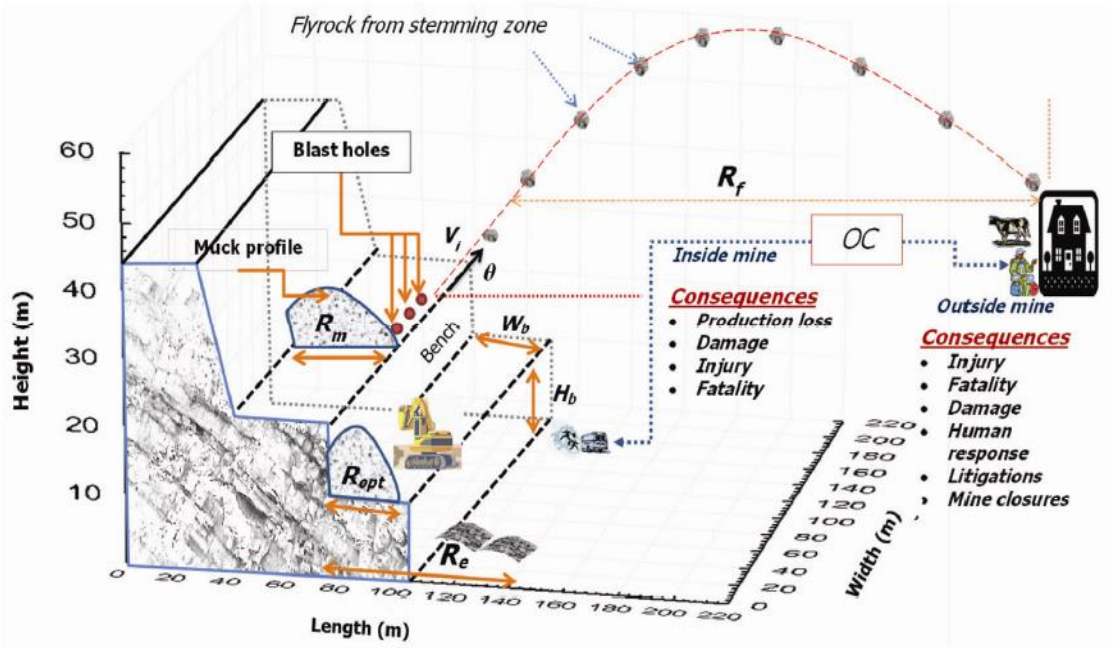

Figure 2.8: Diagram of flyrock [72]

Bajpayee *et al*. [73] carried on investigation on flyrock generated from rock blasting in surface mines. They mentioned injuries due to flyrock and lack of blast area security was 68% of blast injuries in surface coal, metal and non-metal mines during the period 1978-2002. They emphasised on mitigating techniques to reduce blasting related fly rock accident by implementing the proper blasting techniques.

Raina *et al.*[72] predicted a model based on kinematic equation to find out flyrock initial velocity, distance and shape of the fragments. They explained flyrock would be generated due to mismatch of energy generated from explosive with rock strength. They also explained high explosive energy generated high pressure gases emanating of blast hole in the direction of weakest zone causes excessive throw of flyrock.

Trivedi *et al.*[41] predicted blast induced flyrock by using neural network. They specified blast design such as burden, inadequate stemming length, improper drilling, very high explosive concentration, inappropriate delay timing, their sequence, back breaks and loose rock on the top of the bench due to poor previous blasts causes flyrock during their investigation. They used blast design parameters unconfined compressive strength (UCS) and rock quality designation (RQD) as input parameter in ANN and multivariate linear regression analysis (MVRA) to predict flyrock distance.

2.9 Fundamental of Neural network

2.9.1 Biological Basis of Neural Networks

The human brain is a very complex system in terms of thinking, remembering and problem solving .There have been many attempts made to compare the brain function with computer model. As a result some spectacular achievements have been made from

all the attempts. In brain nervous system, a neuron is the part of cellular unit. The path in which a neuron receives and combines signal from other neuron is called dendrites. The neuron produce an output signal along the axon that connects the dendrites with many other neurons if combined input signal is strong enough. An infinitesimal gap in the dendrite that is filled with neurotransmitter fluid that either accelerates or retards the flow of electrical charges through which signals passes is called synapse or synaptic junction. These signals are coming from neuron along a dendrite. The neurotransmitter fluid produces electrical signals that go to the nucleus or soma of the neuron. The adjustment of infinitesimal gap helps memory of brain to 'learn' and stores information. The human neural network contains few thousand artificial neurons and less than a million artificial synaptic junctions.

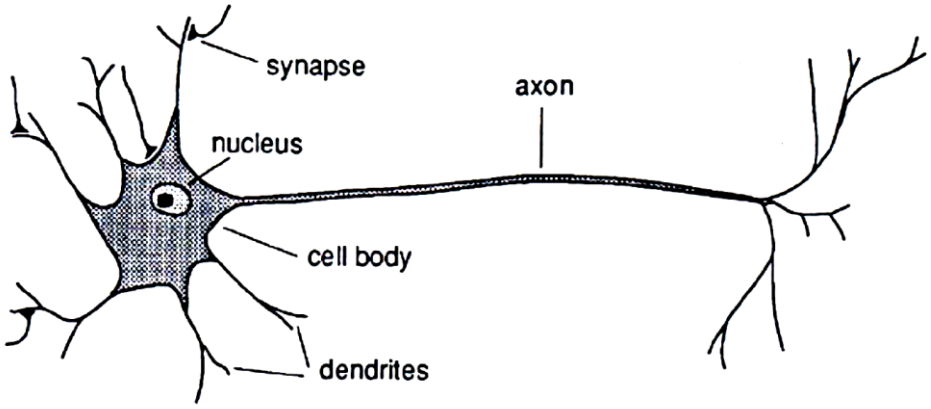

Figure 2.9: Diagram showing neuron of human brain [74]

2.9.2 Artificial Neurons

An artificial neuron is a model which directs analogs to the components of actual neuron. The artificial neuron is first introduced by [75]. The inputs signals are represented by $X_0, X_1, X_3, \ldots\ldots\ldots\ldots, X_n$ .The signals are continuous rather than discrete variable (means discrete electrical pulses in the brain). Each input are initialized by weight (known as synaptic weights) whose function is analogous in abiological junction. These weights are either positive or negative depending upon the acceleration and inhabitation of the flow of electrical signals. The whole process occurs in two parts; such as in first process Aggregate of weighted input signals are resulting a quantity,

$$I = \sum_{i=1}^{n} W_{ij} X_i \tag{34}$$

the second part is called activation function through which combined signals flows [76]. Generally the activation function is a continuous function that falls between two asymmetric values typically 0 and 1;-1 and+1 called sigmoid function. The activation function is the logistic function represented by equation

$$f(I) = \frac{1}{1+e^{-\alpha I}} \tag{35}$$

The logistic function is shown in Figure 2.9

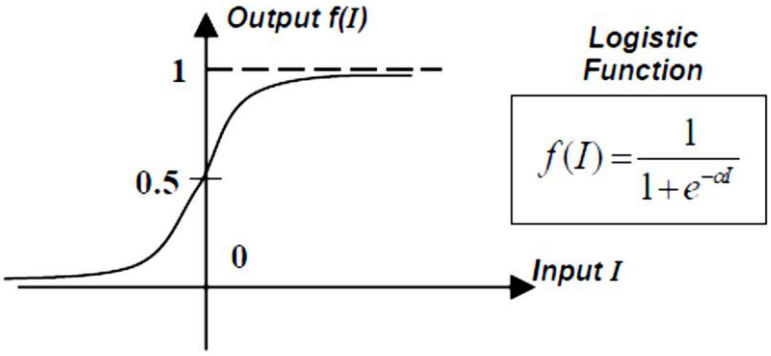

Figure 2.10: Activation function of neurons [74]

2.9.3 Artificial neural network

Artificial neural network can be defined as a large number of inter connected processing element called neurons in an architecture similar to the structure of the cerebral cortex of the brain [74].

The architecture consists of input layer, hidden layer and output layer as shown in the figure.

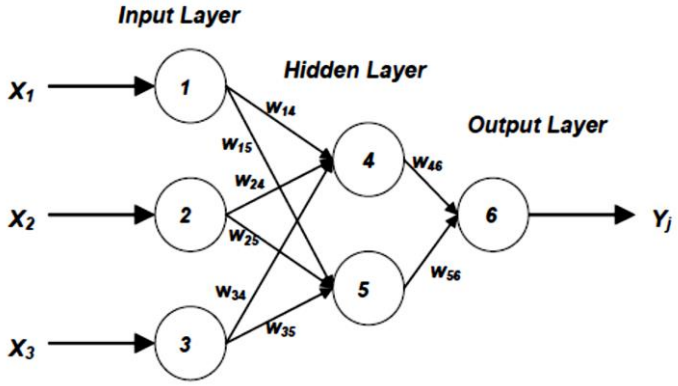

Figurer 2.11 : Architecture of artificial neural network [74]

2.9.4 Back propagation neural network and its error

Neural network gives the data by examining and mapping the inter relationship. The data given by neural network is predicted data. An ANN consists of highly inter connected simple information processing element called neuron or perception. The feed forward neural network is formed by several layers of simple computing neurons or perceptions. A particular network either input or output contain one or more layer in which two or more perception can be combined. The network consists of three layers such as input layer, hidden layer, output layer. Feed forward neural network are special kind of ANN, in which

inputs are received and simply forward through all the next layers (hidden layer) to obtain the output. Here output is compared with measured value. The difference of error between both is called bias which proceed back through the network (backward pass) updating the individual weights of the connection and also biases of individual neurons. All the neurons in the back propagation neural are associated with a bias neuron and a transfer function. The transfer functions are step functions. Those are either linear or non-linear functions designed to map a neurons' or layers' net output to its actual output. This process is repeated for all training pairs in the data till the network error reached to a minimum threshold value defined by a cost function usually the root mean squared error or summed squared error. The following algorithm is typically used for construction of neural network.
The j^{th} neuron is connected with a number of inputs as

$$X_i=(X_1, X_2, X_3, \ldots\ldots\ldots X_n) \tag{36}$$

The *Net* input values in the hidden layer is

$$Net_j = \sum_{i=1}^{n} X_i W_{ij} + \alpha_j \tag{37}$$

Where, X_i is n^{th} no of input units, W_{ij} is the connection between i^{th} neuron of input layer and j^{th} neuron of hidden layer;α_j is the bias neuron.
Usually the calculation of output in the hidden layer is determined with the logarithmic sigmoid function which is non-linear and is defined as

$$f(Net_j) = \frac{1}{1+e^{-Net_j}} = O_j \tag{38}$$

Where, $f_{(Netj)}$ is the weighted sum of inputs for a processing unit of output layer.
In the learning process, the network is presented with pair of patterns; an input pattern and corresponding desired output pattern. The network computes output pattern by using weights and threshold value. The error at any output layer k is determined between the actual output and desired output as

$$e_i = i_k - o_k \tag{39}$$

The total error is given by

$$E = \sum e_i^{\,2} \tag{40}$$

The decent down error surface is made using following rule for optimum weight space of the network,

$$\delta w_n = -n \times \frac{\delta E}{\delta w_n} \tag{41}$$

Where n is the learning rate parameter; W_n is the weight of the connection between the i^{th} neuron of the input layer and the j^{th} neuron of the hidden layer; i^{th} is the actual output; o_j is the desired output.

The update of the weight for the $(n+1)^{th}$ pattern is given as

$$W_n(n+1) = W_n(n) + \delta W_n \tag{42}$$

The connection between the hidden and output layer follows the similar logic. But in the above case linear transfer function is used. Total input in K^{th} unit of output layer is given by

$$Net_k = \sum_{j=1}^{n} W_{jk} O_j + \alpha_k \tag{43}$$

The predicted value by linear transfer function from K^{th} unit is

$$f(net_k) = n \tag{44}$$

Where, W_{jk} is the weight between j^{th} neuron of hidden layer and K^{th} neuron of output layer; α_{th} is the bias neuron; n is predicted value. The process is repeated till the user specified error or epoch goal is reached.

2.10 Multiple regression Analysis

Multiple regression analysis is used to predict linear relationship between a dependent variable and one or more independent variable. It is based on the principle that minimized sum of squares of differences of predicted and measured value and is given by

$$Y = b_0 + b_1 x_1 + b_2 x_2 + ... + b_n x_n + \beta \tag{45}$$

Where, b_0 = intercept, β = error associated with predictor and b_1, b_2, b_3 are coefficient on the n^{th} predictor.

Monjezi *et al.*[77] analysed fragmentation size at Gol-E-Goher iron ore mine by using regression analysis and fuzzy interference system. They considered burden, spacing, hole depth, specific drilling, stemming length, charge per delay, rock density and powder factor as input parameter and fragmentation as output parameter. The result of R^2 and

RMSE value found by them for fuzzy model were 0.96 and 3.26 respectively whereas 0.80 and 6.83 for regression model.

Bahrmi *et al.*[68] implemented ANN to develop a model to predict rock fragmentation in blasting in iron ore mines. They incorporated eight parameter hole diameter, average hole depth, burden, spacing, powder factor ,SMR, blastability index, specific drilling,

stemming length, charge per delay as input parameter. From the model they found that 10-9-7-1 architecture gives optimum R^2 and RMSE value as 0.97 and 0.56.

Monjezi *et al.* [78]predicted fragmentation size by developing a model using artificial neural network in sercheshmech copper mine. For construction of model, they considered burden to spacing ratio, hole diameter, stemming, total charge per delay and point load index as input parameter. They concluded that the model with architecture 9-8-5-1 gives RMSE 0.995 and R^2 of 0.985 as optimum value.

Saydi *et al.* [79] used back propagation neural network (BPNN) and radial basis functional neural network(RBFNN) for prediction of rock fragmentation and back break in limestone mines, Iran. They found that (BPNN) network with architecture 6-10-2 is found to be optimum whereas RBFNN with 6-36-2 with spread factor provides maximum prediction aptitude. So the BPNN model is most preferable model providing maximum accuracy and minimum error.

Mohammadnejad *et al.*[80] adopted novel artificial method, called a 'Support Vector Machine' (SVM) for the prediction of blast-induced ground vibration by taking into consideration the maximum charge per delay and the distance between the blast face and monitoring point. Two limestone quarries have been studied through this research. The results showed a correlation coefficient of 0.944 which has been obtained by comparing measured and predicted values.

Armaghani *et al.*[81] predicted environmental impacts such as peak particle velocity, Air over pressure and fly rock by using two intelligent system such as artificial neural network(ANN) and adaptive neuro fuzzy inference system (ANFIS) at four granite quarry in Malaysia. They investigated total 166 blasting operations to predict PPV, AOP and fly rock. For ANN and ANFIS, they took burden to spacing, stemming length, powder factor, maximum charge per delay, Distance from blast face as input parameter and PPV, AOP and fly rock as output parameter. They found that coefficient of regression (R^2) values of 0.939, 0.947 and 0.959 while 0.771, 0.864 and 0.834 using ANFIS and ANN for prediction of PPV, AOP and fly rock. So they concluded that ANFIS is better than ANN.

Ghoraba *et al.*[82] predicted the ground vibration by artificial neural network at Gol-E-Ghoar iron ore mines, Iran. From total 115 vibration dataset, they used 80% (92 data set) for training; remaining 20% data set for testing for construction of network. They also used the empirical equation for prediction of peak particle velocity (PPV) and found that coefficient of correlation and root mean square error were 0.662 and 14.922 for USBM equation; 0.982 and 3.371 for ANN model. So they found best fit curve for ANN model rather than USBM prediction.

Saadat *et al.*[83] used ANN based approach to predict ground vibration in Gol-e-Gohar iron ore mine. For the prediction they used 65 monitored PPV event in four layer feed

forward back propagation multilayer perception (MLP) algorithm and also in empirical prediction equation.

Hajihassani *et al.*[81] predicted ground vibration by artificial neural network which was optimized by imperialist competive algorithm (ICA).They monitored 95 blastevent(PPV) value in a granite quarry in Malaysia. During prediction they found that ANN was able to fit curve at R^2 =0.911whereICA model fit curve at R^2 =0.976.

Armaghani *et al.*[84] predicted environmental impacts such as peak particle velocity, Air over pressure and fly rock by using two intelligent system such as artificial neural network(ANN) and adaptive neuro fuzzy inference system (ANFIS) at four granite quarry in Malaysia. They investigated total 166 blasting operations to predict PPV, AOP and fly rock. For ANN and ANFIS, they took burden to spacing, stemming length, powder factor, maximum charge per delay, Distance from blast face as input parameter and PPV, AOP and fly rock as output parameter. They found that coefficient of regression (R^2) values of 0.939, 0.947 and 0.959 while 0.771, 0.864 and 0.834 using ANFIS and ANN for prediction of PPV, AOP and fly rock. So they concluded that ANFIS is better than ANN.

Ghoraba *et al*. [82] predicted the ground vibration by artificial neural network at Gol-E-Ghoar iron ore mines, iran. From total 115 vibration dataset, they used 80% (92 data set) for training; remaining 20% data set for testing for construction of network. They also used the empirical equation for prediction of peak particle velocity (PPV) and found that coefficient of correlation and root mean square error were 0.662 and 14.922 for USBM equation; 0.982 and 3.371 for ANN model. So they found best fit curve for ANN model rather than USBM prediction

Chapter 3

Site Description, Field Work

3.1. Site Description

Iron ore mine of Koira and Daitari region are opencast mines and occupies 90 and 1812.99 hector each respectively. Iron ore mine of Koira region is situated under the jurisdiction of koira, Nuagon, Kadodihi and Harishchandrapur, Tehsil Bonai, Sundergragh District Odisha, Where iron ore mine of Daitariregionis situated underthe jurisdiction of Rubana RF, Daitari RF and talpada village, District of Jajpur and Keonjhar (Odisha). The production is achieved by these two mines through drilling, blasting, loading and hauling.

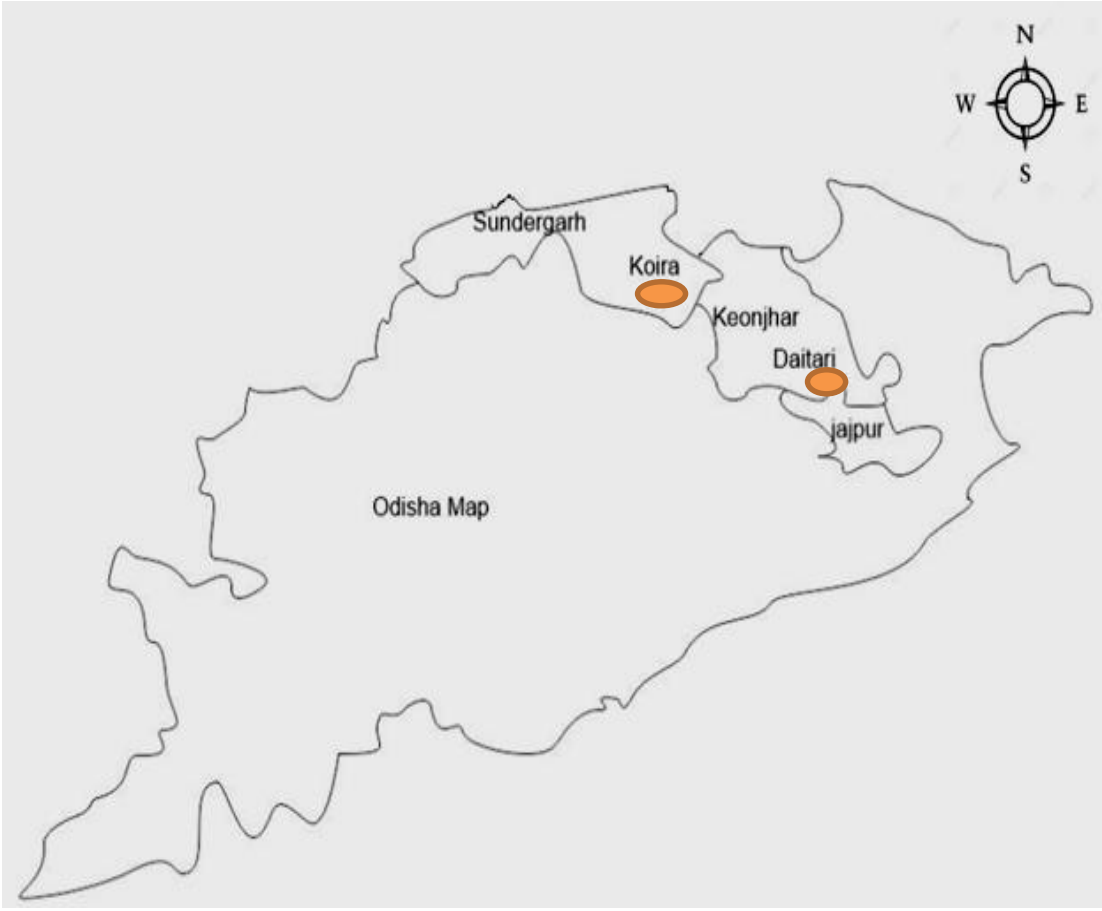

Figure 3.1: Geological location of Koira and Daitari Regions

3.2. Geology

3.2.1. Iron ore Mine of Koira Region:

The Mine site is located at Koira with an average elevation of about 560 - 630 m in northern eastern peak and 570m to 610m in south western peak. The site falls between latitude 21^0 53' 40" to 21^0 54'20" N and longitude 85^0 13' 20" to 85^0 14' 00". The average altitude of the mine area is about 590 m above mean sea level (MSL).The exposed iron ore deposit of Koira group of rocks belongs to Pre-Cambrian age. The iron ore group is represented by basic volcanic, pyroclastices, banded iron ore formation, maganiferous shale/phyllite, sand stone, conglomerates. The Koira Iron ore mine area, of Jamada-Koira valley, exhibit a synclinorial structure, generalized as a NNE trending low plunging syniclinorium with an over turned western cross fold (IC, 2002). The Precambrian Iron Ore Group (IOG) largely contains BIF in addition to the other volcano-sedimentary rocks forming a significant portion of the Singhbhum–North Orissa Cartoon of eastern Indian shield [85]. The major part of the mine does not have top soil. The thickness of the top soil in the mining area is minimum. The Alluvium, yellowish brown in colour, is the top most cover and typically occurs in the western part of the leased boundary. At some places lateritc cover was found. It consists of pebbles of rounded to sub rounded iron ores cemented together in a semi hard lateritic matrixes. Lateritic ore is the dominant texture of the mines. It occurs below laterite and is radish brown to brown in colour that is hard to friable in nature with few portions showing lumpy iron ore. In the NW area conga with iron occurs soft to medium hard. At places loose ruri type iron ore occurs in scatter manner. Massive iron ore is not found. Shale a light yellow to yellowish material also occurs at the bottom shale and ferruginous shale in between main iron ore body as patches. The schematic layout of lithological sequence is given Figure 3.2.

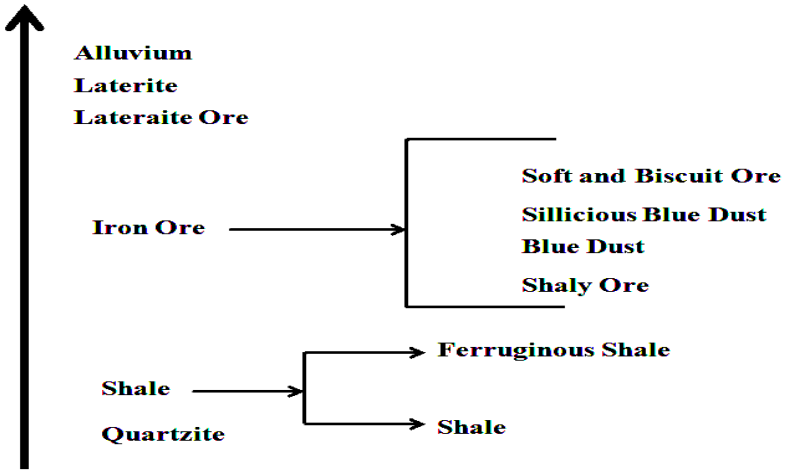

Figure 3.2: Schematic Layout of the Lithologial Sequence of Iron Ore Mine of Koira region

The main iron ore bearing area also consists of blue dust, soft and biscuit ore as well as shaly iron ore. These are of wide variation in physical and mechanical properties.

3.2.2. Iron Ore Mine of Daitari region:

The mine site is located at Daitari with an average elevation of about 840 m. The site falls between latitude 21.633 to 85.583 longitude. Daitari iron ore deposit, a part of a Tomka-Daitari-Kalisagar-Rebana-Harichandanpur basin (Daitari Basin, BIF-2). Banded iron ore formation of Daitari belongs to older proterozoic age. Iron ore formation of Daitari-Tomka basin overlies the granitic basement with an unconformity. The lithology of the area is as below

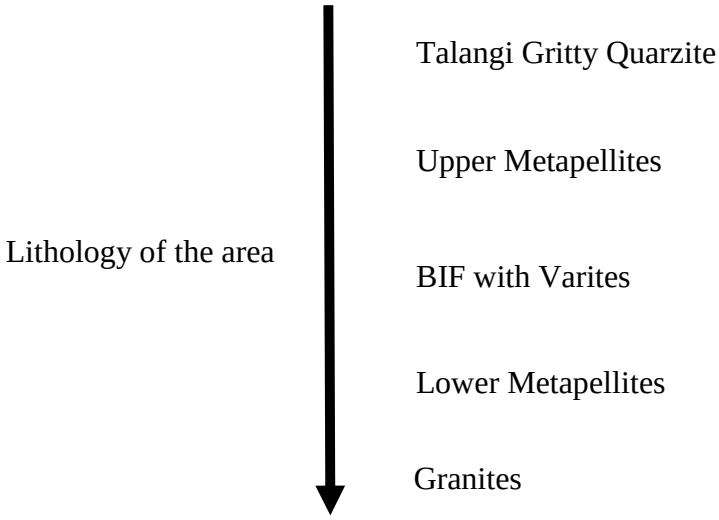

The rocks are highly metamorphosed to green schist facies and intruded by the Chromite bearing Ultramafics of Sukinda. The rocks are typically considered as parametamorphites. Rocks are sedimentary but synsedimentary volcanism also exists in both pre and post BIF stage. Iron ore formation of Daitari-Tomka represents an overturned anticline where the Talapada valley forms the core of anticlinal structure. Sindurmundi hill and the Baghiathali ridge make the southern limb and northern limb of the anticline respectively. Both the limbs strike almost E-W and dip southerly by 62-720.

Daitari iron ore deposit is an isolated deposit forming a conspicuous ridge along the district boundary between Keonjhar and Jajpur towards the north of Sukinda Chromite belt. The lithology of iron ore formation consists of Talangi Gritty quartzite, upper metapellates, BIF with variants, lower Metapellaites, Granites. Stratigraphy of the Daitari area based on various litho units given in Figure 3.3. The iron ore formation of daitari consists of three layer such as upper metapellites (phyllites, ferruginous shale, slate, tremolite-actinolite schist, dolerite with feldspar porphyry etc.); Middle sedimentary

(Banded hematite and chert and its variants and iron ore etc.); and Lower metapellaites (Mn-phyllite, periodite, banded phyllite, pillow lava, quartzite, chlorite, yellow shale.

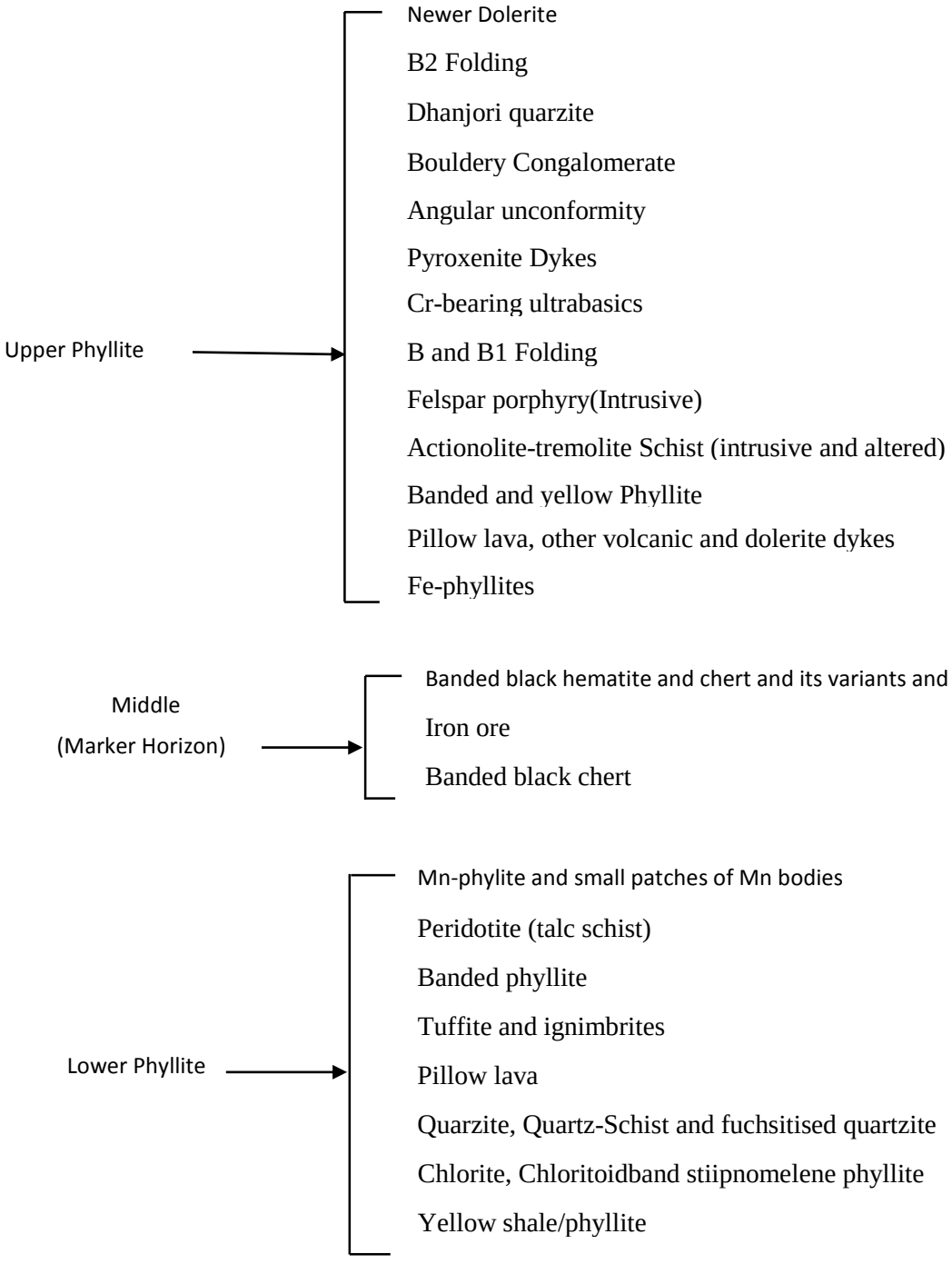

Figure 3.3: Schematic Layout of the Lithologial Sequence of Iron Ore Mine of Daitari region

3.3. Blasting Method Used In Respective Mines

3.3.1. Drilling and Blasting

Drill holes of 102 mm and 100mm diameter holes drilled for iron ore mines of Koira and Daitari region respectively. The explosive used by miners for blasting were Aquadyne, Toe blast, Energel and Supergel.

Table 3.1: Some Properties of Explosives

Sl. No.	Properties	Aquadyne	Toe Blast	Energel	Supergel
1	Sensitivity	Cap sensitivity	Cap sensitivity	Non cap sensitivity	Non cap sensitivity
2	Density	1.2	1.2	1.15	1.15
3	Detonation velocity	4200	4200	3800	3800

3.3.2. Blasting Parameter:

The blast design is used for bench blasting based on blast parameter. The parameters are bench height, hole diameter, hole depth, burden, spacing and stemming, type of explosive, firing pattern and sequence and amount of charge per delay. In below table, all blasting parameters are given for iron ore mine of Koira and Daitari region respectively. The Daitari mine in one instance used a total of 911.84 kg in a series blasting with 15 hole by connecting with cord relay at a time. The figure is joint a representative and does not show the actual blast.

Table 3.2: Blast parameter of Iron ore mine in Koira region

Sl. No.	Parameter	Details	
1	Drilling	Drilling pattern	Staggered
		Spacing(m)	3-4.5
		Burden(m)	2.5-3.5
		Hole diameter(mm)	102-165
		Hole depth(m)	4-9
		Stemming(m)	2-3.5
		Hole dip angle(0)	85-90
2	Explosive	Explosive type/Make	Cartridge/ Idl explosives ltd
		VOD(m/s)	3500-4200
		Density(g/cm^3)	1.2
		Relative Wt strength	82-114
3	Blasting	Sequence	Diagonal/v-pattern
		Time period of delay(ms)	17/25/42
		Charge per delay(kg)	11.12-44.48
4	Detonator	VOD(m/s)	2000

Table 3.3: Blast parameter of Iron ore mine in Daitari region

Sl. No.	Parameter	Details	
1	Drilling	Drilling pattern	Staggered
		Spacing(m)	3-4.5
		Burden(m)	2.5-3.5
		Hole diameter(mm)	100-102
		Hole depth(m)	4-9
		Stemming(m)	1.5-2.5
		Hole dip angle(0)	85-90
2	Explosive	Explosive type/Make	Cartridge/ Idl explosives ltd
		VOD(m/s)	3500-4200
		Density(g/cm^3)	1.2
		Relative Wt strength	82-114
3	Blasting	Sequence	Series
		Time period of delay(ms)	17/42
		Charge per delay(kg)	19.48-911.84
4	Detonator	VOD(m/s)	2000

Diagonal and V-Pattern Blast Conducted in Iron Ore Mine of koira region

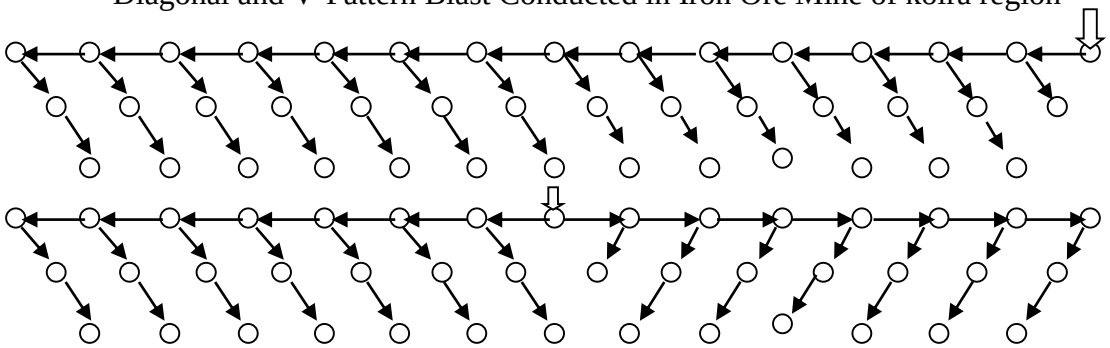

(Series Blast (shown in red arrow) Conducted in Iron Ore Mine of Daitari region)

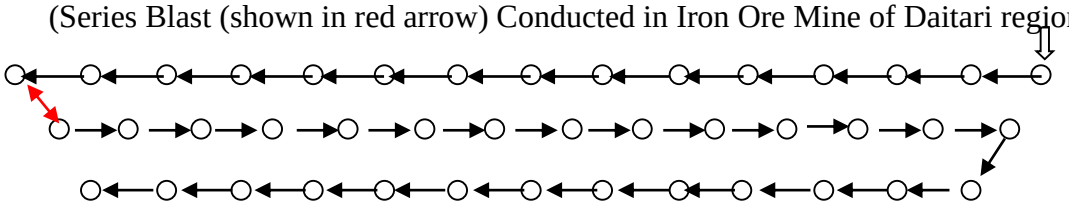

3.4. Field work for research

The site investigations were conducted in two mines for measuring the peak particle velocity and air noise. Also for fragmentation analysis, different image of fragmentation of rock pile after blast were captured. Two seismographs (one minimate and another minimate plus) was used for monitoring ground vibration and air noise. For data

collection one seismograph was placed in front of blast site and the other was placed besides the blast face. The specification of seismograph is summarized below.

- Two seismographs are portable and used for both vibration and air noise.
- It can be used in single shot or a continuous mode.
- Minimate has one geophone and one microphone with four channel but minimate plus has two geophone and two microphones with eight channels.
- The trigger level of geo phone set for recording ground vibration was 0.8 mm/sec
- The geophone can be measured the ground vibration 0 to 37mm/s where microphone measures noise from 80 dB (L) to 135 dB (L).
- Both minimate and minimate plus can record frequency from 2 to 250 Hz.

3.5. Operational procedure of seismograph

Both instantel minimate and minimate plus has transducer and microphone. Transducer measures ground vibration through geophone. The naming of transducer both uniaxial and standard transducer depends upon one or three geophones respectively. Geophone sensor has a coil of wire suspended around a magnet. When magnet moves in a field of magnetic flux line, voltage is produced by coil which is proportional to the relative speed of voltage to coil. The magnet moves by blast energy because it coupled with particle motion of surrounding terrain. The magnet versus coil motion induces a voltage which proportional to particle velocity. Air pressure is generally measured by microphone. Two type of sound pressure measuring scale provided by minimate and minimate plus such as linear and weights. Linear measurement is used to measure the effect of low frequency air pressure without modification. Measured units are absolute, Pascal or relative dB (L). A weight measures noise level in terms of root mean square (RMS). Units were measured using the decibel scale dB (L).

The ground vibration was measured in three directions such as transverse, vertical and longitudinal where microphone measured noise in dB (L) in a linear scale. Transverse, vertical and longitudinal ground vibration shows particles in a side to side, up and down and forward and backward progressing outward motion respectively. The monitoring data was summerised and analyzed by blastware software. For peak particle velocity analyze, maximum charge amounts was observed on spot of blasting and radial distances was measured by the help of handheld GPS and mines Map. For fragmentation analysis, the blasted rock piles were captured by hand held canon digital camera and then the captured image were analyzed by WIPFRAG software.

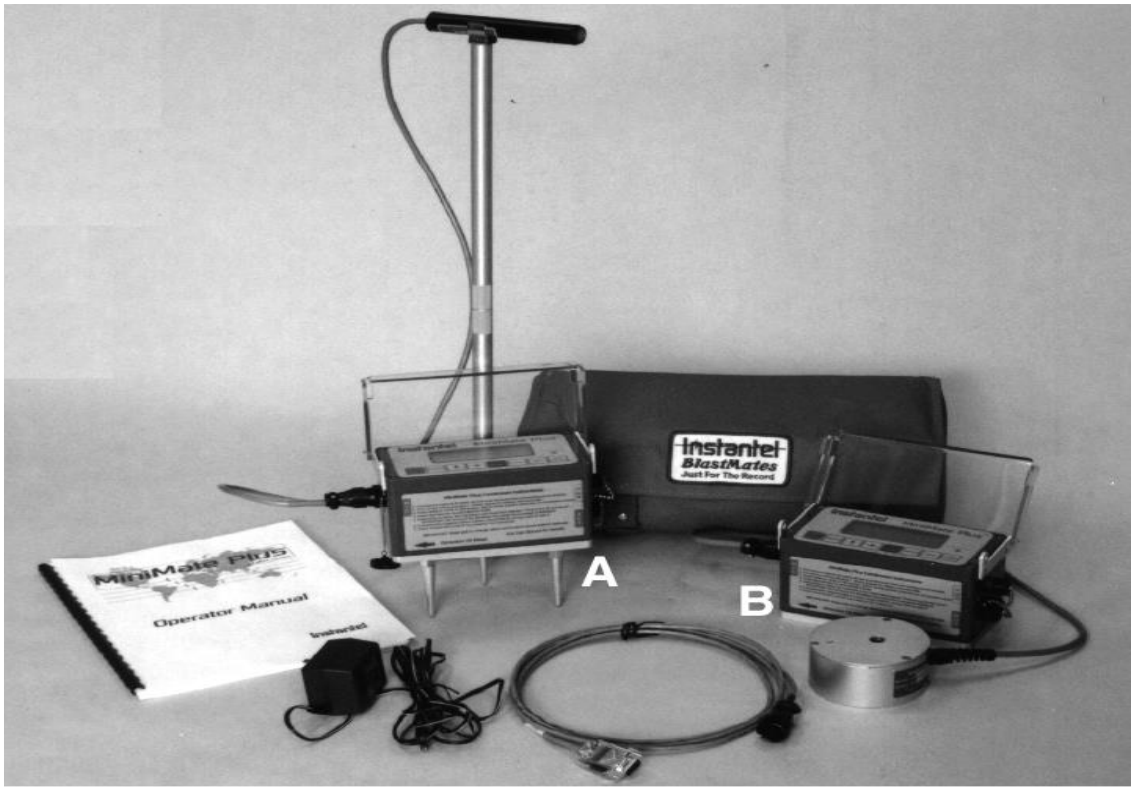

Figure 3.4: (A) Minimate plus with integrated geophone (B) Minimate plus with separate geophone; Sismograph with accessories (make: Instantel Inc. Canada)

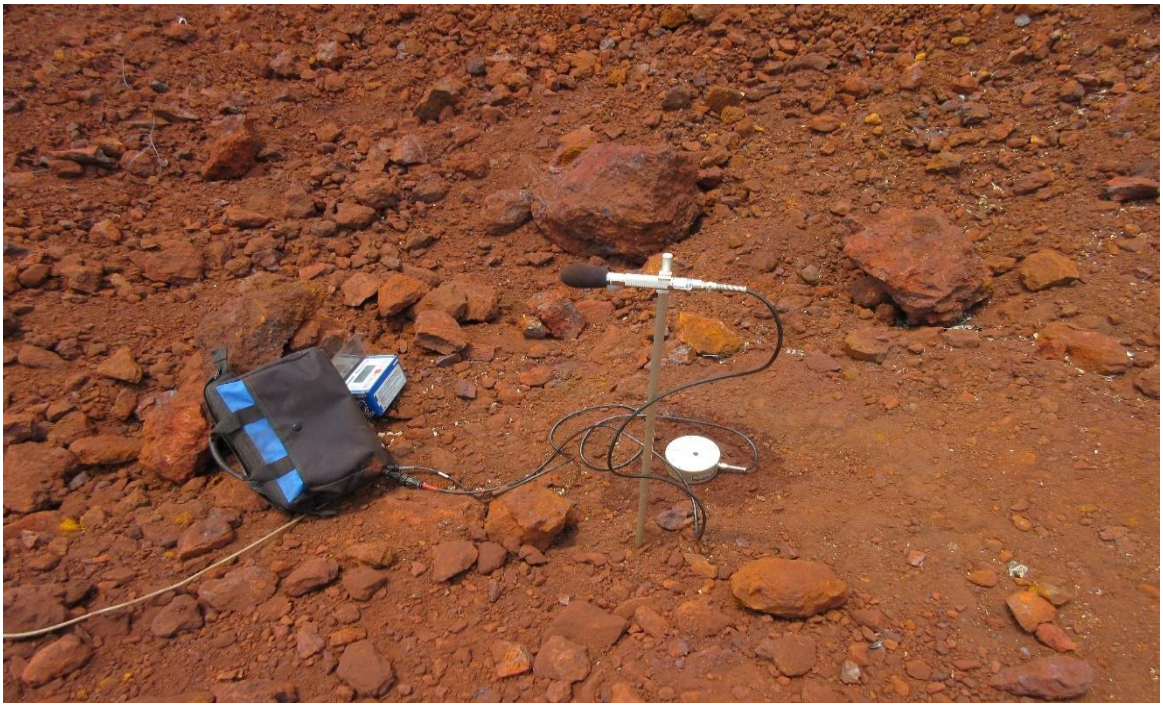

Figure 3.5: Sample image of field instrumentation

Chapter 4
Data Analysis

Introduction

Blasting is an important operation in most of the iron ore mines. In this study two mines have been investigated. The aim of the investigation was to develop purpose an equation to minimise ground vibration, air over pressure as well as fly rock. The specific objectives are to access to current situation evaluation by maintaining ground vibration, establish statistically a reliable empirical formula from the scaled distance and peak particle velocity, predict the maximum charge weights per delay as well as determine or predict the potential use of artificial neural network predicting the peak particle velocity these studies involved evaluation of rock properties, rock mass behaviour, properties of explosives etc. Among all variable the behaviour of rock mass i.e. mechanical properties as well as those of explosive play major role in blasting process. This investigation has been divided into following three section addresses the aim and specific objectives.

A. Determination of rock properties
B. Determination of peak particle velocity, air over pressure, fly rock and fragmentation
C. Evaluation of applicability of ANN approach

4.1 Determination of Rock Properties

Rock properties play the most important role in the fragmentation process. The physic-mechanical properties are discussed here.

(A) Physical and mechanical properties

Physical and mechanical properties of rock and rock mass play an important role in the transmission of sheet waves as well as fragmentation. The typical engineering properties that affect these are uniaxial compressive test, uniaxial tensile test, angle of internal friction, cohesion etc. Typically the higher the strength value, the higher is the transmission of waves. In this study, rocks were collected freshly exposed surfaces, kept in an airtight container sealed and shake proof container and transported to lab. Coring was carried out by a diamond bit NX size coring machine (make: HEICO, India, model-HR72-10) (Figure4.1).The required sizes were then prepared as per standard practice suggested [ASTM D2845].

The physical parameters as density varied between 4.2 gm/cc and 3.5 gm/cc with average value being at 4.0 gm/cc. There was little moisture in the intact iron ore samples tested.

4.1.1 Uniaxial compressive strength

Rock mass experience compressive loading at the next moment of blasting. The first shock wave compressive the rock mass surrounding the blast hole. So the determination of the compressive strength is very important. Unconfined compressive strength of rocks was determined as suggested by [ASTM D7012]. The specimen were prepared and tests carried out in a computer controlled machine (make: HEICO, India, Figure4.1) at a stress rate of 0.5 to 1 MPa/sec. All the samples failed within 10 to 12 minutes. The value of compressive strength varied between 72.19 and 122.7MPa (Table 4.1). The mean values of compressive and tensile strength of rock sample of both mines are 98.547 and 6.754 where standard deviation values are 21.755 and 1.254 respectively.

Table 4.1: Compressive Strength Test Results

Sample No.	UCS (MPa)
1	72.19
2	91.3
3	108
4	122.7

Figure 4.1: Cylindrical iron ore sample Testing

4.1.2 Brazilian Tensile Strength

When the shock wave reaches the free faces it reflects back in the medium. The shock wave on its return path influences the rock mass to undergo tensile loading. Hence it is necessary to know the tensile strength of rock for better design. The tensile strength of rocks was determined as per [ASTM D3967].The test is an indirect method of determination of tensile property. The length to diameter of samples varied between 0.44 and 0.55. The strength tests were conducted (Figure 4.2) and the values of varied between 6.24 and 11.04 MPa (Table 4.2)

Table 4.2: Tensile Strength Test Results

Sample No.	UTS (MPa)
1	5.455
2	6.24
3	6.914
4	8.41

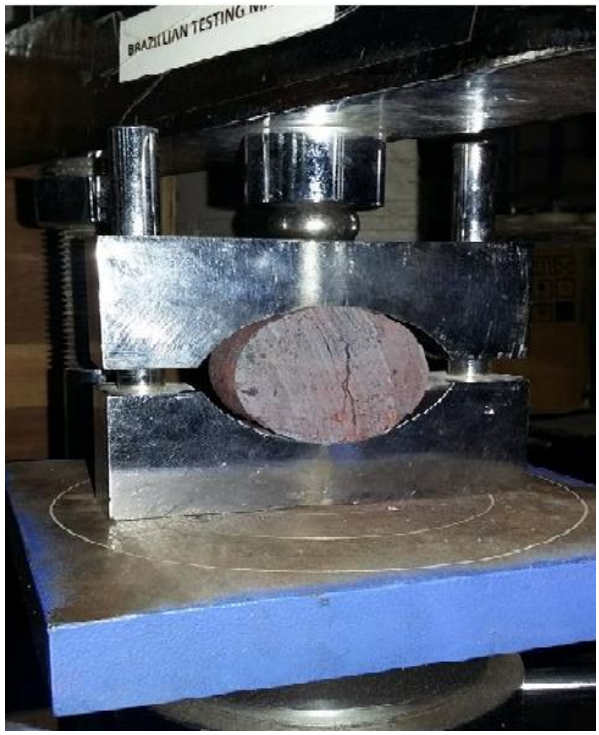

Figure 4.2: Indirect tensile test of rock sample

4.1.3 Ultrasonic Velocity Test

It is one of the widely used testing methods for rock material characterisation. It was carried out with a non-destructive test unit (make: GCTS, USA) and P and S wave were recorded (Figure 4.3). The specimen dimensions were as that of a unconfined compressive strength tests, as suggested elsewhere [92]. The P-wave velocity of rocks was between 5841m/s to 5871m/sand similar values for S-wave were 3250 m/s to 3263m/s.

Table 4.3: Non Destructive Test Results

Sl. No.	P wave	S wave
1	5856	3247
2	5860	3255
3	5865	3257
4	5871	3258

Figure 4.3: Ultrasonic test of rock sample

4.1.4 Elasticity and Poisson Ratio

The two basic material properties are elasticity and Poisson ratio. Elasticity i.e. elastic modulus value is typically determined by uniaxial compressive loading. These values are determined as per IS 9221.The young's modulus and Poisson ratio were determined for the rocks. The E values varied between 10 and 15 GPa with Poisson ratio from 0.021 to 0.054. Mean values of Poisson's ratio and young's modulus are 0.0335 and 11.7 where standard deviation values are 0.0147 and 2.521 respectively.

Table 4.4: Elastic parameters of the Samples

Sample No.	Poisson's ratio	Young's modulus(GPa)
1	0.021	9
2	0.025	10.8
3	0.034	12
4	0.054	15

4.2 Blast data Analysis

Introduction

A large amount of energy is released when an explosive is detonated. An efficient designed blast utilise the energy to obtain the appropriate fragmentation without ground vibration, air over pressure as well as fly rocks. However though there are many design approaches available, the generation of ground vibration and air overpressure has not been completely eliminated, often leading to problem associated with ground vibration and noise.

So it is necessary in many cases to evaluate the performance of blasting compared to those with established empirical approaches. In this investigation five different empirical approaches have been considered and the discussed as below.

4.2.1 Analysis of blast events by Different predictor approaches

Seismic waves are the waves that travel through earth material or body i.e. the transmission of energy through the solid material or earth. These seismic waves typically

man-made are sensible i.e. they can be felt and typically referred as vibration. The different vibration parameter as displacement, velocity, acceleration and frequency are the fundamental properties that constitute the ground vibration of those four parameters. The velocity i.e. speeds at which rock particles move is an important parameter. The two principal factors that affect the vibration level are distance and explosive charge size. There exist numerous mathematical relationships between the vibration level, charge size and distance. But a general reliable approach is yet to be universally established due to complexity of ground vibration, blasting as well as test site factors, so experimental investigation are still necessary to minimise environmental problem [91].

There are some approaches that have suggested site parameters specific to type of iron ore mines and those are in vogue. In these investigations, a few of those developed relations have been analysed with respect to applicability in two iron ore major areas of Odisha. The relations developed by USBM [29], Langefours-Khilstrom [10], Ambraseys-Hendron [30], Indian standard [31], CMRI [32] have been considered and analysed. The actual blasting data as collected from the experimental blasts during investigations have been given in the appendices. These are used along with the site constants suggested by the respective approaches [36] to estimate the correlation between the measured and predicted values. These are reported in following sections.

4.2.1.1 Prediction by USBM approach

The USBM [29] recommended equation is

$$303.736\left(\frac{D}{\sqrt{Q}}\right)^{-1.80138} \tag{46}$$

Mean and standard deviation of predicted values with correlation coefficient are 1.508 and 2.971. The relation between measured and predicted peak particle velocity shows direct relationship of correlation coefficient (0.237). The equation shows slope of 0.306 and constant of -0.265.

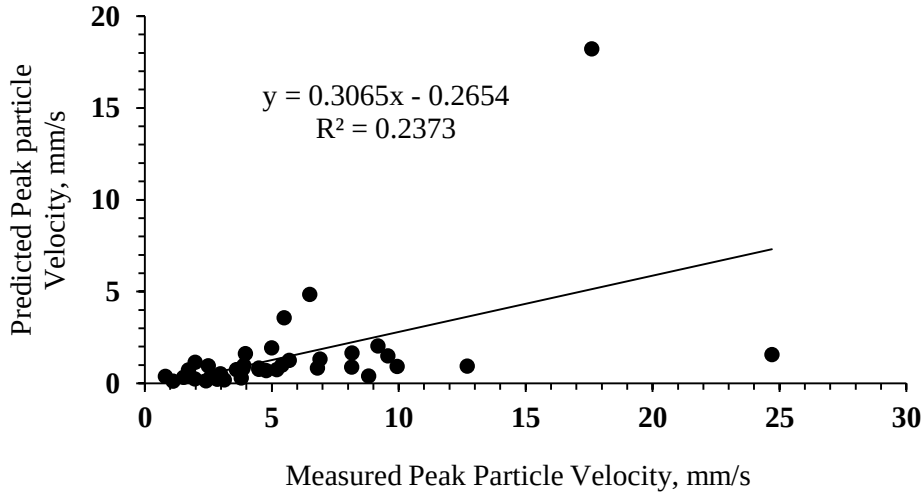

Figure 4.4: Relation between measured and predicted PPV [after USBM Equation]

4.2.1.2 Prediction by Langefors-Kilstrom approach

The Langfors-Khilstrom [10] equation is

$$\upsilon = 30.0096\left(\sqrt{\frac{Q_{MAX}}{R^{\frac{2}{3}}}}\right)^{2.50391} \tag{47}$$

Mean and standard deviation of predicted values with correlation coefficient are 2161.063 and 11262.69 (0.179).The relation between measured and predicted peak particle velocity shows direct relationship with slope and constant of 1010 and-3689 respectively.

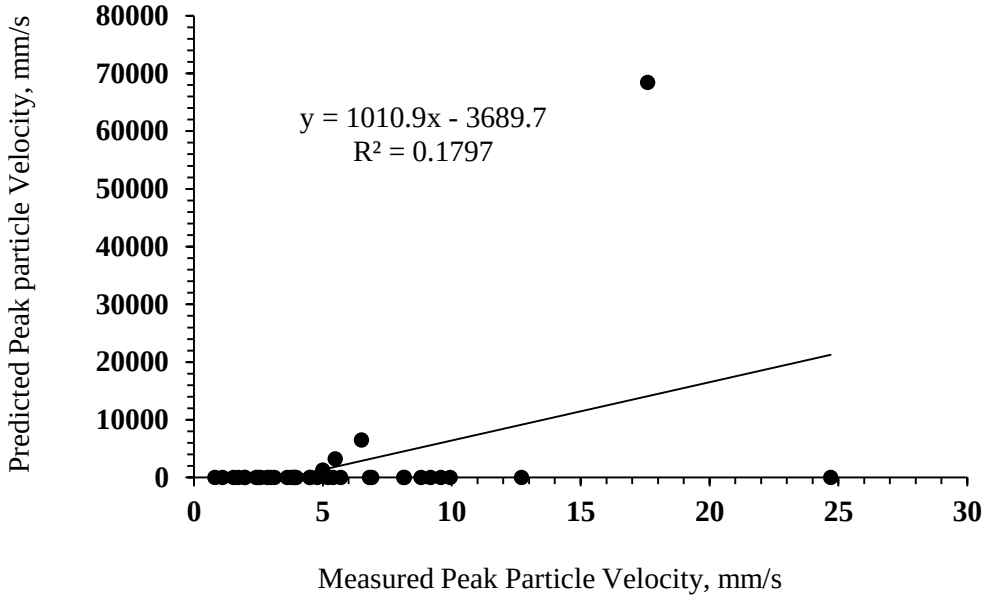

Figure 4.5: Relation between measured and predicted PPV [after Langefors-Kilstrom Equation]

4.2.1.3 Prediction by Ambraseys-Hendron approach

The Ambraseys-Hendron [30] equation is

$$2471.13\left(\frac{D}{Q^{\frac{1}{3}}}\right)^{-1.72116} \tag{48}$$

The predicted PPV from the equation shows mean and standard deviation values are 4.026 and 3.801. The correlation coefficient between measured Peak Particle velocities and predicted Peak Particle velocities shows (0.338) with slope and constant of 0.468 and 1.314.

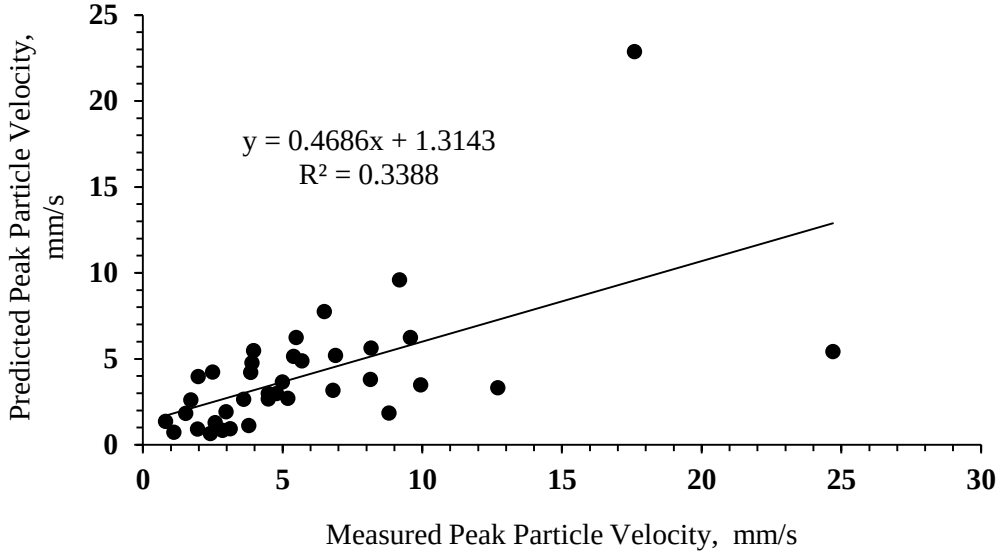

Figure 4.6: Relation between measured and predicted PPV [after Ambraseys-Hendron Equation]

4.2.1.4 Prediction by Indian Standard approach

The recommended Indian Standard [31] equation with their own calculated site constant for iron ore mine is

$$30.0096\left(\frac{Q^{\frac{2}{3}}}{D}\right)^{1.87793} \tag{49}$$

The predicted PPV values shows mean 0.705 and standard deviation 2.322 with correlation coefficient between measured PPV and predicted PPV is 0.195. The measured PPV is directly proportional to predicted PPV with slope of 0.217 and constant of -0.551.

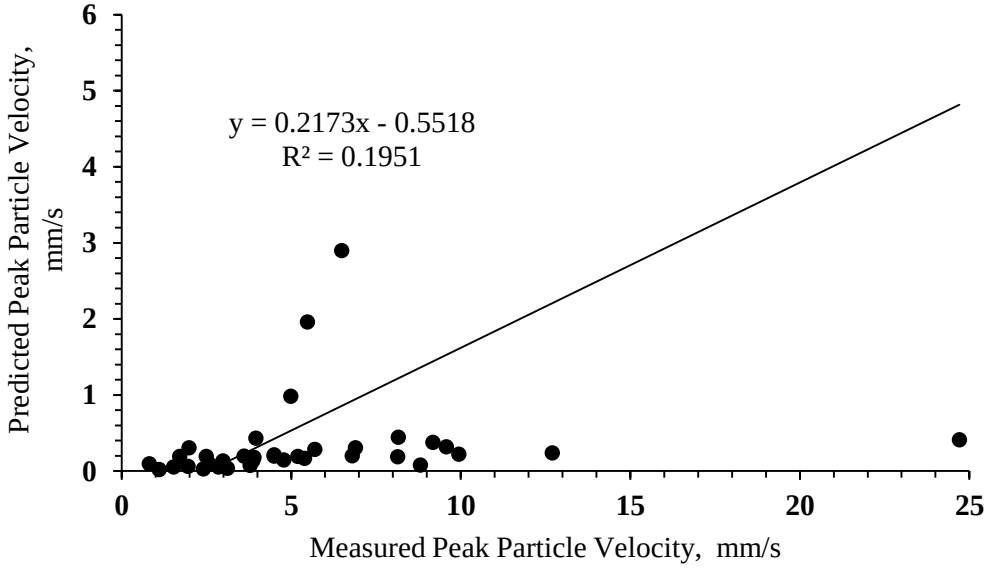

Figure 4.7: Relation between measured and predicted PPV [after Indian Standrad Equation]

4.2.1.5 Prediction of PPV by CMRI approach

CMRI [32]after many field investigation recommended the following equation based on wave propagation law [86]. The decrease in amplitude of ground vibration was considered as only due to geometrical spreading and was given by

$$V = n + k\left(\frac{D}{\sqrt{Q}}\right)^{-1} \tag{50}$$

(Where, V = PPV, D = Distance of measuring instrument from the source of blasting, Q = maximum explosive per delay, n and K are site specific constants)

The recommended values for site constants n and k applicable to iron ore mines are 91.9117 and 0.28874 respectively. These values were considered to predict the peak particle velocity (PPV) for the investigated iron ore mines. The mean PPV predicted value is 4.360 with standard deviation of 3.068. This average value is different than that with the measured value of 37 vibration readings (Figure4.8).The correlation coefficient value is only (0. 295).

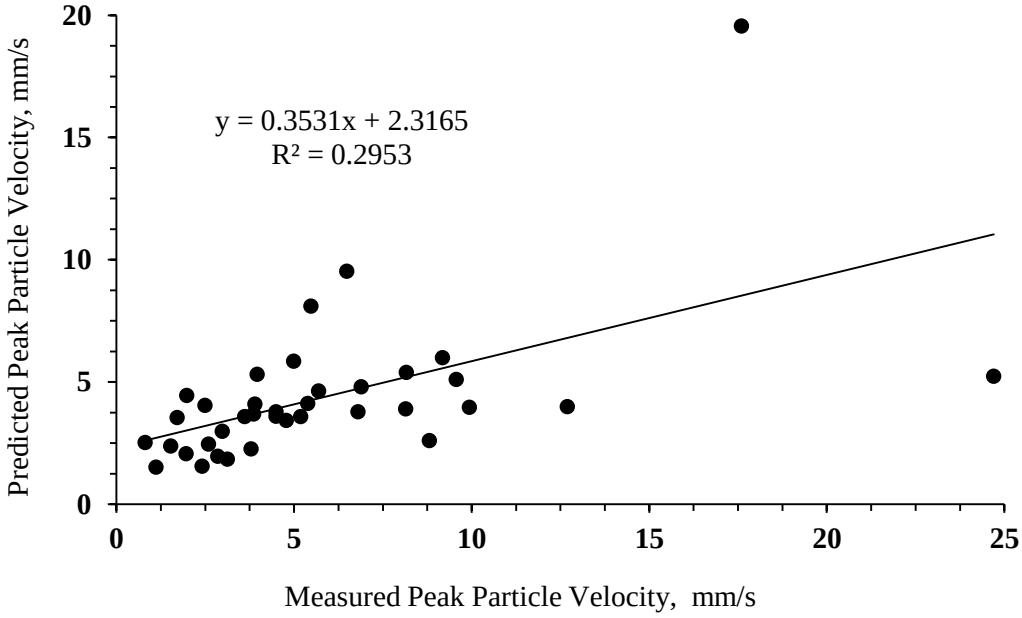

Figure 4.8: Relation between measured and predicted PPV [after CMRI approach]

The above analyses show that the recommended site specific constants or values have limited applicability on the iron ore major areas of Odisha under investigation as there are wide variations in the measured and predicted PPV values. However as the empirical equations suggested are established, hence those equations are considered to predict the site constants for the mines as below.

4.2.2.1 USBM Predictor Equation

USBM equation is one of the oldest approaches of blast vibration analysis and is still popular in many places. The USBM predictor equation shows scaled distance as the function of radial distance and square root of maximum charge per delay. The standard equation is

$$\upsilon = K\left(\frac{R}{\sqrt{Q_{MAX}}}\right)^{-B} \tag{51}$$

Where, V=PPV, R=radial Distance and Q= maximum charge per delay.

The site constant values K and B are determined by plotting the PPV and scaled distance in log-log scale. It is used in those 37 blast event cases. The relation between scaled distance and the PPV were determined for two regions separately and then for all data combined (Figure 4.11). It is observed that the data of koira region exhibit a better correlation than that of Daitari region. The explosive used for mines for Koira and Daitari region was cartridge explosive. The correlation coefficient for the combined data was 0.409.

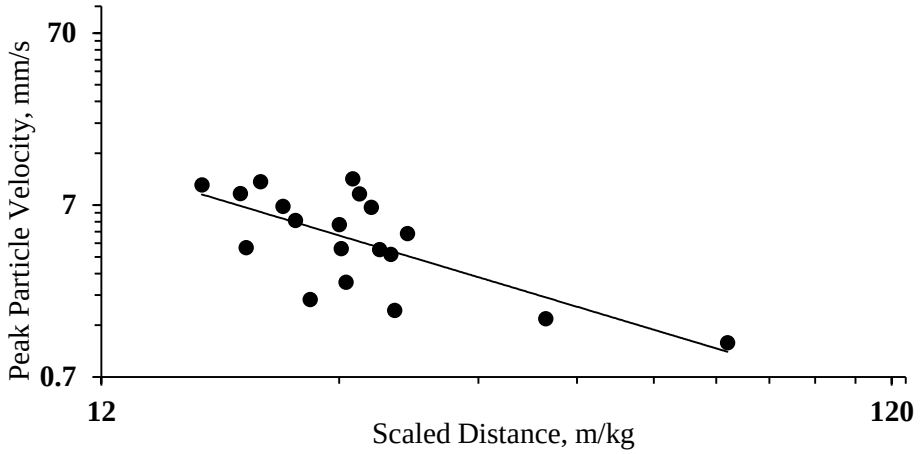

Figure 4.9: Peak particle velocity vs. scaled distance (koira region)

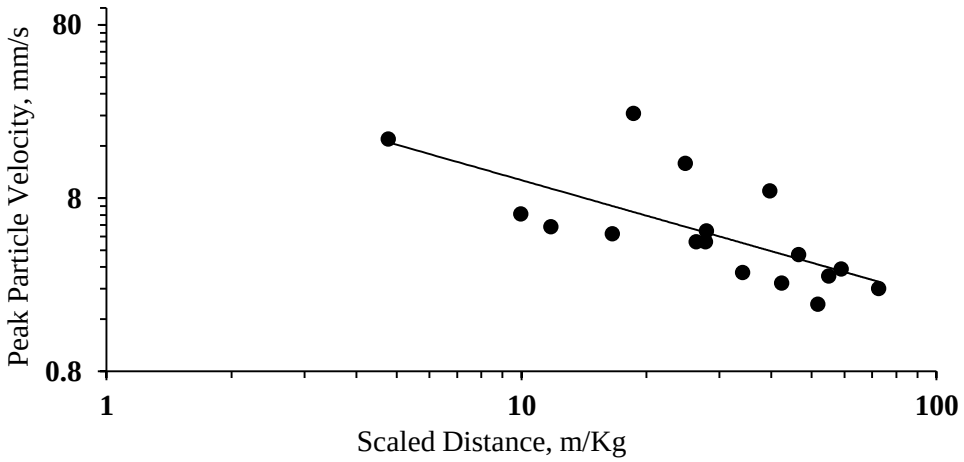

Figure4.10: Peak Particle Velocity vs. Scaled Distance (Daitari region)

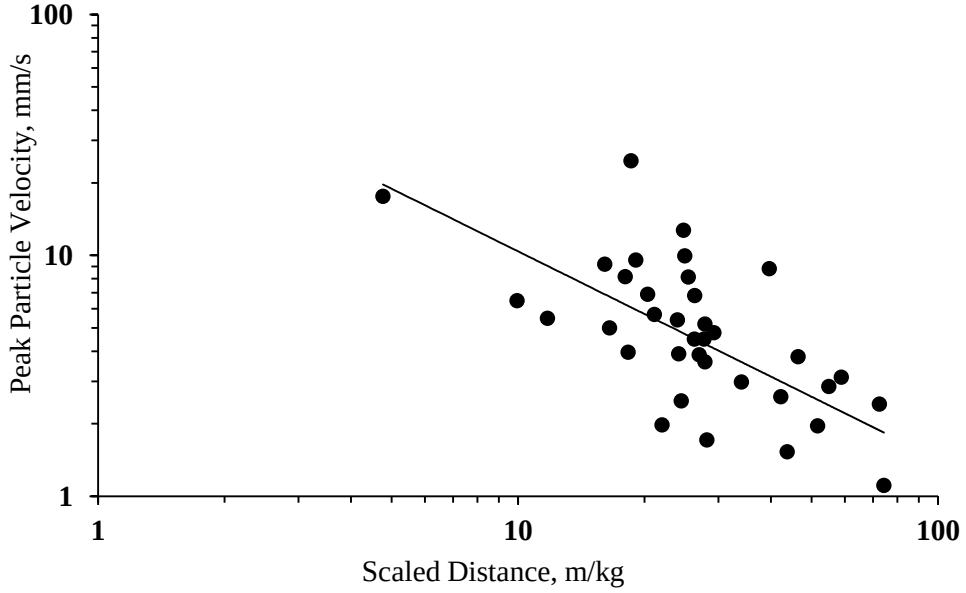

Figure 4.11: Peak Particle Velocity vs. Scaled Distance (Koira and Daitari region)

As per USBM, the relations that exist between Peak particle velocity and scaled distance for Koira region, Daitari region and combined iron mine of Koira and Daitari region is given in below table.

Table 4.5: USBM equation's constant parameter with correlation determination

USBM Equation	B	K	R^2
Koira region	669.2	1.57	0.543
Daitari region	48.70	0.68	0.471
Combined data	75.90	0.86	0.409

4.2.2.2 Langefors-Kilstrom Equation

According to langefors-kilstrom, scaled distance is the square root of charge per delay divided by two third of radial distance. The standard equation is

$$\upsilon = K\left(\sqrt{\frac{Q_{MAX}}{R^{\frac{2}{3}}}}\right)^{B} \tag{52}$$

The site constant K and B is determined by plotting PPV with scaled distance in Graph. It is used in those 37 blast event cases. The relation between scaled distance and the PPV were determined for two mines separately and then for all data combined (Figure 4.14). It is observed that the data of Koira region exhibit a better correlation than that of Daitari region. The explosive used for mines of Koira and daitari region was cartridge explosive. The correlation coefficient for the combined data was 0.350.

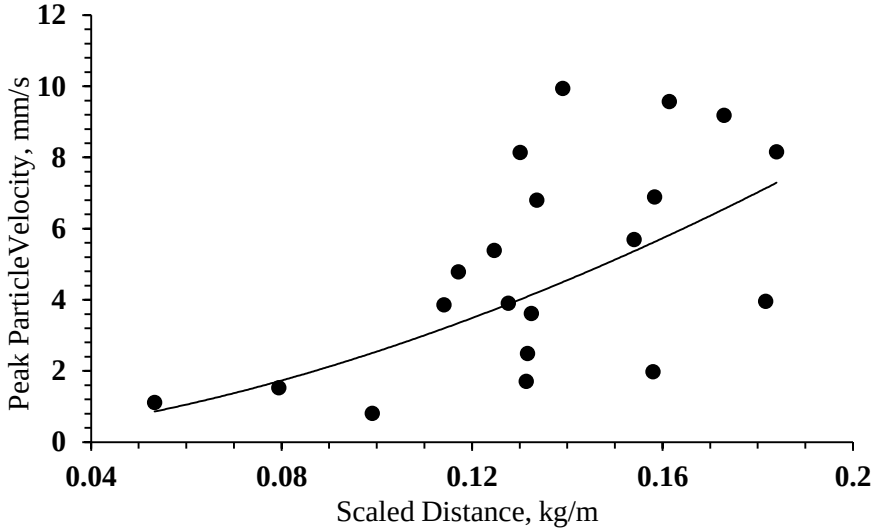

Figure 4.12**:** Peak particle velocity vs. scaled distance (koira region)

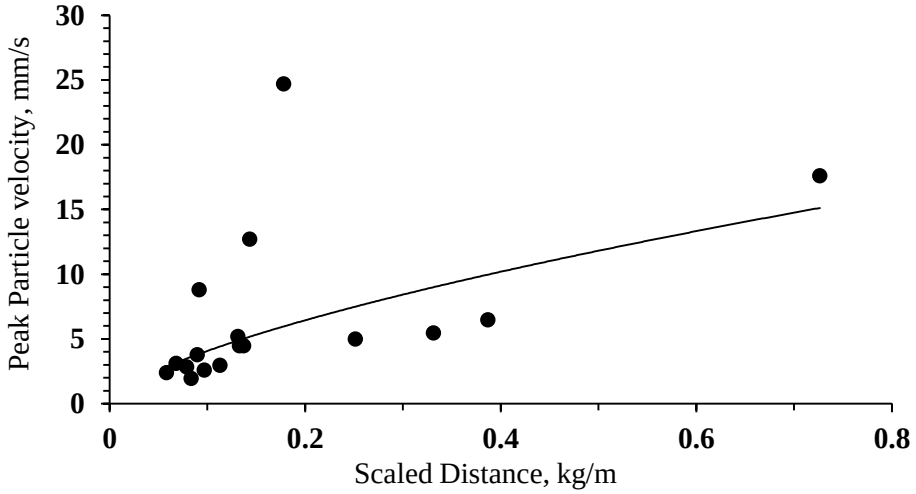

Figure 4.13: Peak Particle Velocity vs. Scaled Distance (Daitari region)

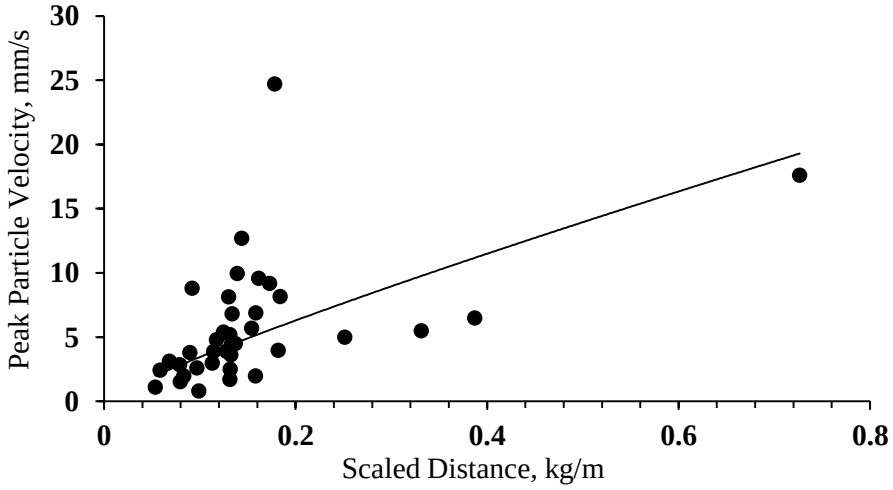

Figure 4.14: Peak Particle Velocity vs. Scaled Distance (Koira and Daitari region)

As per Langefors-Kilstrom, the relation that exists between Peak particle velocity and scaled distance for Koira region, Daitari region and combined iron ore mine is given in below table.

Table 4.6: Langefors-Kilstrom equation's constant parameter with correlation coefficient

Langefors-Kilstrom Equation	B	K	R^2
Koira region	135.4	1.726	0.449
Daitari region	18.67	0.661	0.393
Combined data	25.46	0.868	0.350

4.2.2.3 Ambraseys-Hendron Equation

According to Ambraseys-hendron, scaled distance is the ratio of radial distance to the cube root of maximum charge. The peak particle velocity equation is denoted by

$$\upsilon = K\left(\frac{R}{\sqrt{Q^{\frac{1}{3}}_{MAX}}}\right)^{-B} \tag{53}$$

The site constant equation is determined by plotting PPV and scaled distance in log-log scale. It is used in those 37 blast event cases. The relation between scaled distance and the PPV were determined for two areas separately and then for all data combined (Figure-4.17). It is observed that the Daitari region exhibit a better correlation than that of Koira region. The correlation coefficient for the combined data was 0.443.

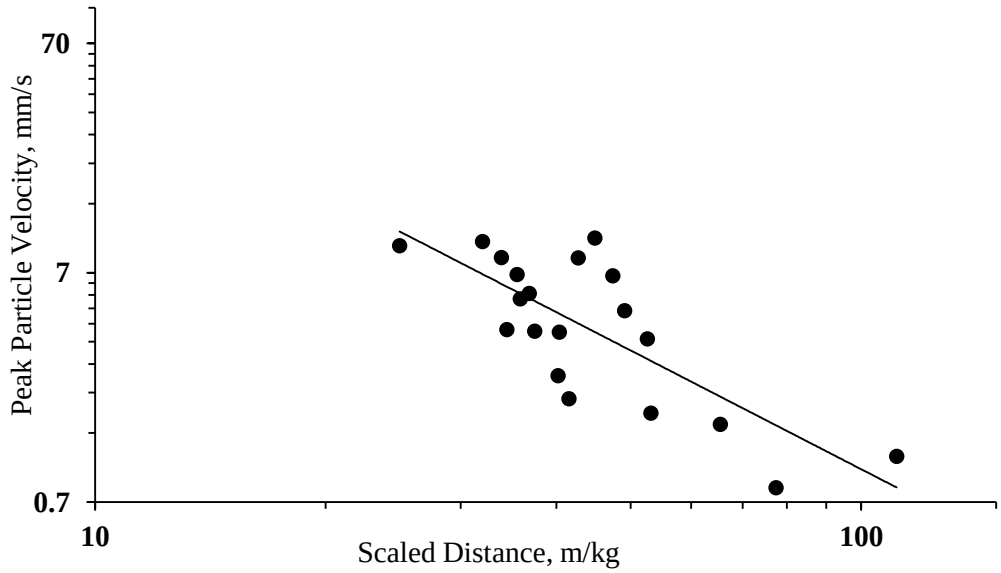

Figure 4.15: Peak particle velocity vs. scaled distance (koira region)

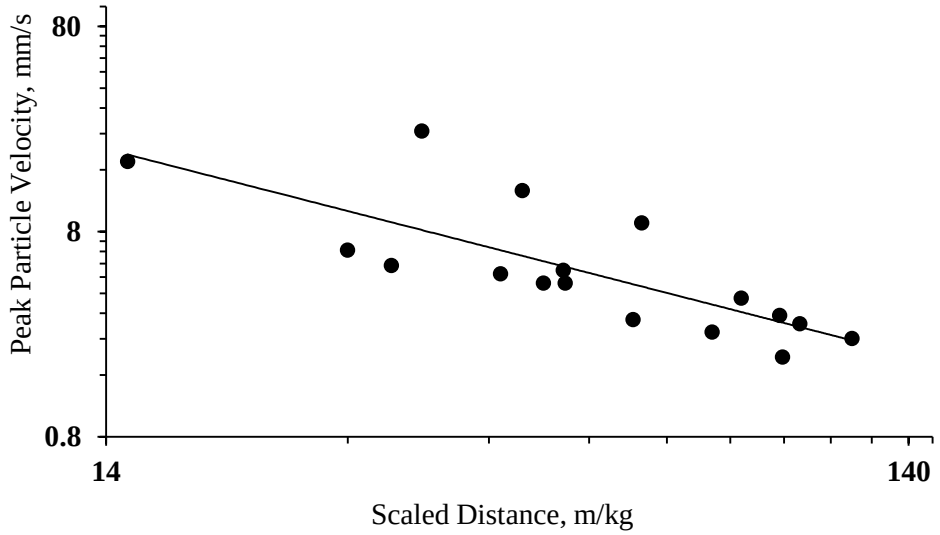

Figure 4.16: Peak Particle Velocity vs. Scaled Distance (Daitari region)

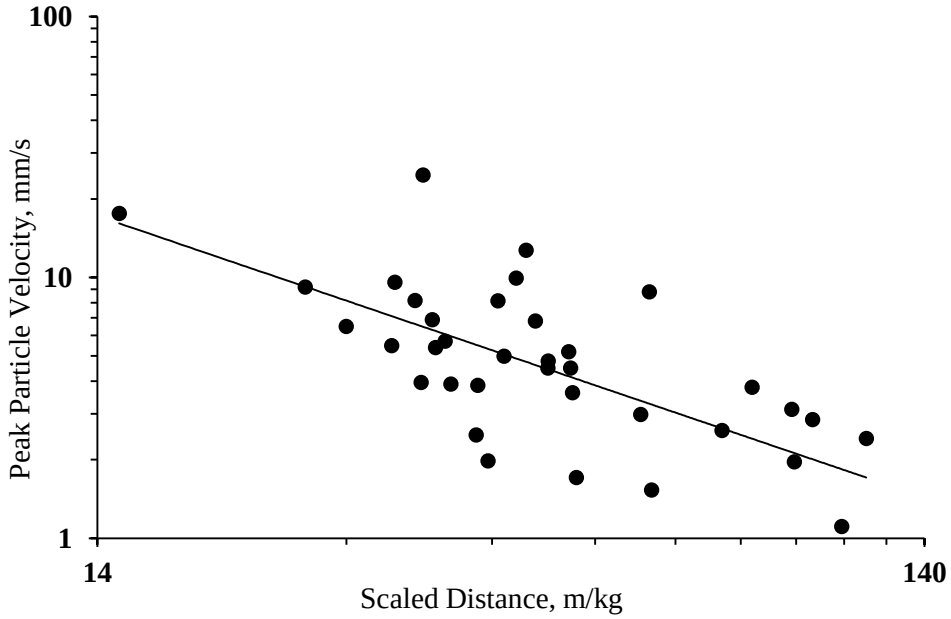

Figure 4.17: Peak Particle Velocity vs. Scaled Distance (Koira and Daitari region)

As per Ambraseys-Hendron, the relation that exists between Peak particle velocity and scaled distance for Koira region, Daitari region and combined iron mine is given in below table.

Table 4.7: Ambraseys-Hendron equation's constant parameter with correlation Coefficient

Ambraseys-Hendron Equation	B	K	R^2
Koira region	2690	1.72	0.591
Daitari region	284.9	1.00	0.593
Combined data	296.3	1.07	0.443

4.2.2.5 Indian Standard Equation

According to Indian standard, scaled distance is the ratio of two third of maximum charge per delay to the radial distance. The PPV equation is denoted by

$$\upsilon = K\left(\frac{Q_{MAX}{}^{\frac{2}{3}}}{R}\right)^{B} \tag{54}$$

The site constant K and B are determined by plotting PPV and scaled distance in graph. It is used in those 37 blast event cases. The relation between scaled distance and the PPV were determined for two areas separately and then for all data combined (Figure 20).
It is observed that the Koira region exhibit a better correlation than that of Daitari region. The correlation of coefficient for the combined data was 0.350.

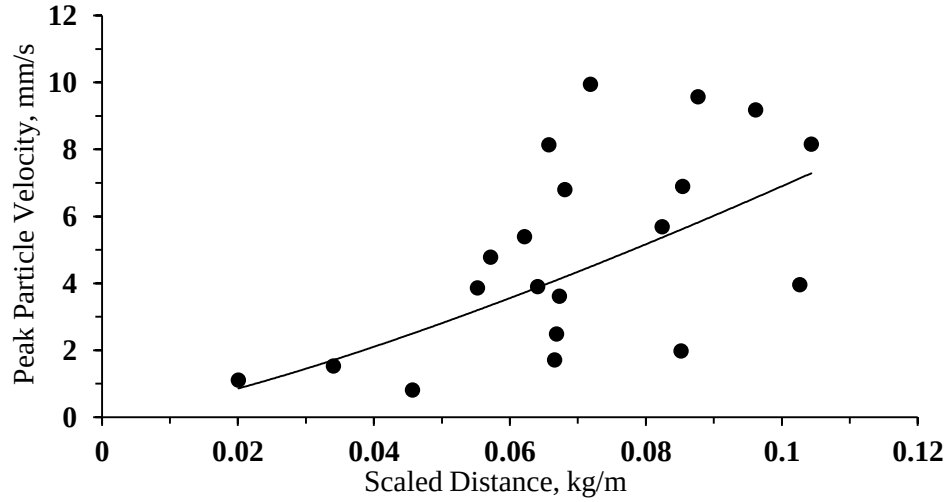

Figure 4.18: Peak particle velocity vs. scaled distance (koira region)

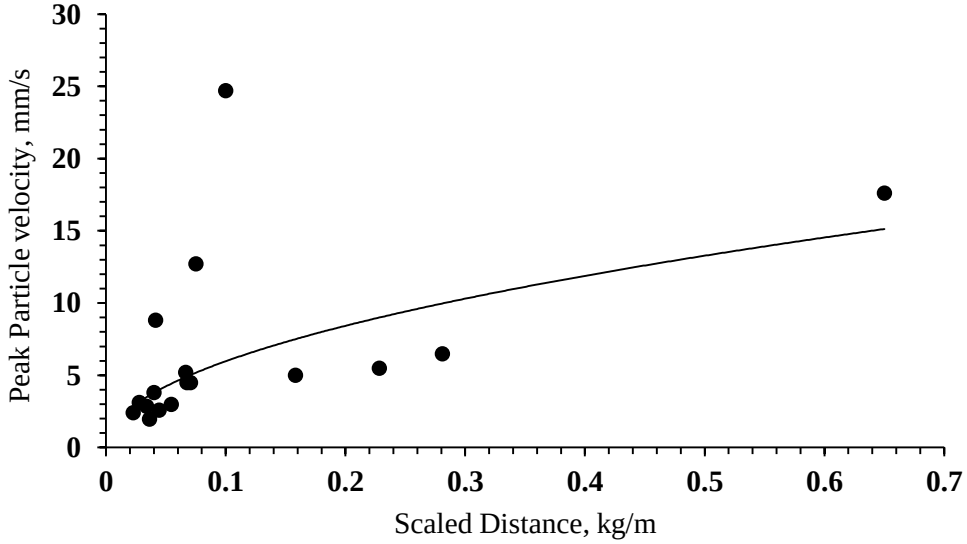

Figure 4.19: Peak Particle Velocity vs. Scaled Distance (Daitari region)

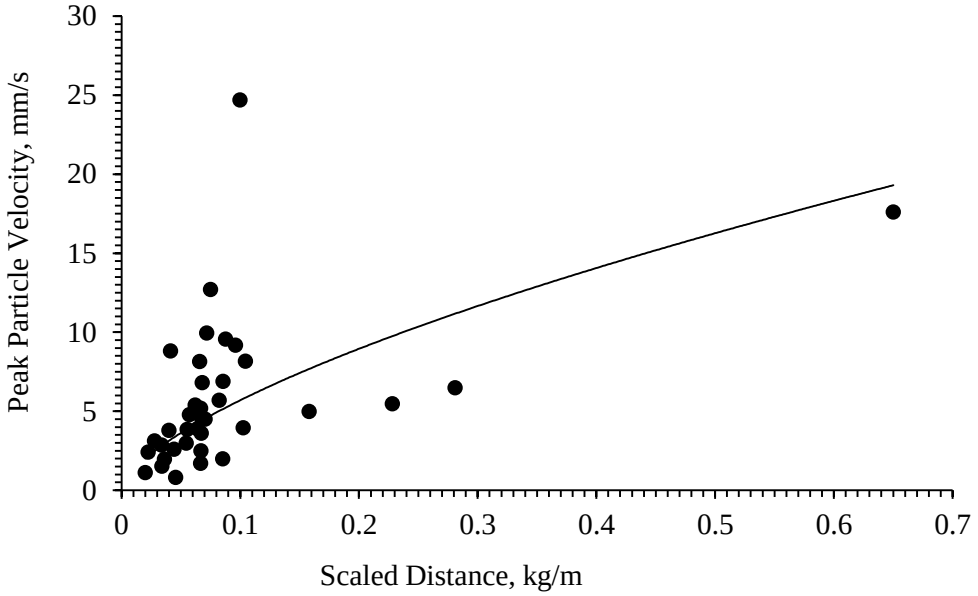

Figure 4.20: Peak Particle Velocity vs. Scaled Distance (Koira and Daitari region)

As per Indian Standard, the relation that exists between Peak particle velocity and scaled distance for Koira region, Daitari region and combined iron mine is given in below table.

Table 4.8: Indian Standard equation's constant parameter with correlation coefficient

Indian Standard Equation	B	K	R^2
Koira region	136.3	1.295	0.449
Daitari region	18.72	0.496	0.393
Combined data	25.25	0.651	0.350

4.2.2.5 CMRI Equation

CMRI after many field investigations recommended the following equation based on wave propagation law [86]. The decrease in amplitude of ground vibration was considered as only due to geometrical spreading and was given by

$$V = n + k\left(\frac{D}{\sqrt{Q}}\right)^{-1} \tag{55}$$

(Where, V = PPV, D = Distance of measuring instrument from the source of blasting, Q = maximum explosive per delay, n and K are site specific constants.)

It is used in those 37 blast event cases. The relation between scaled distance and the PPV were determined for two areas separately and then for all data combined (Figure4.22). It is observed that the Daitari region exhibit a better correlation than that of Koira region. The correlation coefficient for the combined data was 0.295.

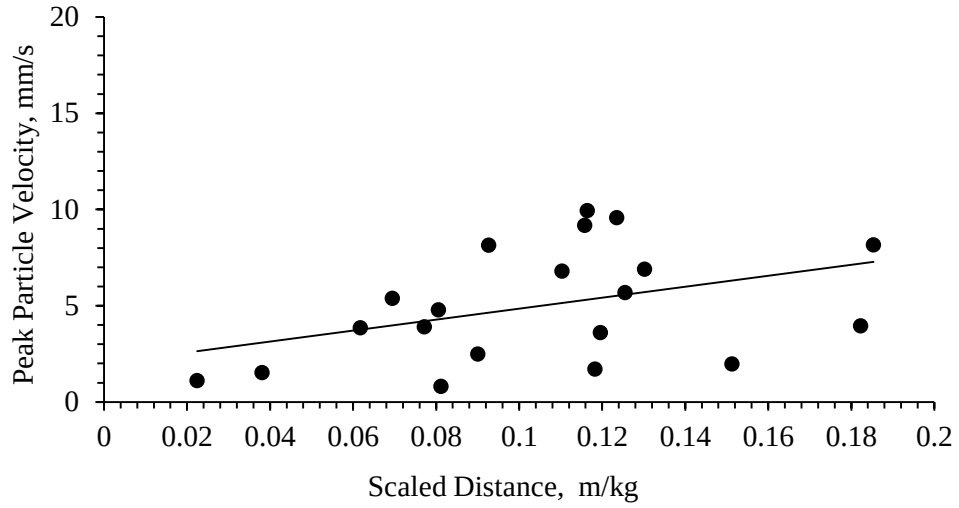

Figure 4.21: Peak particle velocity vs. scaled distance (koira region)

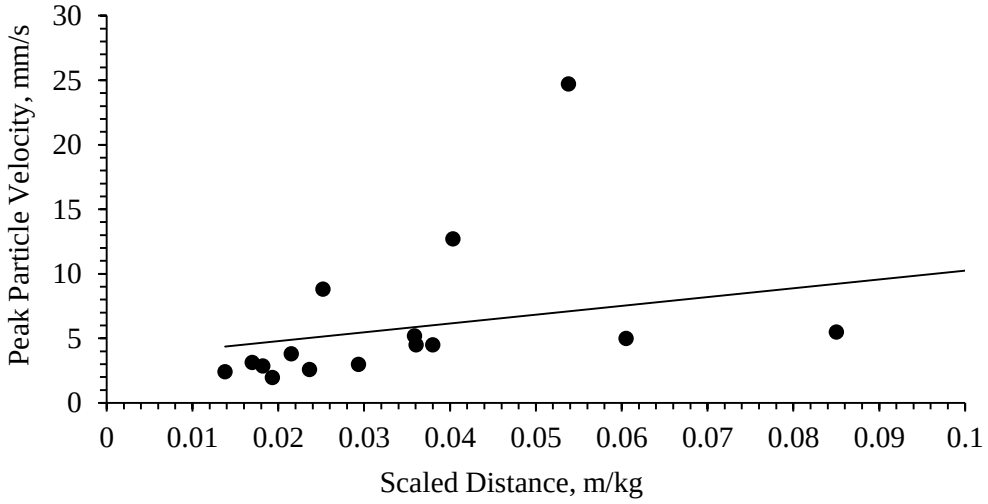

Figure 4.22: Peak Particle Velocity vs. Scaled Distance (Daitari region)

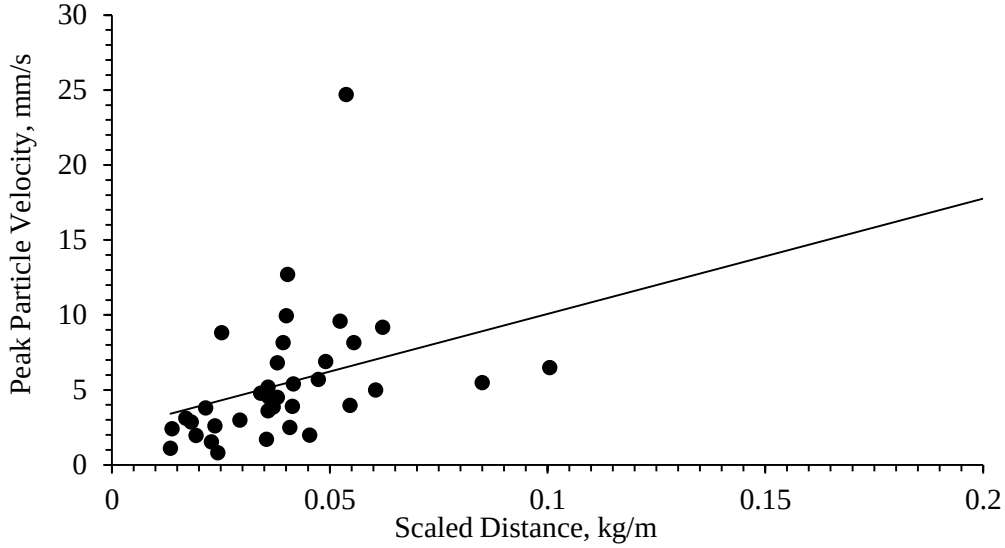

Figure 4.23: Peak Particle Velocity vs. Scaled Distance (Koira and Daitari region)

As per CMRS, the relation that exists between Peak particle velocity and scaled distance for Koira region, Daitari region and combined iron mine is given in below table.

Table 4.9: CMRS equation's constant parameter with correlation coefficient

CMRI Equation	K	N	R^2
Koira region	28.48	1.994	0.162
Daitari region	68.19	3.422	0.282
Combined data	76.87	2.382	0.295

4.2.3 Prediction of PPV by empirical formulas and compared with measured value

The site constants as determined from the combined data were considered to predict the PPV to evaluate applicability of those five approaches. Those are then compared with measured PPV values as below.

4.2.3.1 Prediction by USBM approach

The USBM equation was changed as below and using the same the predicted values were

$$75.90\left(\frac{D}{\sqrt{Q}}\right)^{-0.86} \tag{56}$$

calculated. The PPV ranged between 2.419 to 19.806. The mean and standard deviation values are 5.086 and 3.092 respectively. These values when compared with the measured data show the slight improvement correlation coefficient of 0.305 with slope and constant of 0.361 and 2.992 respectively.

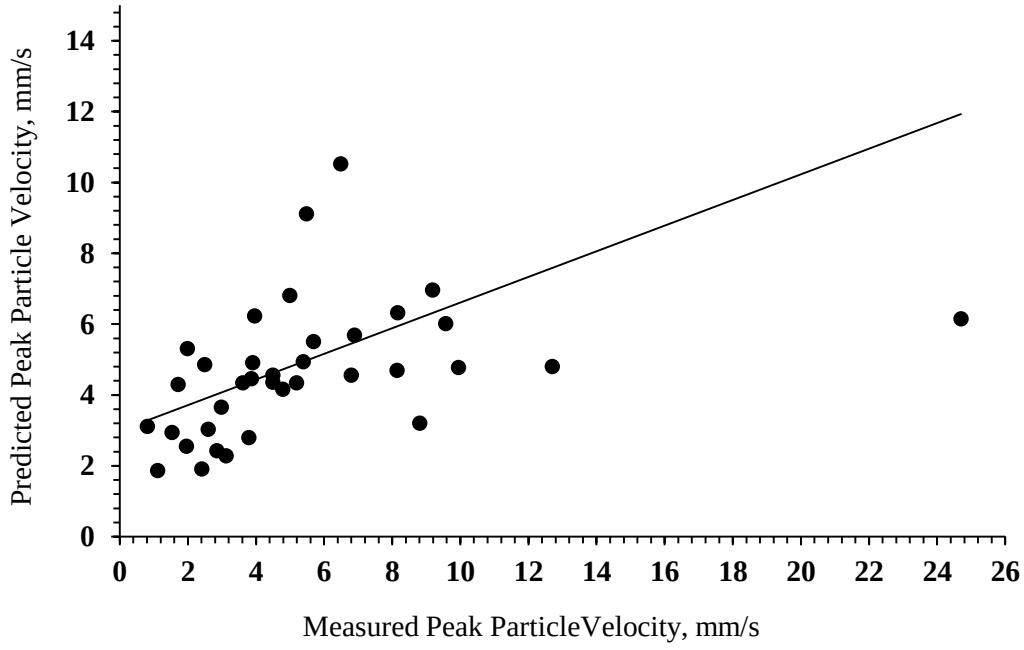

Figure 4.24: Relation between predicted PPV and measured PPV [USBM approach]

4.2.3.2 Prediction by LANGEFORS-KILSTROM approach

The graph 4.16 is plotted between predicted Peak particle velocities by USBM approach from equation

$$25.46\left(\sqrt{\frac{Q}{D^{\frac{3}{2}}}}\right)^{0.868} \tag{57}$$

and measured Peak Particle velocities values. The mean and standard deviation values are 4.981 and 3.034 respectively. These values when compared with the measured data show correlation coefficient of 0.256 with slope and constant of 0.325 and 3.099.

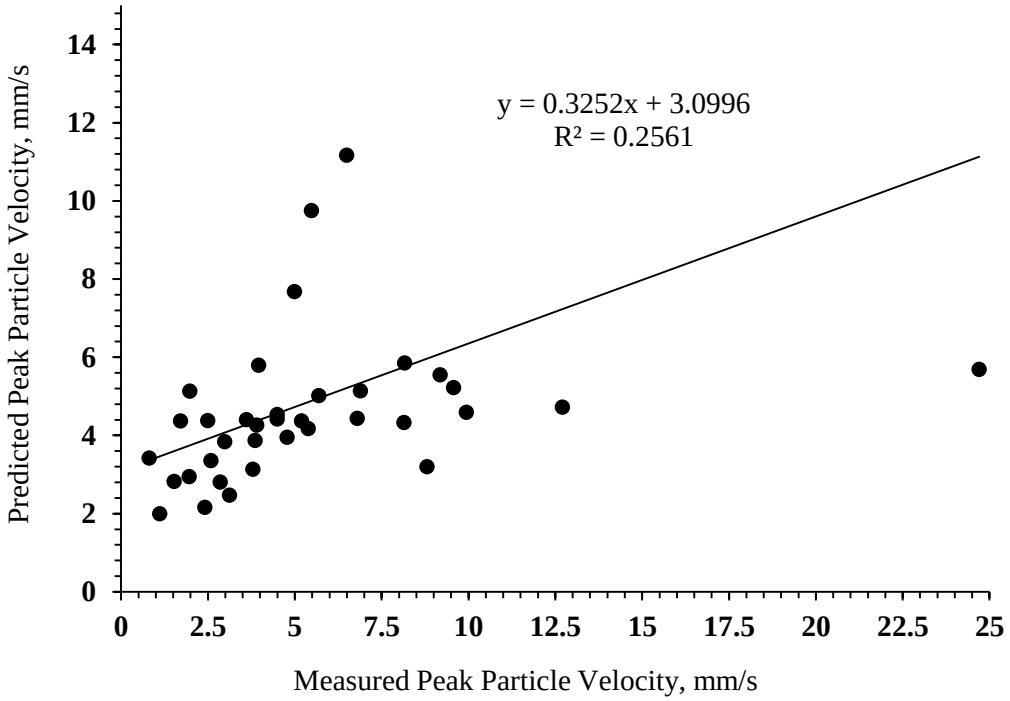

Figure 4.25: Relation between predicted PPV and measured PPV [Langfors Khilstrom approach]

4.2.3.3 Prediction by Ambraseys-Hendron approach

The graph 4.26 is plotted between predicted Peak particle velocities by USBM approach from the developed equation using the field data and measured Peak Particle velocities values.

$$296.3\left(\frac{D}{Q^{\frac{1}{3}}}\right)^{-1.07} \tag{58}$$

The mean and standard deviation values are 5.173 and 2.687 respectively. These values when compared with the measured data show correlation coefficient of 0.363 with slope and constant of 0.343 and 3.188.

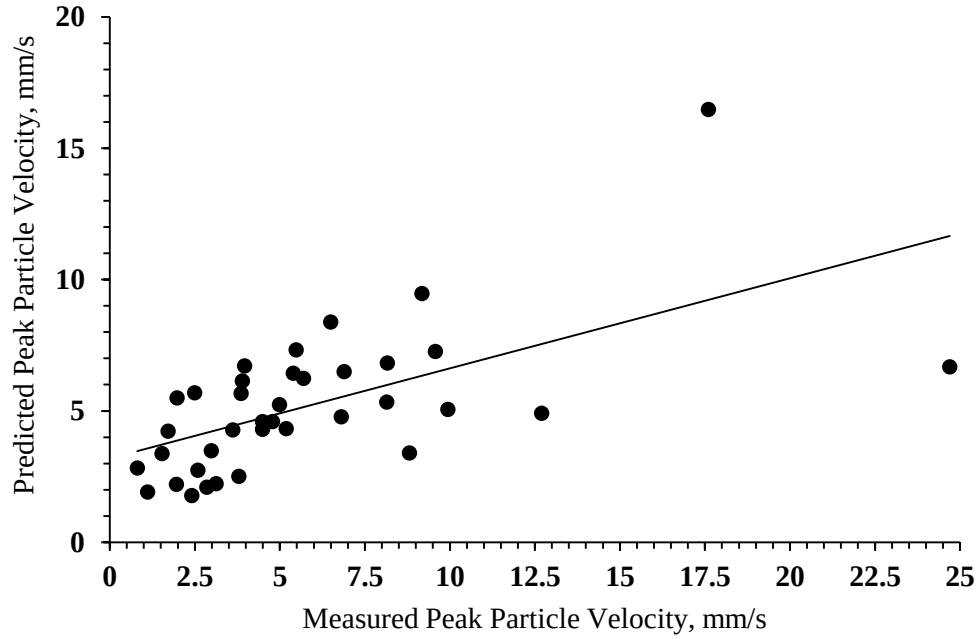

Figure 4.26: Relation between predicted PPV and measured PPV [Ambraseys Hendron approach]

4.2.3.4 Prediction by Indian Standard approach

The graph 4.27 is plotted between predicted Peak particle velocities by USBM approach from equation and measured Peak Particle velocities values. The mean and standard

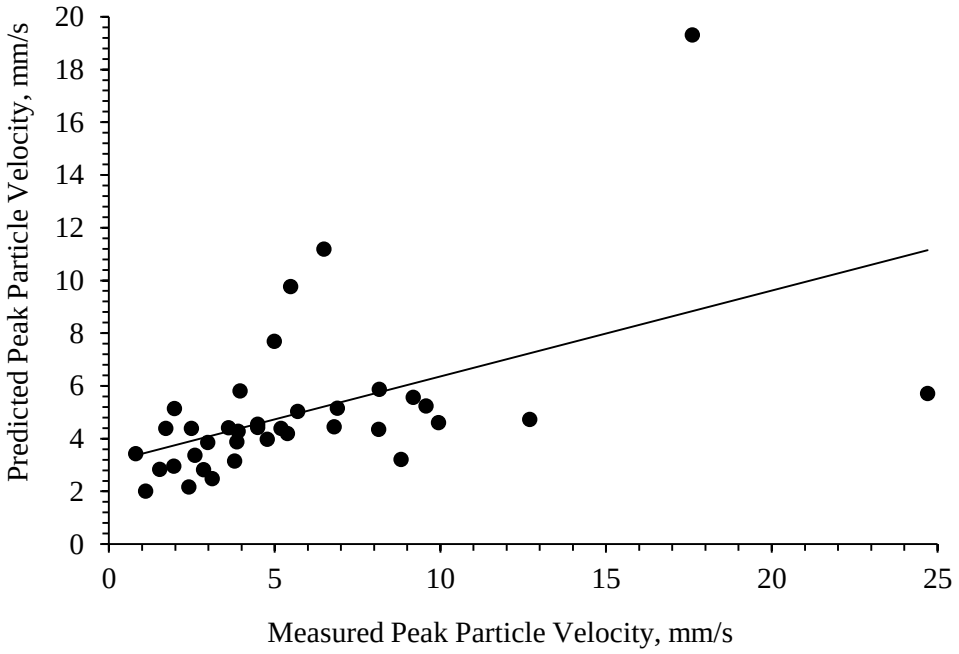

Figure 4.27: Relation between predicted PPV and measured PPV [Indian Standrad approach]

deviation values are 4.990 and 3.035respectively.These values when compared with the measured data show direct relation having correlation of determination of 25.6% with slope and constant of 0.325 and 3.106.

4.2.3.5 Prediction by CSIR approach

The graph 4.28 is plotted between predicted Peak particle velocities by USBM approach from equation and measured Peak Particle velocities values. The mean and standard

$$76.87(\frac{D}{\sqrt{Q}})^{-1} + 2.382 \quad (59)$$

deviation values are 5.787 and 2.566respectively.These values when compared with the measured data show direct relation having correlation coefficient of 0.295 with slope and constant of 0.295 and 4.077.

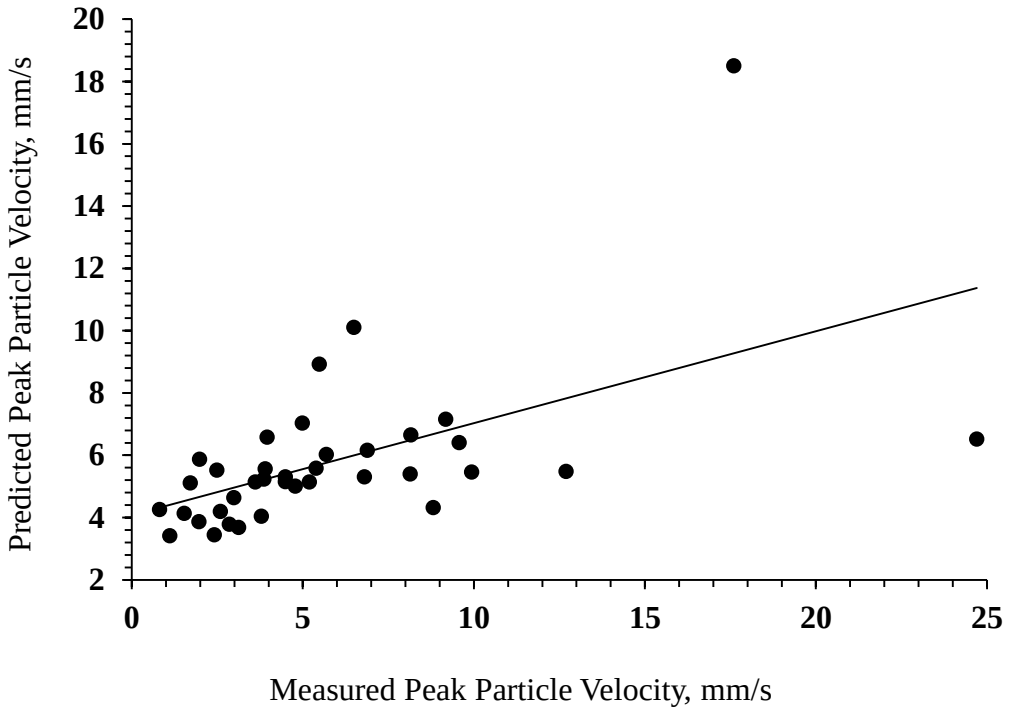

Figure 4.28: Relation between predicted PPV and measured PPV [CSIR approach]

4.2.4 Prediction by ANN

Introduction

Artificial neural network is a computer algorithm which works as human brain. Neural network commonly makes mistake as human brain. But it corrects mistakes by modifying the weight applied to each input parameter. The process of modifying the weights goes on until the network reaches the user friendly accuracy. The neural network model is used to predict the peak particle velocity on the basis of back propagation algorithm. Multilayer supervised learning network one of the best model of neural network to solve the problem

of training of neural network with best fit curve. This model consists of number of input patterns and the correct output.

4.2.4.1 Algorithm of back propagation neural network

Back propagation is a gradient descent system that tries to minimise the mean squared error. The following algorithm is implemented to minimise the mean square error.

Decide the neural network architecture

(# Hidden layers, #Neurons in each Hidden layer)

Decide the learning parameter and momentum

Initialize the network with random weights

While MSE is unsatisfactory

Do for each input pattern

Compute First hidden layer's nodes inputs;

Compute First hidden layer's nodes outputs;

Compute inputs to the output nodes

Compute the network outputs

Compute the MSE between the Predicted and Actual outputs

Back propagate the error and adjust the weights

(Weights adjustment between output layer and first hidden layer, then weight adjustment between first hidden layer and input layer)

End-Do

4.2.4.2 Prediction of PPV by ANN and compared with measured value

Steps as initialization of weights; feed-forward; back propagation of errors and updating of weights and biases are necessary for network training. Four input parameters such as distance, explosive, stemming, depth are considered and each parameter are represented by one neuron in the input layer. These four parameters chosen as they are known to influence the output parameter PPV significantly. Each input and target parameter consists of 37 data-set. For the training network 4-5-1 (Figure 4.21), all 37 datasets are divided using MATLAB code. The datasets for training (70%), validation (15%) and testing (15%) were selected randomly [94]. All these data sets exhibited statistical similarity. The various parameters for ANN has been selected iteratively and an optimal network has been found for the objective. ANN with different number of hidden layers are constructed and

different number of neuron in the hidden layers are constructed and the software was run. Then based upon the least error criterion, the optimised network having

one hidden layer with five neuron was chosen. Since the relationship of input parameters with the output is nonlinear in nature, a sigmoidal function was chosen. The hidden layer is made with five neurons. The training data were used for weight matrix (W) and bias vector (b) while test and validation data were used to monitor the accuracy and validation of the network. The logarithmic sigmoid function was used in hidden layer and linear transfer function was used in the output layer for function approximation. The network architecture is given in Figure4.21.

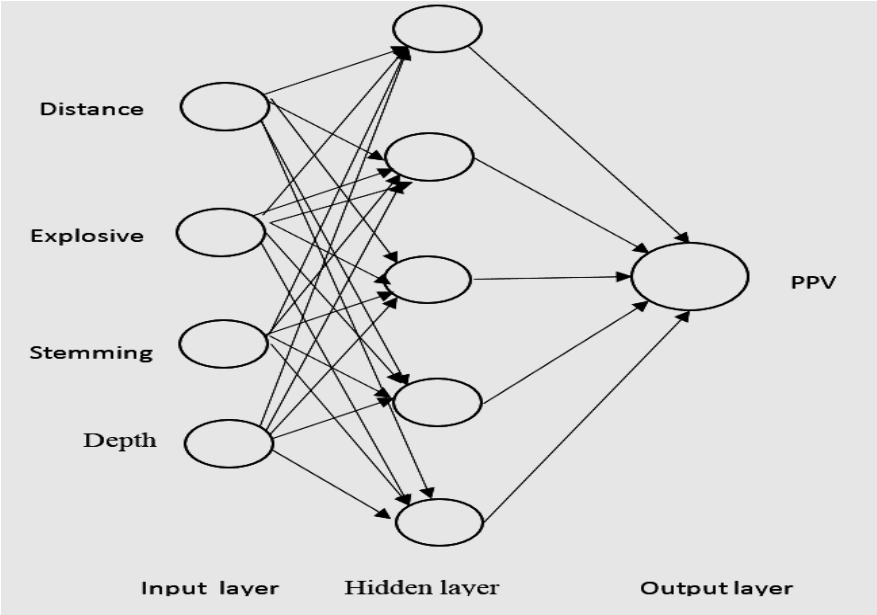

Figure 4.29 : 4-5-1 Architecture of ANN

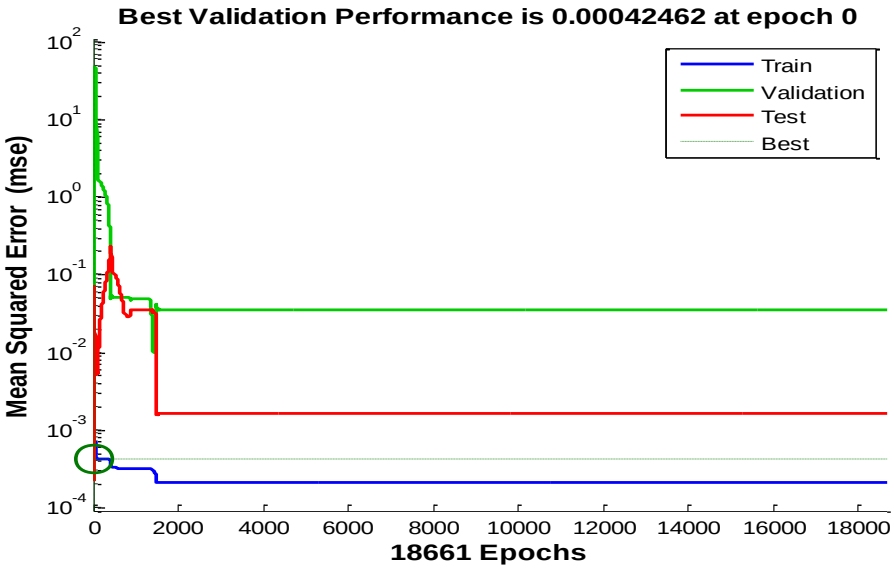

Figure 4.30: Mean square error vs. epochs for training, testing and validation

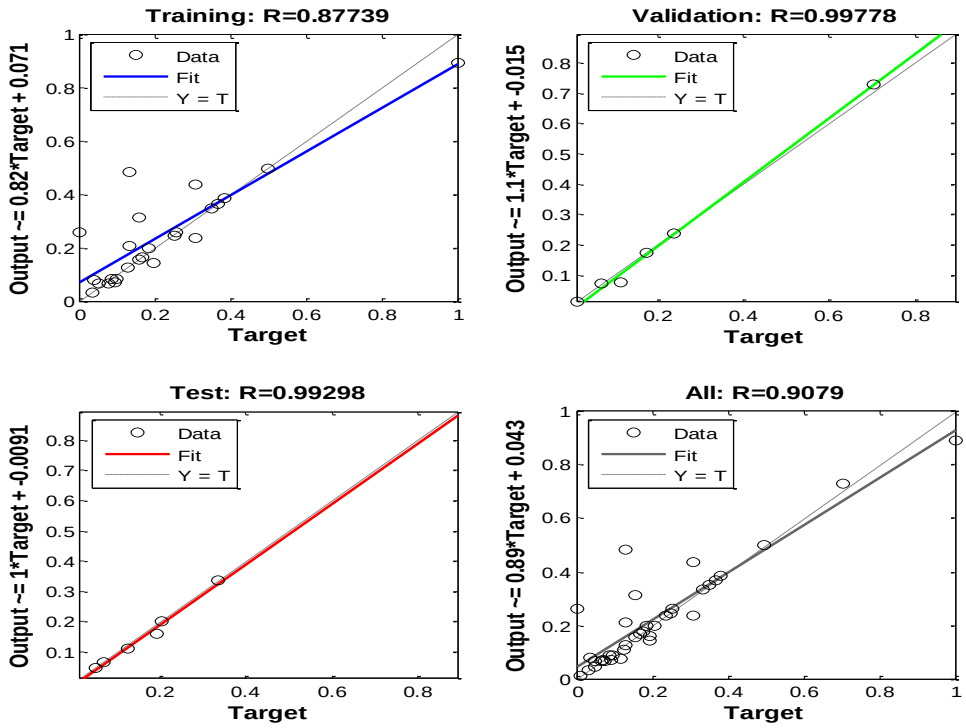

Figure 4.31: Training, validation and testing with all graph shows output vs. target

The predicted PPV values so determined from the ANN analysis were compared to that of the measured values (Figure 4.24). It shows direct relation having high correlation coefficient (R^2=0.824) with slope and constant of 0.886 and 1.123.

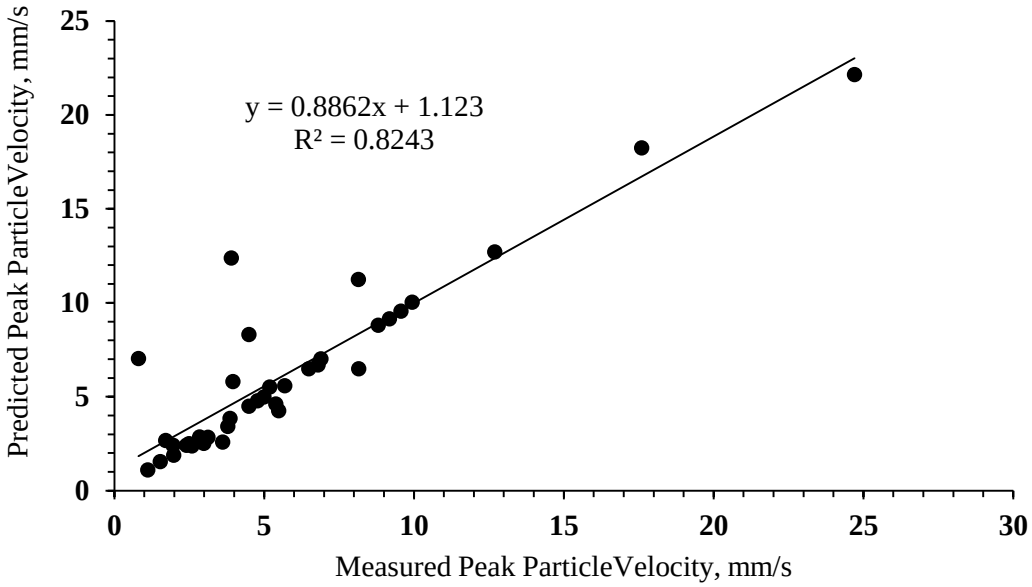

Figure 4.32: Predicted PPV vs. Measured PPV by ANN model

The mean and standard deviation values of predicted PPV values are 6.251 and 4.609 respectively.

Similar exercises between the ANN developed PPV and measure PPV values were carried out (Figure 4.30). The predicted PPV by ANN is much closer to the measured values as other predicted value of empirical equations. The PPV values predicted by empirical approaches show either an under-estimate or over-estimate as compared to that of measured PPV values. But predicted PPV by ANN show much closer value compared to PPV values predicted by empirical approaches.

4.2.5 Frequency vs. PPV for Koira and Daitari regions

4.2.5.1 Frequency vs. PPV for Koira region

Three component of PPV are plotted against three components of zero crossing and FFT frequency for iron ore mine in Figure 4.23 and 4.24. In case of FFT frequency, both transverse and longitudinal component shows maximum 23.1 Hz FFT frequency at 1.22 mm/s peak particle velocity. The longitudinal components shows maximum 32 Hz zero crossing frequency at 1.52 mm/s peak particle velocity where minimum 0 Hz zero crossing frequency at 0.254mm/s peak particle velocity. From both FFT and zero crossing graphs it is concluded that longitudinal component shows greater frequency at lower particle velocity.

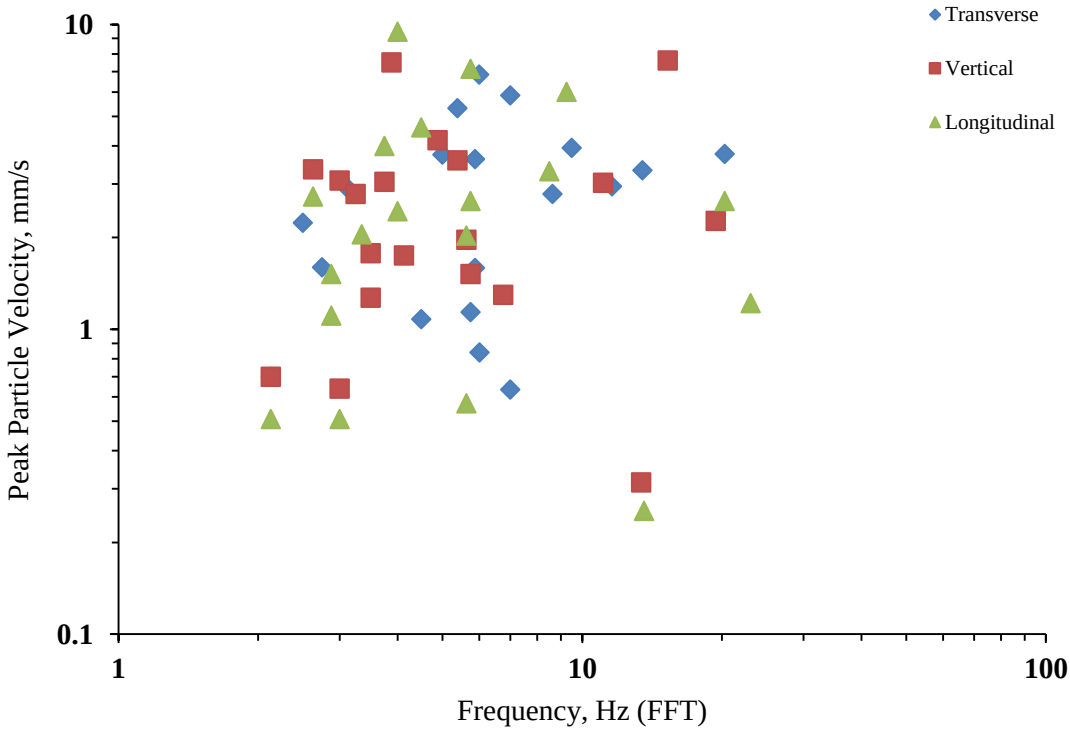

Figure 4.33: Three component of PPV vs. three component of FFT frequency

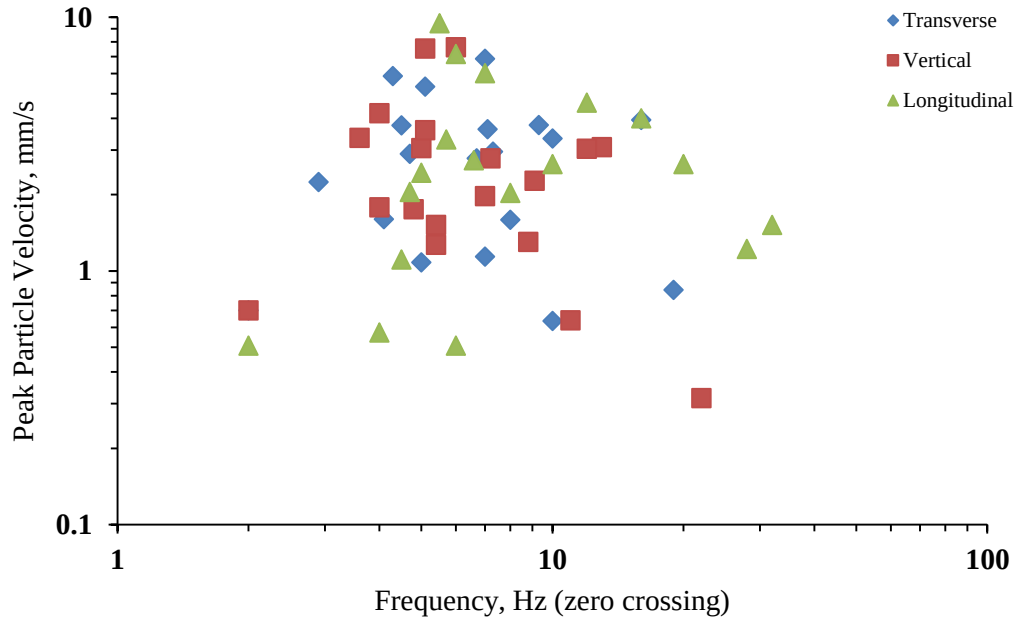

Figure 4.34: Three component of PPV vs. three component of ZC frequency

4.2.5.2 Frequency vs. PPV for Daitari region

Same as iron ore mines of Koira region, all the three component of PPV are plotted against FFT and ZC frequency of ground vibration in Figure 2.46 and 2.47. In case of FFT frequency transverse component shows maximum 11 Hz frequency at 7.37 mm/s where minimum 2 Hz frequency at 16.5 mm/s peak particle velocity. The longitudinal component shows maximum 17 Hz zero crossing frequency at 5.08 mm/s peak particle velocity and minimum 0 Hz frequency at 10.2 mm/s peak particle velocity. The longitudinal component shows maximum 17 Hz zero crossing frequency.

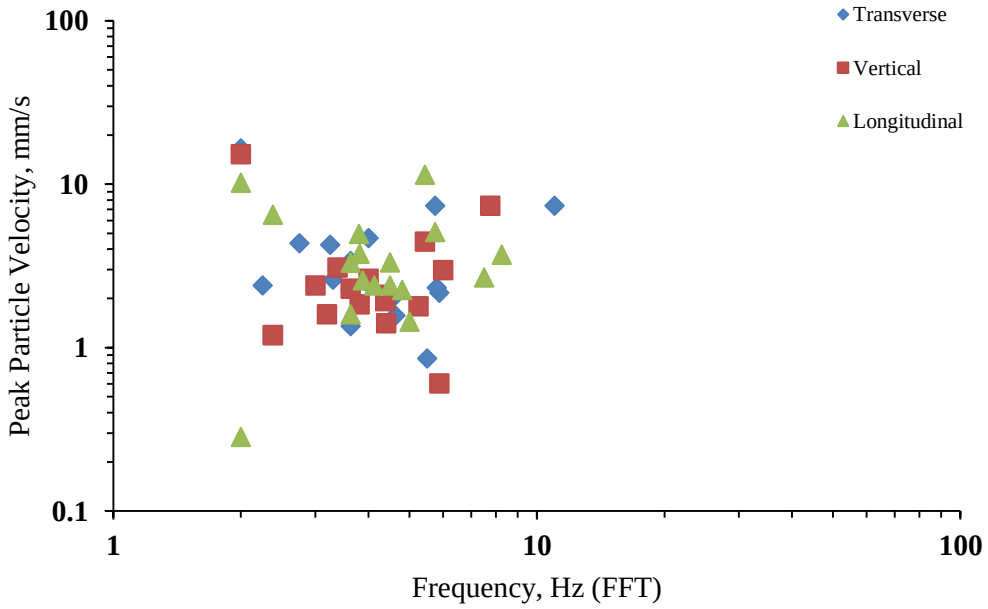

Figure 4.35: Three component of PPV vs. three component of FFT frequency

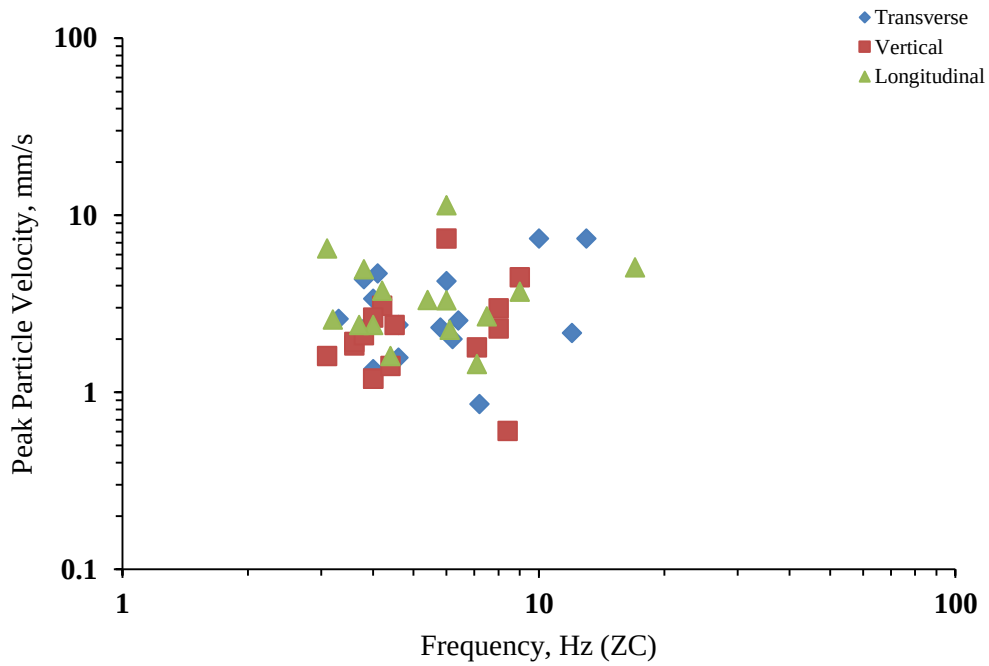

Figure 4.36: Three component of PPV vs. three component of ZC frequency

4.2.6 Statistical Analysis of maximum charge per delay

The maximum charge per delay has been calculated by using different predictor's equation by back calculation while PPV as constant 10 mm/s according to DGMS guidelines. The graph(Figure 28) plotted between maximum charge per delay by different predictor equation and assumed distance from 50 to 600 with interval fifty shows higher trend in case of Ambraseys-Hendron equation and lower trend in case of Langfors-Khilstrom equation.

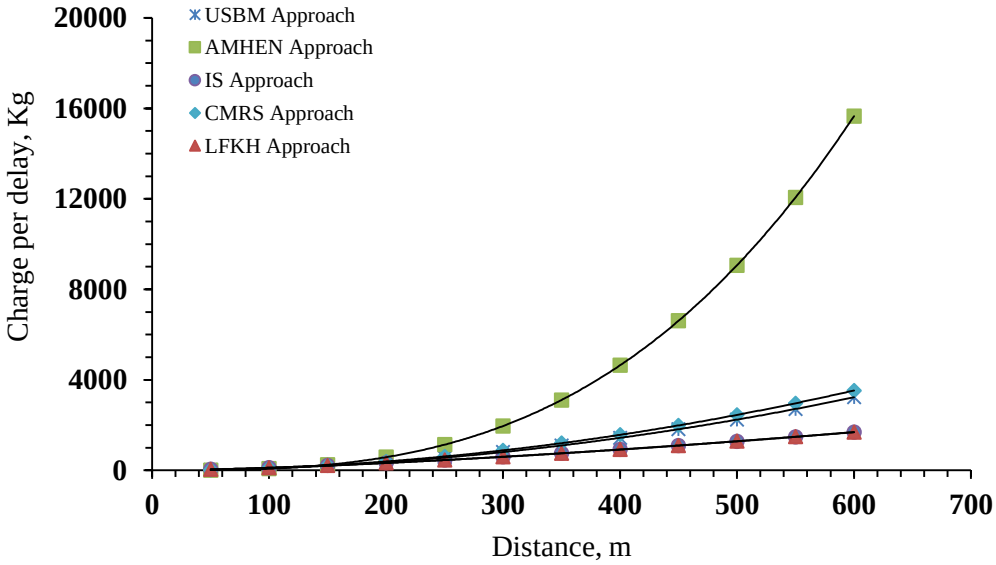

Figure 4.37: Charge per delay vs. Distance

4.2.7 Statistical Analysis of Air Noise

4.2.7.1 Analysis of Air Noise for iron ore mine Koira region

Air over pressure was recorded for iron ore mine varied from 100 dB to 142 dB. Air over pressure is the function of radial distance and cube root of maximum charge per delay. Air over pressure is plotted against cube root of scaled distance and the mutual relationship is expressed in exponential trend line as per [75].

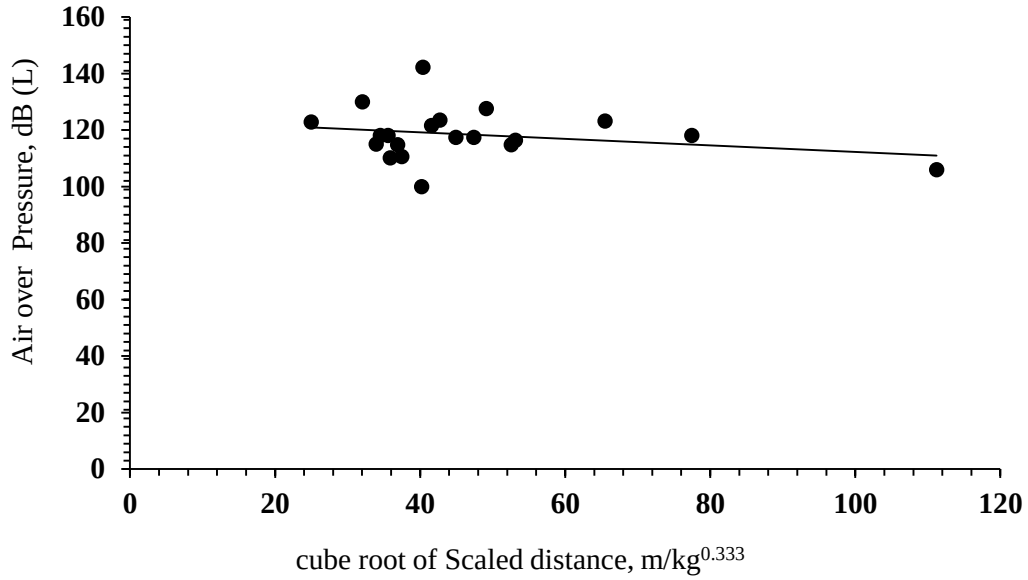

Figure 4.38: Relation between Air noise pressure and cube root scaled distance

4.2.7.2 Analysis of Air Noise Daitari region

Air over pressure was recorded for iron ore mine varied from 110.2 dB to 146dB. Air over pressure is the function of radial distance and cube root of maximum charge per delay. Air over pressure is plotted against cube root of scaled distance and the mutual relationship is expressed in exponential trend line as per [75].

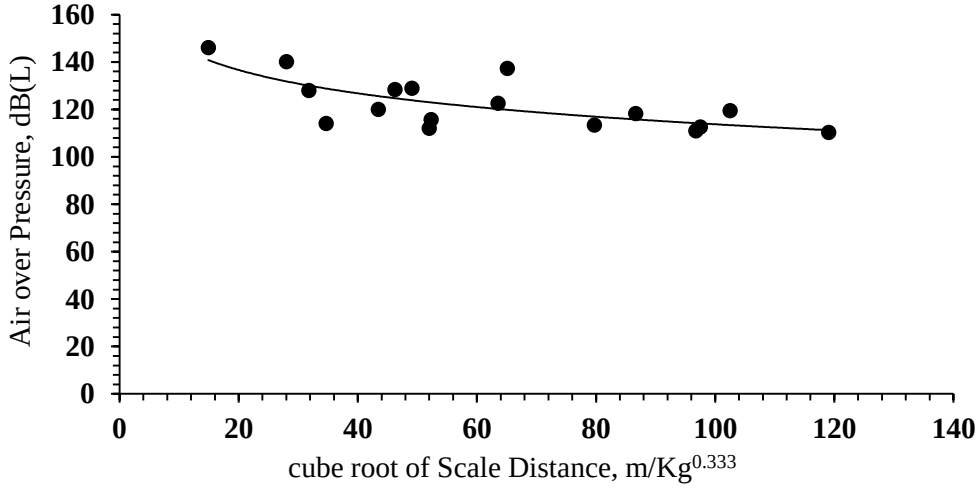

Figure 4.39: Relation between Air noise pressure and cube root scaled distance

4.2.8 Statistical Analysis of Rock Fragmentation

4.2.8.1 Determination of Average size (X_{50}) from image analysis

Fragmentation analysis of the 9 blast event of iron ore mine of Koira and Daitary region were carried out by dedicated software code WIPFRAG (ver. 2010). It is an image analysis system for sizzling materials such as blasted and crushed rock [87]. The methodology used in WIPFRAG consists of image input, image processing and output stage of analysis. First stage,image of fragmented rock after blasting captured by digital camera used as input in WIPFRAG. Second stage consists of image processing by transform the rock fragments image in to binary image consisting of net of block outlines. The algorithim of WIPFRAGconsist automatic identification of individual blocks and create outline "net" by using by using state of the art edge detection. It measures the image in a 2D net and then convert the same to 3D, using principle of geometric probability [88]. Third stage consists of generating the cummulative curve in terms of graphs by using the Rosin–Rammler equation. Several images of each patch analysed individually by WIPFRAG and merged into single cumulative graph. The average percentage of passing size (X_{50}) of rock fragments with powder factor, explosive amount and rock factor were considered for analysis.

Table 4.10: Average percentage of passing size (X50) of rock fragments with powder factor, explosive amount and rock factor

Sl. No.	Powder factor (kg/m^3)	Explosive amount per each hole (Kg)	Rock Factor	Average size, (X_{50})
1	0.367	13.9	2.88	8.79
2	0.37	12.97	3.22	7.68
3	0.549	41.7	6.3	9.03
4	0.499	44.48	5.76	9.53
5	0.292	41.7	2.22	8.42
6	0.371	19.48	4.54	6.33
7	0.399	29.537	4.87	25.47
8	0.447	29.844	5.34	16.47
9	0.431	17.622	6.15	35.56

4.2.8.2 Analysis of effect of average size (X_{50}) with respect to explosive density/powder factor (Kg/m^3)

Variation in powder factor from 0.292 to 0.549 (Kg/m^3**)** affect mean size while it is plotted against mean fragmentation size. The graph shows with increase in powder factor, the mean fragmentation size increase. So the graph 4.32 shows direct relationship between mean fragmentation size and powder factor.

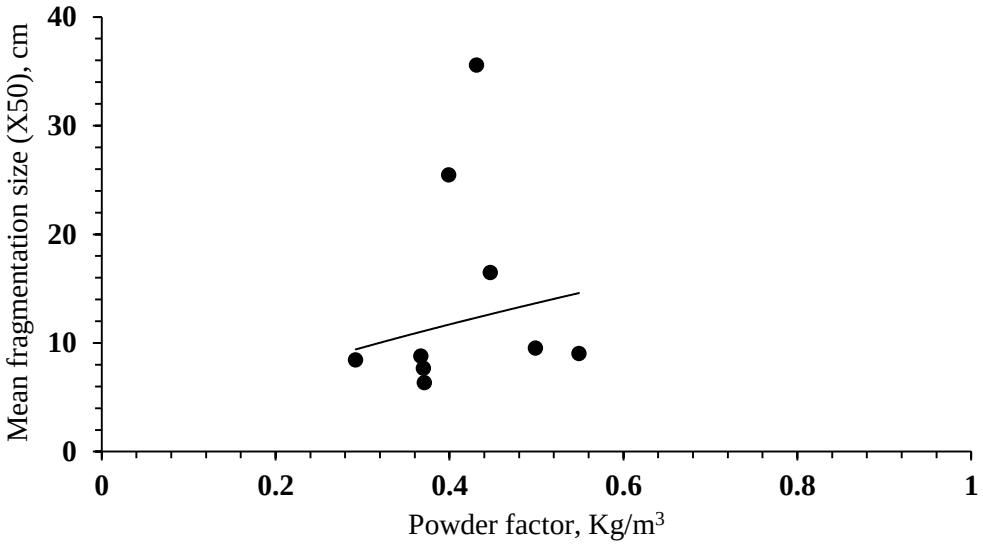

Figure 4.40: Mean fragmentation size (X_{50}), (cm) vs. Powder factor (Kg/m^3)

4.2.8.3 Analysis of effect of average size (X_{50}) with respect to explosive charge (Kg)

Variations in explosive charge per hole from 13.9 to 44.48 (Kg) affects mean size while it is plotted against mean fragmentation size. The graph shows with increase in explosive charge, the mean fragmentation size decrease. So the graph 4.32 shows inverse relationship between mean fragmentation size and explosive charge.

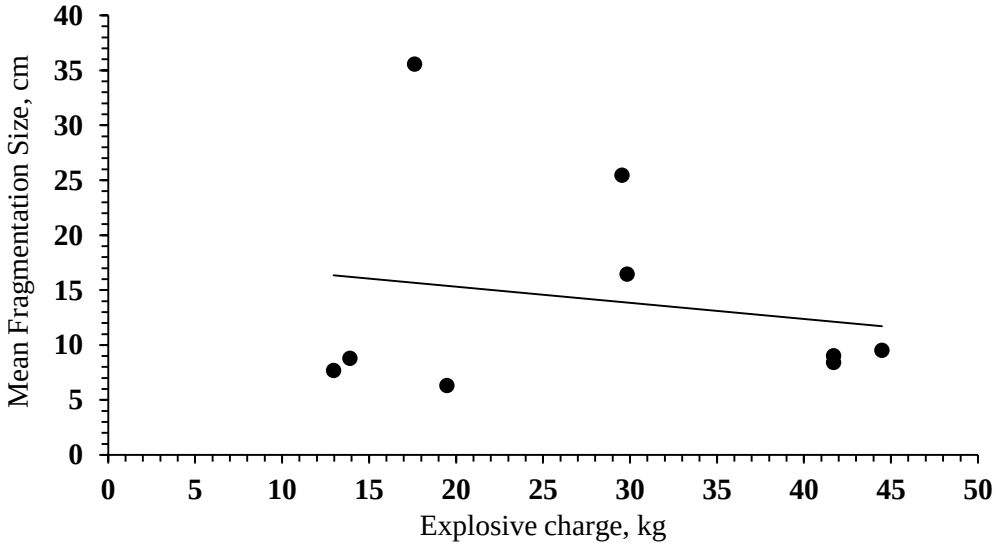

Figure 4.41: Mean fragmentation size vs. Explosive charge

4.2.8.4 Analysis of effect of average size (X_{50}) with respect to hole depth (m)

Variation in hole depth from 5 to 7.95 (m) affect mean size while it is plotted against mean fragmentation size. The graph shows with increase in hole depth, the mean

fragmentation size sharply decrease. So the graph 4.32 shows inverse relationship between mean fragmentation size and hole depth.

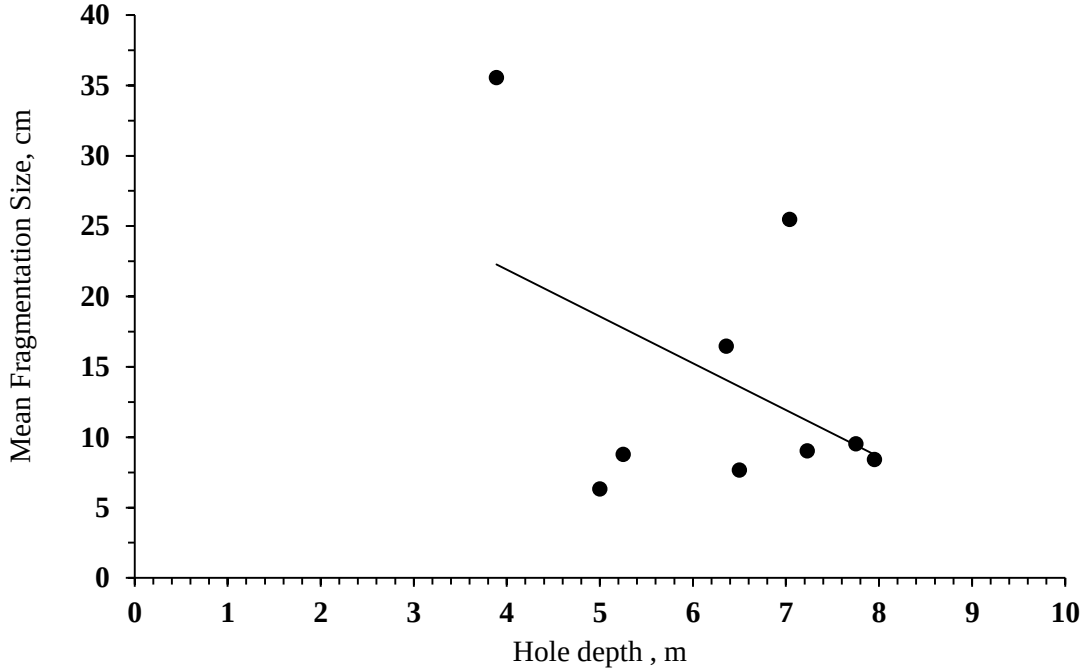

Figure 4.42: Mean fragmentation size (X_{50}) vs. hole depth (m)

4.2.8.5 Mean fragmentation size Prediction by Multiple Linear Regression Analysis

Multiple regression analysis is used to predict linear relationship between a dependent variable and one or more independent variable. It is based on the principle that minimized sum of squares of differences of predicted and measured value and is given by

$$y = b_0 + b_1x_1 + b_2x_2 + \ldots\ldots\ldots\ldots + b_nx_n + \beta \quad (60)$$

(Where, b_0=intercept, β=error associated with predictor and b_1,b_2,$b_n$are coefficient on the n^{th} predictor)

The multiple regression analysis was carried out to predict the mean fragmentation size at corresponding powder factor, explosive quantity and rock factor at 95 % confidence interval. The governing relation is obtained from the regression analysis as below.

$$X_{50} = 32.194 - 0.108(\exp lossive) - 149(powderfactor) + 10(rockfactor) \quad (61)$$

The predicted values of mean fragmentation size were compared with that of the measured values (Figure4.41). There exists a good correlation between the two approaches(R=0.772) with slope and constant of 0.596 and 5.706.

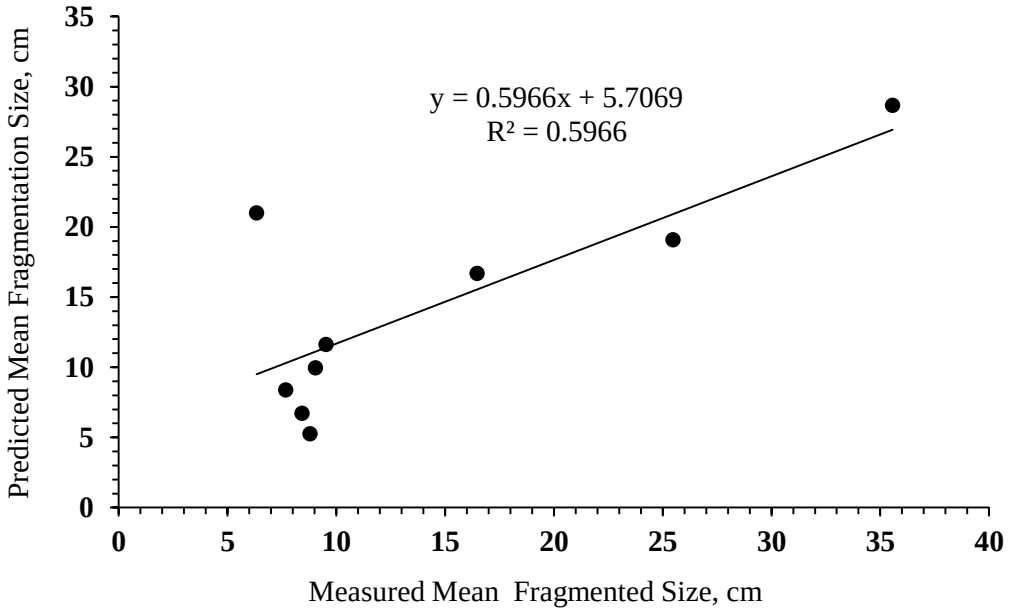

Figure 4.43: Predicted Mean fragmentation size vs. Measured Mean fragmentation size

4.2.9 Flyrock

Fly rocks are dangerous effects of blasting operation. It depends upon blast design layout and drilling and loading of explosive. In the last stage of gas expansion when the burden released, the remaining pressure used to heave and throw the rock. Fly rock distance value with respect to specific charge and diameter of hole of some blasts of both Koira and Daitari region iron ore mine.

Table 4.11: Blasting parameter with flyrock Distances

Sl. No.	Specific charge (Kg/m^3)	Diameter (m)	Stemming (m)	Depth (m)	Flyrock (m)	Flyrock(m)×Diameter(m)
1	0.367	0.1	2.72	7.23	38	3.8
2	0.424	0.1	2	7.75	46	4.6
3	0.305	0.1	3.8	8	47	4.7
4	0.330	0.1	1.7	4	47	4.7
5	0.241	0.1	2.4	5	52	5.2
6	0.395	0.1	2.3	7.04	65	6.5
7	0.446	0.1	1.32	6.36	56	5.6
8	0.421	0.1	1.5	4	57	5.7
9	0.431	0.1	1.04	3.89	65	6.5
10	0.691	0.1	1.35	4.5	95	9.5
11	0.794	0.1	1.25	3.5	118	11.8
12	0.384	0.102	3.21	6.5	63	6.43
13	0.35	0.102	1.8	4	57	5.81
14	0.395	0.102	3.21	6.5	64	6.53
15	0.355	0.102	2.74	6.5	67	6.83

4.2.9.1 Fly rock (m) with respect to stemming length (m)

The relation between fly rock and stemming length shows inverse relationship by plotting stemming length against fly rock which means increase in stemming length decrease in fly rock distance. The graph 4.36 shows linear decreasing trend line between fly rock and stemming length.

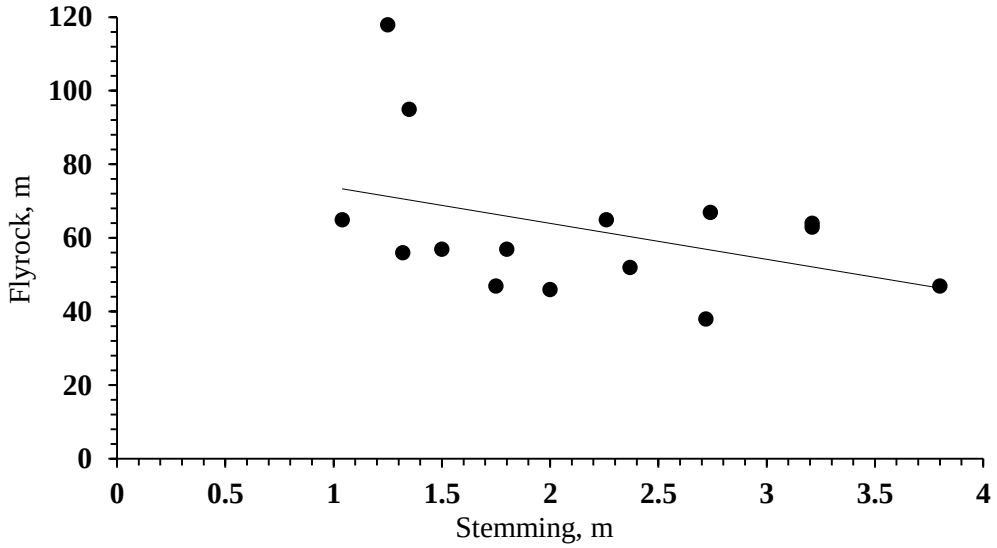

Figure 4.44: Fly rock, m VS. Stemming length, m

4.2.9.2 Fly rock (m) with respect to hole depth (m)

The relation between fly rock and hole depth shows inverse relationship by plotting hole depth against fly rock which means increase in hole depth decrease in fly rock distance. The graph 4.37 shows linear decreasing trend line between fly rock and hole depth.

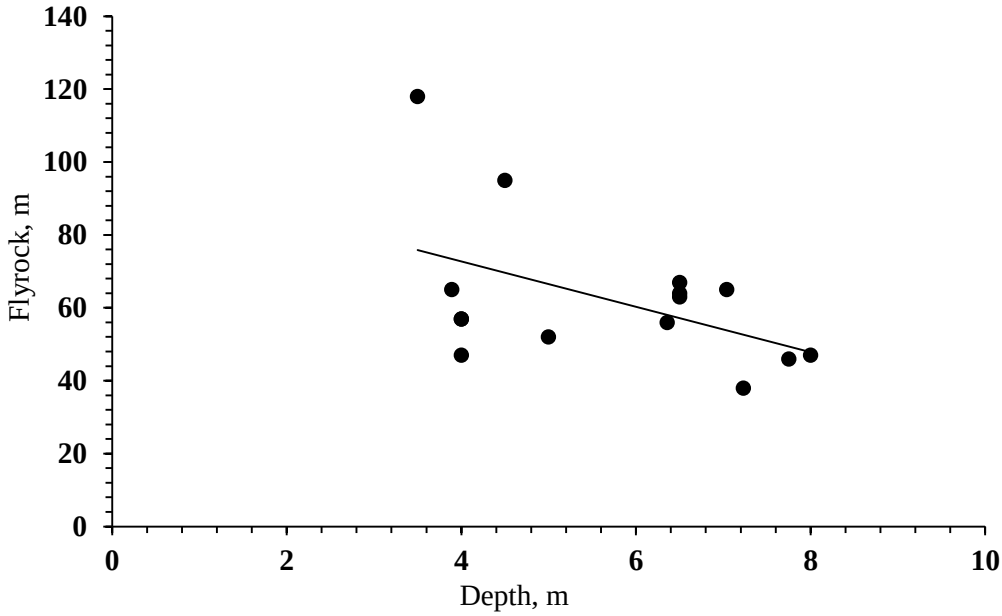

Figure 4.45: Fly rock (m) vs. Depth (m)

4.2.10 Relationship between Specific charge(Kg/m^3) and Fly rock (m)

The graph (Figure 4.45) between specific charge (Kg/m^3) and flyrock (m)×Diameter(m) was plotted and resultant equation [89]with correlation coefficient (0.774) is

$$\frac{12.56\times\alpha+0.997}{\varphi} \tag{62}$$

Where α and φ are specific charge (Kg/m^3) and hole diameter (m) respectively.

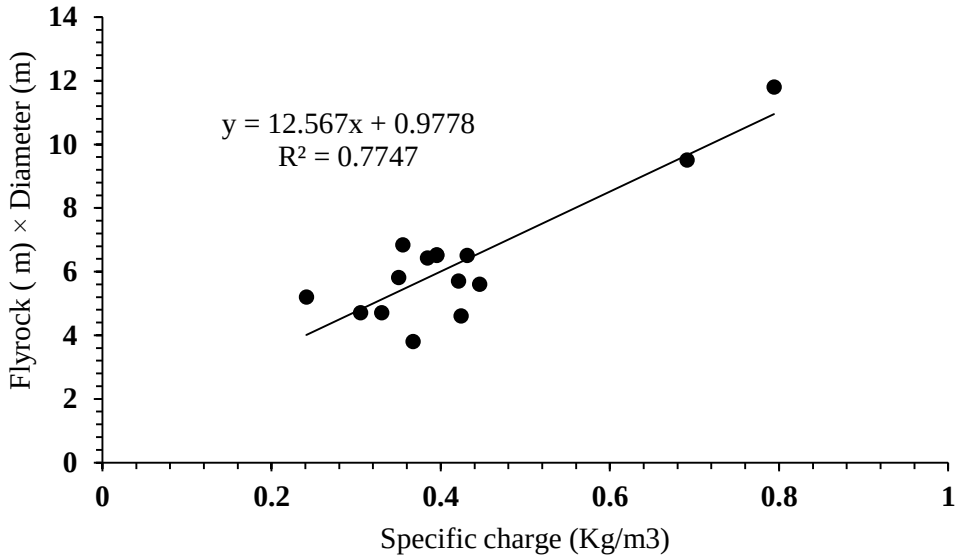

Figure 4.46: Flyrock (m) × Diameter (m) vs. Specific charge (Kg/m^3)

Chapter 5
Conclusion

- The compressive and tensile strength of rock sample collected from both iron ore mine of Koira and Daitary region from 72.19 to122.7 MPa and 5.455 to 8.41 MPa respectively where elastic parameter such as Poisson's ratio and young's modulus varied from 0.021 to 0.054 and 9 to15 GPa. The mean values of compressive and tensile strength of rock sample of both mines are 98.547 and 6.754 where standard deviation values are 21.755 and 1.254 respectively. Also mean values of Poisson's ratio and young's modulus are 0.0335 and 11.7 where standard deviation values are0.0147 and 2.521 respectively.
- The P-wave and S-wave value of rock sample varied from 5856 to 5871 m/s and 3247 to 3258 m/s respectively. The mean values of P-wave and S-wave of rock samples are 5863 and 3254.25 where standard deviation values are 6.480 and 4.9916.
- The site constants recommended by USBM, Ambraseys–Hendron, Langefors–Kihlstrom, Indian Standard and CMRI approaches for iron ore mines were used. But the PPV values obtained did not compare favorably with the measured PPV.
- The site constant values were determined using those five equations with measured PPV. The Ambraseys–Hendron approach exhibited best relation with R^2 (0.36).
- ANN approach was used to evaluate the blast vibration.
- The ANN derived PPV values compared favorably with the measured PPV values. The correlation coefficient obtained was 0.82.
- The frequency of PPV varied between 0 to 32 Hz (Koira region) and 0 to 17 Hz (Daitari region).The longitudinal component showed maximum frequency at lower PPV.
- Three component of PPV plotted against three component of zero crossing graph in both case of iron ore mine of Daitari and Koira region. It is concluded that longitudinal component shows greater frequency at lower particle velocity. But in case of iron mine of Koira region transverse component shows maximum 11 Hz frequency at 7.37mm/s where longitudinal component shows maximum 17 Hz zero crossing frequency.
- The maximum charge per delay calculated from different predictor equation by back calculation shows linear trend. Ambraseys-Hendron equation shows higher trend while Langefors-Khilstrom equation shows lower trend.
- Air over pressure was recorded for varied from 100 to142 dB and 110.2 to 146 dB for iron ore mines located in Koira region and Daitari region respectively. The relation between air over pressure and cube root of scaled distance shows inverse linear trend in both cases. The Air over Pressure data collected from Daitari region shows better correlation coefficient of 50.7%. than Koira region.

- Total nine blast photograph of rock pile after blasting was analyzed by WIPFRAG software to find average fragmentation size(X_{50}).The average passing size was plotted against powder factor or explosive density, explosive charge with hole depth. The graph shows linear trend in case of powder factor where inverse linear trend shown by explosive charge and hole depth. Multiple linear regression analysis was used for average size prediction and there exists good correlation of 59.6% between predicted and measured value.
- Fly rock distance of fifteen blast event of both iron ore mine of Koira and Daitari region were combined. A resultant equation of fly rock distance ($\frac{12.56\times\alpha+0.997}{\varphi}$) were generated with correlation of coefficient (0.774). The trend of fly rock distance with explosive, stemming length and hole depth show linear relation in case of explosive and inverse relation in case of stemming length and hole depth.

Scope for further Research

This investigation was a limited exercise by time as well as parameters. This should be investigated for more no of operating iron ore mines to collect more data and hence a comprehensive conclusion.

Bibliography

1. Eloranta, J. *The efficiency of blasting versus crushing and grinding*. in *Proceedings of the 23rd Conference of Explosives and Blasting Technique. Las Vegas, Nevada. February*. 1997.
2. Beyglou, A.H., *Improvement of blast-induced fragmentation and crusher efficiency by means of optimized drilling and blasting in Aitik.* 2012.
3. Bhandari, S., *Engineering rock blasting operations.* A. A. Balkema. 388, 1997: p. 388.
4. Kutter, H. and C. Fairhurst. *On the fracture process in blasting*. in *International Journal of Rock Mechanics and Mining Sciences & Geomechanics Abstracts*. 1971: Elsevier: P.189-202.
5. Siskind, D.E. and R.R. Fumanti. *Blast-produced fractures in Lithonia granite: 23F. US. Bur. Mines, RI 7901, 1974, 38P*. in *International Journal of Rock Mechanics and Mining Sciences & Geomechanics Abstracts*. 1974: Pergamon.
6. Singh, S. *The Effect of Shock and Gas Energies on Rock Fracturing Process*. in *Proceedings Of The Annual Conference On Explosives And Blasting Technique*. 1999: International Society Of Explosives Engineers.
7. Konya, C.J. and E.J. Walter, *Surface blast design*. 1990: Prentice-Hall.
8. P.K.Rajmeny, A.j., Sushil Bhandari, *Blast Designing: Theory & Practical.* 2006: p. 83-84.
9. Konya, C.J., *Spacing of explosive charges.* MS Thesis, Department of Mining and Petroleum Engineering, University of Missouri at Rolla, 1968.
10. Langefors, U. and B. Kihlström, *The modern technique of rock blasting*. 1978: John Wiley & Sons.
11. Ash, R.L., *The design of blasting rounds*, in *Surface mining*. 1968, AIME, New York. p. 373-397.
12. Vutukuri, V. and S. Bhandari. *Some aspects of design of open pit blasts*. in *National Symposium on Rock Fragmentation, Adelaide, February 26-28, 1973*. 1973: Institution of Engineers, Australia.
13. Rajmeny, P., U. Singh, and S. Rathore, *A new model to estimate rock mass strength accounting for the scale effect.* International Journal of Rock Mechanics and Mining Sciences, 2004. 41(6): p. 1013-1021.
14. Bhandari, S. and V. Vutukuri, *Rock fragmentation with longitudinal charges.* Proc. 3rd Int. Cong. Rock Mech. Denver, US, 1974: p. 1337-1342.
15. Rajmeny, P., A. Joshi, and S. Bhandari, *Blast designing: theory and practice.* Himanshu, Publ.New Delhi, 2006.
16. Singh, T. and R. Dubey, *A study of transmission velocity of primary wave (p-wave) in coal measure sandstone.* Journal Of Scientific And Industrial Research, 2000. **59**(6): p. 482-486.

17. Nobel, D., *Blasting and Explosives Quick Reference Guide-2010.* 2010, REF0110/0210/AZZAUS.
18. Hino, K., *Theory and practice of blasting*. 1959.Asa ,Japan : Nippon Kayaku Company.
19. Persson, P., N. Lundborg, and C. Johannsson, *The basic mechanisms in rock blasting*. 1970.
20. Monjezi, M. and H. Dehghani, *Evaluation of effect of blasting pattern parameters on back break using neural networks.* International Journal of Rock Mechanics and Mining Sciences, 2008. 45(8): p. 1446-1453.
21. Armaghani, D.J., et al., *Neuro-fuzzy technique to predict air-overpressure induced by blasting.* Arabian Journal of Geosciences, 2015. 8(12): p. 10937-10950.
22. Hustrulid, W.A., *Blasting principles for open pit mining: general design concepts*. 1999: Balkema Publications.
23. Ricker, N., *Transient waves in visco-elastic media*. Vol. 10. 2012: Elsevier Scientific Publication Company, Amsterdam, Oxford, New York.
24. Khandelwal, M. and T. Singh, *Prediction of blast-induced ground vibration using artificial neural network.* International Journal of Rock Mechanics and Mining Sciences, 2009. 46(7): p. 1214-1222.
25. Amnieh, H.B., A. Siamaki, and S. Soltani, *Design of blasting pattern in proportion to the peak particle velocity (PPV): Artificial neural networks approach.* Safety science, 2012. 50(9): p. 1913-1916.
26. Michel M.Wood, K.E., carol Asial and wayne pennington *earthquake:Upseis, An educational site for building and seismologists,online publication.* michigen Technological university 2007.
27. Duvall, W.I. and D.E. Fogelson, *Review of criteria for estimating damage to residences from blasting vibrations*. 1962: US Department of the Interior, Bureau of Mines.
28. Nicholls, H.R., C.F. Johnson, and W.I. Duvall, *Blasting vibrations and their effects on structures*. 1971: US Government Printers.
29. Dowding, C., *Monitoring and control of blast effects.* SME Mining Engineering Handbook publication, 1992.
30. Adhikari, G., et al., *Role of blast design parameters on ground vibration and correlation of vibration level to blasting damage to surface structures.* Indian National Institute of Rock Mechanics (September 2005), 2005.
31. Mines, U.S.B.o. and D. Siskind, *Structure response and damage produced by ground vibration from surface mine blasting*. 1980: US Department of the Interior, Bureau of Mines.
32. Ambraseys, N., *Rock mechanics in engineering practice*. 1968: John Wiley & Sons, Incorporated, 111 River Street Hoboken, NJ 07030-6000 USA.p.455
33. Standard, I., *Criteria for safety and design of structures subjected to under ground blast.* ISI., IS-6922, 1973.

34. Roy, P., *Putting ground vibration predictions into practice.* Colliery Guardian, 1993. 241(2): p. 63-7.
35. Roy, P.P., *Vibration control in an opencast mine based on improved blast vibration predictors.* Mining Science and Technology, 1991. 12(2): p. 157-165.
36. Singh, B., ed. *investigation of blasting pattern and geo technical properties of the sorrounding rock mass on the ground vibration, fragmentation, fly rock etc*. 1991. p.7-87.
37. Esen, S. and H. Bilgin. *Evaluation of Blast Vibrations From Sekkoy Surface Coal Mine in Turkey*. in *Proceedings Of The Annual Conference On Explosives And Blasting Technique*. 2001: ISEE; 1999.
38. Mandal, B., *Implementation of DGMS Guidelines for ergonomics risk assessment of mining operations.*
39. Skipp, B.O., *Ground vibration–codes and standards.* Ground dynamics and man-made processes. The Institution of Civil Engineers, United Kingdom, 1998: p. 29-41.
40. Nick, S., *Preliminary Vibration Assessment* ,2002.
41. Trivedi, R., T. Singh, and A. Raina, *Prediction of blast-induced flyrock in Indian limestone mines using neural networks.* Journal of Rock Mechanics and Geotechnical Engineering, 2014. 6(5): p. 447-454.
42. Carcedo, F.A., C.L. Jimeno, and C. Jimeno, *Drilling and blasting of rocks.* AA Balkema, Rotterdam, Netherlands, 1995.
43. Morhard, R.C., *Explosives and rock blasting*. 1987: Atlas Powder Company.
44. Linehan, P. and J. Wiss, *Vibration and air blast noise from surface coal mine blasting.* 1980.
45. Kuzu, C., A. Fisne, and S. Ercelebi, *Operational and geological parameters in the assessing blast induced airblast-overpressure in quarries.* Applied Acoustics, 2009. 70(3): p. 404-411.
46. Kamperman, G.W. and M.A. Nicholson, *The Transfer Function of Quarrry Blast Noise and Vibration Into Typical Residential Structures*. 1977: Environmental Protection Agency, Office of Noise Abatement and Control.
47. Khandelwal, M. and P. Kankar, *Prediction of blast-induced air overpressure using support vector machine.* Arabian Journal of Geosciences, 2011. **4**(3-4): p. 427-433.
48. Siskind, D.E., et al., *Structure response and damage produced by airblast from surface mining*. 1980, Bureau of Mines, Twin Cities, MN (USA). Twin Cities Research Center.
49. Hopler, R.B., *Blasters' Handbook*. 1998: International Society of Explosives Engineers.
50. Armaghani, D.J., et al., *Blasting-induced flyrock and ground vibration prediction through an expert artificial neural network based on particle swarm optimization.* Arabian Journal of Geosciences, 2014. **7**(12): p. 5383-5396.
51. Kahriman, A., *Analysis of parameters of ground vibration produced from bench blasting at a limestone quarry.* Soil Dynamics and Earthquake Engineering, 2004. **24**(11): p. 887-892.

52. Khandelwal, M. and T. Singh, *Evaluation of blast-induced ground vibration predictors.* Soil Dynamics and Earthquake Engineering, 2007. **27**(2): p. 116-125.

53. Uysal, Ö., E. Arpaz, and M. Berber, *Studies on the effect of burden width on blast-induced vibration in open-pit mines.* Environmental geology, 2007. **53**(3): p. 643-650.

54. Nateghi, R., *Prediction of ground vibration level induced by blasting at different rock units.* International Journal of Rock Mechanics and Mining Sciences, 2011. 48(6): p. 899-908.

55. Stojadinovic, S., M. Zikic, and R. Pantovic, *A New Approach to Blasting Induced Ground Vibrations and Damage to Structures.* Acta Montanistica Slovaca, 2011. 16(4): p. 344.

56. Dehghani, H. and M. Ataee-Pour, *Development of a model to predict peak particle velocity in a blasting operation.* International Journal of Rock Mechanics and Mining Sciences, 2011. 48(1): p. 51-58.

57. Caylak, C., et al., *Importance of ground properties in the relationship of ground vibration–structural hazard and land application.* Journal of Applied Geophysics, 2014. 104: p. 6-16.

58. Hosseini, M. and M.S. Baghikhani, *Analysing the Ground Vibration Due to Blasting at AlvandQoly Limestone Mine.* International Journal of Mining Engineering and Mineral Processing, 2013. **2**(2): p. 17-23.

59. Mandal, S.K., N. Bhagat, and M. Singh, *Magnitude of vibration triggering component determines safety of structures.* Journal of Mining and Environment, 2014. **5**(1): p. 35-46.

60. M. A. Saliu, A.F.A., I. A. Okewale, *Correlation between Blast Efficiency and Uniaxial Compressive Strength.* International Journal of Engineering and Technology, 2013. **3** (8).

61. Choudhary, B.S. and K. Sonu, *Assessment Of Powder Factor In Surface Bench Blasting Using Schmidt Rebound Number Of Rock Mass.*

62. Mohan, V. and N. Dey, *Assessment of Ground Vibration and Plotting of Contour Map of Surface Mine Blasting.* Journal of The Institution of Engineers (India): Series D, 2014. 95(1): p. 1-6.

63. H.P. Karkar, S.S.R., *Evaluation and Assesment of blast induced ground vibration and flyrock in Iron Ore Mine.* The Indian Mining and engineering journal., 2016. 55(1): p. 08-15.

64. Esen, S., I. Onederra, and H. Bilgin, *Modelling the size of the crushed zone around a blasthole.* International Journal of Rock Mechanics and Mining Sciences, 2003. 40(4): p. 485-495.

65. Kuznetsov, V., *The mean diameter of the fragments formed by blasting rock.* Journal of Mining Science, 1973. 9(2): p. 144-148.

66. Cunningham, C. *Fragmentation estimations and the Kuz-Ram model-Four years on*. in *Proc. 2nd Int. Symp. on Rock Fragmentation by Blasting*. 1987.

67. Gheibie, S., et al., *Modified Kuz—Ram fragmentation model and its use at the Sungun Copper Mine.* International Journal of Rock Mechanics and Mining Sciences, 2009. 46(6): p. 967-973.

68. Bahrami, A., et al., *Prediction of rock fragmentation due to blasting using artificial neural network.* Engineering with Computers, 2011. 27(2): p. 177-181.
69. Verakis, H. and T. Lobb. *An analysis of blasting accidents in mining operations*. in *Proceedings Of The Annual Conference On Explosives And Blasting Technique*. 2003: ISEE; 1999.
70. IME, *Glossary of commercial explosives industry terms.* 1997.
71. Persson, P.-A., et al., *BOOK REVIEW: Rock Blasting And Explosives Engineering*. Journal of Energetic Materials, 1994. 12(1): p. 85-88.
72. Raina, A.K., V. Murthy, and A.K. Soni, *Flyrock in surface mine blasting: understanding the basics to develop a predictive regime.* Current Science, 2015. 108(4): p. 660.
73. Bajpayee, T., H. Verakis, and T. Lobb. *An analysis and prevention of flyrock accidents in surface blasting operations*. in *Proceedings of the annual conference on explosives and blasting technique*. 2004: ISEE; 1999.
74. Tsoukalas, L.H. and R.E. Uhrig, *Fuzzy and neural approaches in engineering*. 1996: John Wiley & Sons, Inc.
75. McCulloch, W.S. and W. Pitts, *A logical calculus of the ideas immanent in nervous activity.* The bulletin of mathematical biophysics, 1943. 5(4): p. 115-133.
76. Tsoukalas, L.H. and R.E. Uhrig, *Fuzzy and neural approaches in engineering. Jhon Wiley & Sons.* Inc, New York, 1996.
77. Monjezi, M., M. Rezaei, and A.Y. Varjani, *Prediction of rock fragmentation due to blasting in Gol-E-Gohar iron mine using fuzzy logic*. International Journal of Rock Mechanics and Mining Sciences, 2009. 46(8): p. 1273-1280.
78. Monjezi, M., et al., *Prediction of rock fragmentation due to blasting in Sarcheshmeh copper mine using artificial neural networks.* Geotechnical and Geological Engineering, 2010. 28(4): p. 423-430.
79. Sayadi, A., et al., *A comparative study on the application of various artificial neural networks to simultaneous prediction of rock fragmentation and backbreak.* Journal of Rock Mechanics and Geotechnical Engineering, 2013. 5(4): p. 318-324.
80. Mohamadnejad, M., et al., *Prediction of blast-induced vibrations in limestone quarries using Support Vector Machine.* Journal of Vibration and Control, 2011: p. 1077546311421052.
81. Hajihassani, M., et al., *Ground vibration prediction in quarry blasting through an artificial neural network optimized by imperialist competitive algorithm.* Bulletin of Engineering Geology and the Environment, 2015. 74(3): p. 873-886.
82. Ghoraba, S., et al., *Prediction of ground vibration caused by blasting operations through a neural network approach: a case study of Gol-E-Gohar Iron Mine.* Iran. J Zhejiang Univ Sci A. doi, 2015. 10: p. 1631.

83. Saadat, M., M. Khandelwal, and M. Monjezi, *An ANN-based approach to predict blast-induced ground vibration of Gol-E-Gohar iron ore mine, Iran.* Journal of Rock Mechanics and Geotechnical Engineering, 2014. 6(1): p. 67-76.

84. Armaghani, D.J., et al., *Application of two intelligent systems in predicting environmental impacts of quarry blasting.* Arabian Journal of Geosciences, 2015. 8(11): p. 9647-9665.
85. Saha, A., S. Ray, and S. Sarkar, *Early history of the Earth: evidence from the eastern Indian Shield.* Precambrian of the Eastern Indian Shield. Mem. Geol. Soc. India, 1988. 8: p. 13-37.
86. Roy, P.P., *Rock blasting: effects and operations*. 2005: CRC Press.
87. Palangio, T., J. Franklin, and N. Maerz. *WipFrag-A breakthrough in fragmentation measurement*. in *Proc 6th High-tech seminar on state of the art blasting technologie, instrumentation, and explosives. Boston, Mass*. 1995.
88. Maerz, N.H., *Image sampling techniques and requirements for automated image analysis of rock fragmentation.* Proceedings of the FRAGBLAST, 1996. 5: p. 115-120.
89. Lundborg, N., *Risk for flyrock when blasting.* BFR Report R, 1981. 29.
90. Heck, Joy Sr. *Effect of blasting Air overpressure on Residential Structures.* FIRMATEK,2014,http://firmatek.com/?p=663
91. Bilgin, H.A., Cakmak, B. B., *Environmental Impact Assessment for Blasting at Raw Material Quarry of Konya Cement Factory*. 2006, Project Code: 06-03-05-1-00-12, METU, Ankara, Final Report, . p. 58
92. Aydin, A., *ISRM suggested method for determination of the Schmidt hammer rebound hardness*: revised version, in The ISRM Suggested Methods for Rock Characterization, Testing and Monitoring: 2007-2014. 2008, Springer. p. 25-33.
93. Akeil,S.,*Comparative Study on ground Vibration by statistical and neural netwoks approches at tuncbilk coal mine, Panel ByH*. MS thesis, Department of mining engineering .Middle East Technical university.
94. Monjezi,M, Ghafurikalajahi.M, Bahrami. V. *Prediction of blast-induced ground vibration using artificial neural networks.* Tunnelling and Underground Space Technology 26 (2011) .p. 46–50.

Dissemination

Journal Articles

1. Parida, A. and Mishra M.K, Blast vibration analysis by different predictor approaches-a comparison. Proceedia of Earth and Planetary Science, Elsevier Publ, 11, 2015: p. 337-345

Conference Presentations

1. Parida, A., Mishra, M.K., Kumar, H., and Parida, K. T., Rock Fragmentation Analysis in Iron ore Mine. National Seminar on Sustainable Technology for Cleaner Environment – 2016 (STCE-16); IE(I), Rourkela Center, Feb 13-14, 2016:p.58.

Resume

AbinashParida
At-Katramala, Po-Sekhpur, Dist-Kendrapara, State-Odisha
Tel- 8895155455
Home-9437054791
Email-aparida@gmail.com

Education:

B. Tech. in Mining Engineering, OSME, Keonjhar

Principal subjects: Rock Mechanics, Mine survey, Surface Mine Method, U/G Mining Method, Mine Machinery.

Experience: Adhunik Metalicks, Jharkhand; July 2012 to July 2013
Project Asst., Dept of Mining Engg., NIT Rourkela in a DST sponsored project MN –ESS (for 09 months)

Index

Appendices

Blast monitoring data

Region	Distance(m)	Max. charge per delay (Kg)	PPV(mm/s)	Depth (m)	stemming(m)
Daitari	160	41.7	12.7	9.05	2
	180	41.7	5.19	9.05	2
	220	41.7	2.98	9.05	2
	170	41.7	4.49	9.05	2
	282	44.48	2.59	9.77	2.25
	345	44.48	1.96	9.77	2.25
	120	41.7	24.7	9.55	2.5
	300	41.7	3.79	9.55	2.5
	355	41.7	2.85	9.55	2.5
	175	19.48	8.81	4.89	1.6
	260	19.48	3.12	4.89	1.6
	320	19.48	2.41	4.89	1.6
	185	44.48	4.49	9.77	2.5
	220	489	6.49	8.5	1.92
	230	382.5	5.48	8.5	1.92
	144	911.84	17.6	8	3.77
	298	325.26	4.99	6.5	3.21
Koira	138	22.24	4.78	6.5	3.3
	90	22.24	9.57	6.5	3.3
	120	22.24	8.14	6.5	3.3
	60	13.9	9.18	6.5	3.2
	80	11.12	5.39	4	2.25
	90	13.9	3.9	6.5	3.2
	108	19.46	2.49	6.5	3.2
	248	11.12	1.11	4	2.25
	90	11.12	3.86	4	2.25
	146	11.12	1.53	4	2.25
	108	28.125	6.89	6	3.75
	112	28.125	5.69	6	3.75
	153	33.76	6.8	6.3	3.5
	145	33.76	9.94	6.3	3.5
	122	44.48	3.96	7	4
	120	44.48	8.16	7	4
	186	44.48	3.61	7	4
	188	44.48	1.71	7	4
	147	44.48	1.98	7	4
	274	44.48	0.81	7	4

Event report of PPV (12.7 mm/s)

Instantel

Event Report

Microphone	Linear Weighting
PSPL	128.3 dB(L) at 6.018 sec
ZC Freq	39 Hz
Channel Test	Passed (Freq = 20.0 Hz Amp = 308 mv)

	Tran	Vert	Long	
PPV	7.37	4.45	11.4	mm/s
PPV (Ponderated)	7.45	5.17	13.3	mm/s
ZC Freq	10	9.0	6.0	Hz
Time (Rel. to Trig)	8.389	8.282	8.406	sec
Peak Acceleration	0.0530	0.0398	0.0663	g
Peak Displacement	0.115	0.0875	0.243	mm
Sensor Check	Passed	Passed	Passed	
Frequency	7.8	7.8	8.0	Hz
Overswing Ratio	3.6	3.9	3.6	

Peak Vector Sum 12.7 mm/s at 8.400 sec

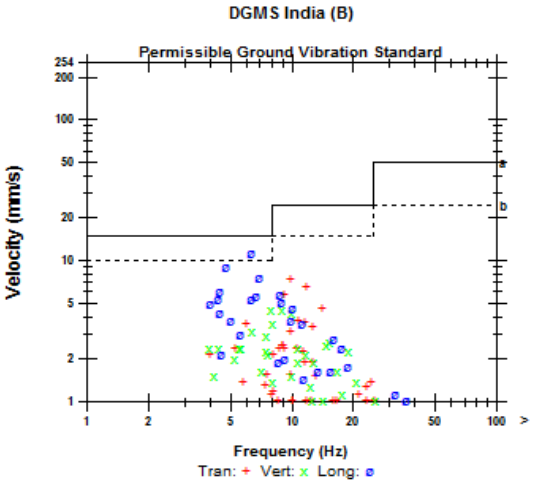

a) Industrial buildings
b)Domestic houses/structures

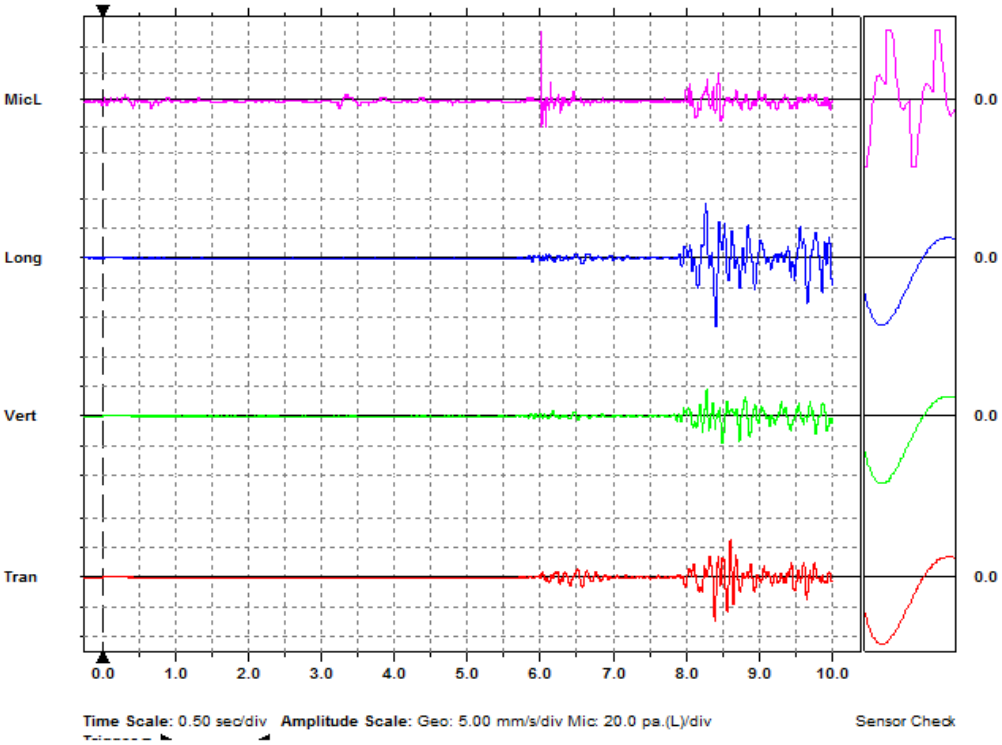

Time Scale: 0.50 sec/div **Amplitude Scale:** Geo: 5.00 mm/s/div Mic: 20.0 pa.(L)/div Sensor Check

Zero crossing frequency (Hz) and Fourier frequency (Hz) with respect to PPV (mm/s)

T PPV(mm/s)	V PPV(mm/s/)	L PPV(mm/s)	T ZC(Hz)	V ZC(Hz)	L ZC(Hz)	T FFT(Hz)	V FFT(Hz)	L FFT(Hz)
7.37	4.45	11.4	10	9	6	11	5.44	5.44
2.16	2.29	5.08	12	8	17	5.88	3.63	5.75
2	1.6	2.57	6.2	3.1	3.2	4.56	3.19	3.88
2.54	1.84	3.75	6.4	3.6	4.2	3.94	3.81	3.81
2.29	1.19	2.4	3.8	4	4	3.63	2.38	4.13
1.35	1.19	1.6	4	4	4.4	3.63	2.38	3.63
16.5	15.2	10.2	0	0	0	2	2	2
3.37	1.79	3.32	4	7.1	5.4	3.63	5.25	4.5
2.32	1.41	2.68	5.8	4.4	7.5	5.8	4.4	7.5
7.37	7.37	0.284	13	6	0	5.75	7.75	2
2.4	1.92	2.4	4.6	3.6	3.7	2.25	4.38	4.5
1.57	2.1	2.25	4.6	3.8	6.1	4.63	4.38	4.8
4.25	2.98	3.3	6	8	6	3.25	6	3.63
4.68	3.08	6.49	4.1	4.2	3.1	4	3.38	2.38
2.6	2.64	4.95	3.3	4	3.8	3.3	4	3.8
0.857	0.603	1.44	7.2	8.4	7.1	5.5	5.88	5
4.35	2.4	3.7	3.8	4.5	9	2.75	3	8.25
5.86	3.08	6.02	4.3	13	7	7	3	9.25
2.24	3.35	2.05	2.9	3.6	4.7	2.5	2.63	3.35
2.78	1.52	3.3	6.7	5.4	5.7	8.63	5.75	8.5
1.6	1.27	1.11	4.1	5.4	4.5	2.75	3.5	2.88
1.14	1.78	1.52	7	4	32	5.75	3.5	2.88
0.635	0.639	0.508	10	11	6	7	3	3
3.94	3.05	4	16	5	16	9.5	3.75	3.75
5.32	7.52	9.48	5.1	5.1	5.5	5.38	3.88	4
2.89	4.18	7.16	4.7	4	6	3.13	4.88	5.75
3.33	2.78	2.64	10	7.2	10	13.5	3.25	5.75
2.95	3.03	4.6	7.3	12	12	11.6	11.1	4.5
6.86	7.62	0.254	7	6	0	6	15.3	13.6
3.62	3.59	2.73	7.1	5.1	6.6	5.88	5.38	2.63
3.75	1.75	2.44	4.5	4.8	5	5	4.13	4
1.08	0.315	0.572	5	22	4	4.5	13.4	5.63
1.59	1.97	2.03	8	7	8	5.88	5.63	5.63
0.699	0.699	0.508	2	2	2	2.13	2.13	2.13
0.841	1.3	1.22	19	8.8	28	6.01	6.76	23.1
3.76	2.27	2.64	9.3	9.1	20	20.3	19.4	20.3

Sample Images of Blasted rock and Fragmentation Analysis

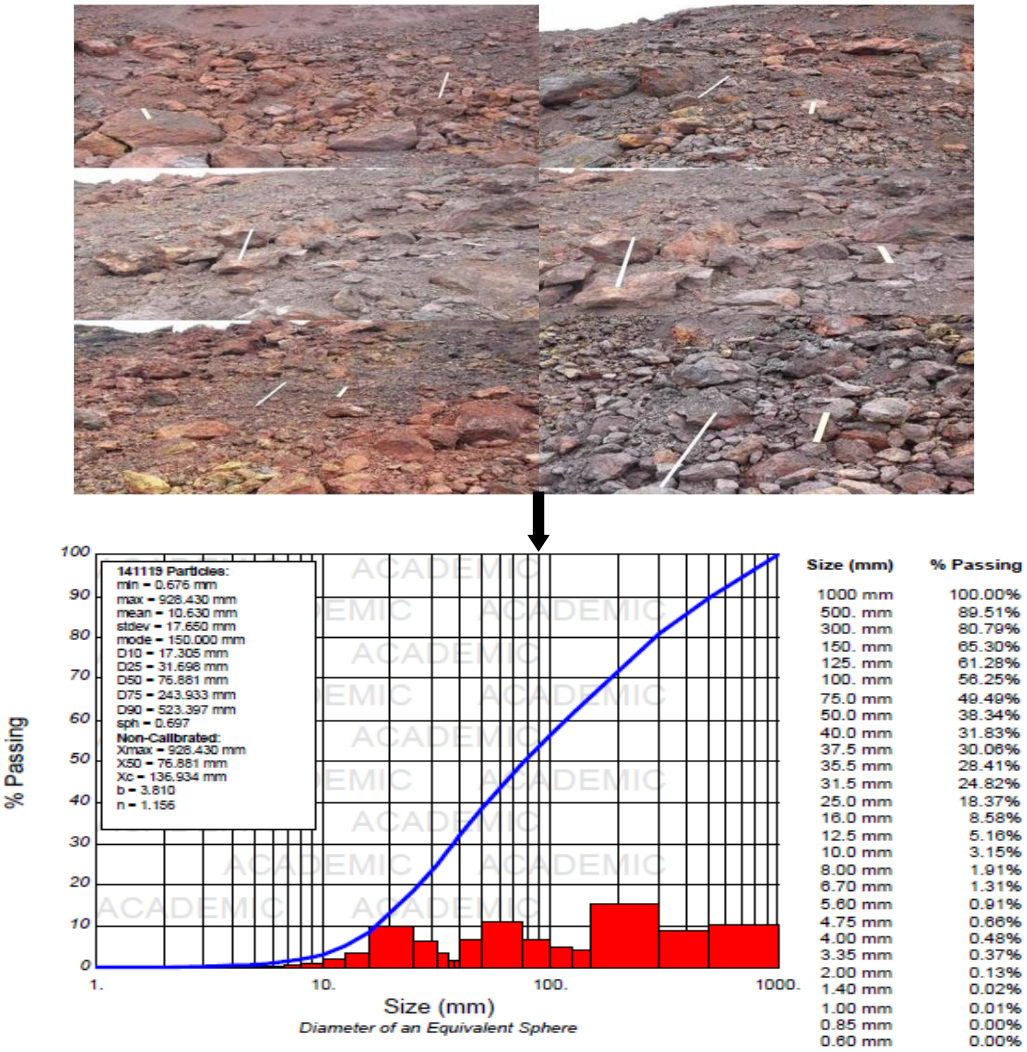

Size Distribution Profile of Merged Events